CRITERIA FOR PREDICTING SPIN SUSCEPTIBILITY OF FIGHTER-TYPE AIRCRAFT

Robert Weissman

Aeronautical Systems Division
Wright-Patterson Air Force Base, Ohio

June 1972

ASD-TR-72-48

CRITERIA FOR PREDICTING SPIN SUSCEPTIBILITY OF FIGHTER-TYPE AIRCRAFT

ROBERT WEISSMAN

TECHNICAL REPORT ASD-TR-72-48

JUNE 1972

DEPUTY FOR ENGINEERING
AERONAUTICAL SYSTEMS DIVISION
AIR FORCE SYSTEMS COMMAND
WRIGHT-PATTERSON AIR FORCE BASE, OHIO

RM

102

NOTICE

When Government drawings, specifications, or other data are used for any purpose other than in connection with a definitely related Government procurement operation, the United States Government thereby incurs no responsibility nor any obligation whatsoever; and the fact that the government may have formulated, furnished, or in any way supplied the said drawings, specifications, or other data, is not to be regarded by implication or otherwise as in any manner licensing the holder or any other person or corporation, or conveying any rights or permission to manufacture, use, or sell any patented invention that may in any way be related thereto.

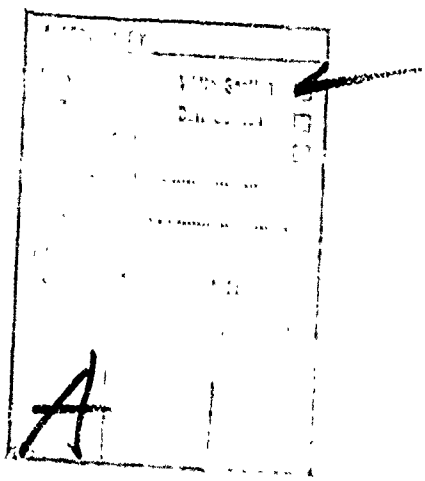

Copies of this report should not be returned unless return is required by security considerations, contractual obligations, or notice on a specific document.

AIR FORCE/56780/15 September 1972 — 100

UNCLASSIFIED

Security Classification

DOCUMENT CONTROL DATA - R & D

(Security classification of title, body of abstract and indexing annotation must be entered when the overall report is classified)

1. ORIGINATING ACTIVITY (Corporate author)	2a. REPORT SECURITY CLASSIFICATION
Deputy for Engineering Wright-Patterson AFB, Ohio 45433	UNCLASSIFIED
	2b. GROUP

3. REPORT TITLE

CRITERIA FOR PREDICTING SPIN SUSCEPTIBILITY OF FIGHTER-TYPE AIRCRAFT

4. DESCRIPTIVE NOTES (Type of report and inclusive dates)

5. AUTHOR(S) (First name, middle initial, last name)

Robert Weissman

6. REPORT DATE	7a. TOTAL NO. OF PAGES	7b. NO. OF REFS
June 1972	85	4

8a. CONTRACT OR GRANT NO.	9a. ORIGINATOR'S REPORT NUMBER(S)
b. PROJECT NO.	ASD-TR-72-48
c.	9b. OTHER REPORT NO(S) (Any other numbers that may be assigned this report)
d.	

10. DISTRIBUTION STATEMENT

Approved for Public Release; distribution unlimited.

11. SUPPLEMENTARY NOTES	12. SPONSORING MILITARY ACTIVITY
	Deputy for Engineering Wright-Patterson AFB, Ohio 45433

13. ABSTRACT

An investigation was conducted to determine if there is a correlation between lateral-directional static stability characteristics and spin susceptibility. The effects of longitudinal static stability and adverse or proverse yaw were also considered. The motion of an airplane entering the high angle of attack, low speed flight regime is analyzed in six degrees of freedom. The $C_{n_\beta,dynamic}$ and aileron-alone divergence parameters are calculated for four aerodynamic cases. Results show that these parameters have promise as criteria for predicting spin susceptibility of fighter-type aircraft in the early stages of design and development. An airplane whose $C_{n_\beta,dynamic}$ and aileron-alone divergence parameters are both negative at near-stall angles of attack tends to be susceptible to spinning and an airplane with positive values for these parameters tends not to be susceptible to spinning.

Ia

DD FORM 1 NOV 68 1473

UNCLASSIFIED

Security Classification

UNCLASSIFIED

Security Classification

14. KEY WORDS	LINK A		LINK B		LINK C	
	ROLE	WT	ROLE	WT	ROLE	WT
Spin Susceptibility of Fighter-Type Aircraft						
Stall/Post-Stall/Spin Characteristics of Fighter-Type Aircraft						

*U.S.Government Printing Office: 1972 —759-485/58

Ib

UNCLASSIFIED

Security Classification

ASD-TR-72-48

CRITERIA FOR PREDICTING SPIN SUSCEPTIBILITY OF FIGHTER-TYPE AIRCRAFT

ROBERT WEISSMAN

IC

FOREWORD

This work was accomplished by the author as a member of the Stability and Control Branch, Aeromechanics Division, Directorate of Airframe Subsystems Engineering, Aeronautical Systems Division, as an in-house effort. The work was done between March and December 1970 and originally submitted to the School of Engineering, University of Dayton, in partial fulfillment of the requirements for the Degree of Master of Science in Engineering.

The author wishes to express his gratitude to Mr. John W. Carlson for his help and understanding and to Dr. Jack G. Crouch, University of Dayton, for his guidance during the course of the work.

This report was submitted by the author during April 1972.

Publication of this report does not constitute Air Force approval of the report's findings or conclusions.. It is published only for the exchange and stimulation of ideas.

Richard H. Kleinger
Chief, Aeromechanics Division
Directorate of Airframe
Subsystems Engineering

ABSTRACT

An investigation has been made to determine if there is a correlation between lateral-directional static stability characteristics and spin susceptibility. The effects of longitudinal static stability and adverse or proverse yaw were also considered. The motion of an airplane entering the high angle of attack, low speed flight regime is analyzed in six degrees of freedom utilizing a digital computer. The basic aerodynamic characteristics used as input data are representative of a fighter-type airplane and the motion of the airplane is first computed utilizing these basic data and then recomputed with variations in lateral-directional static stability characteristics and a variation in pitching moment. The $C_{n\beta,dynamic}$ and aileron-alone divergence parameters are calculated for four aerodynamic cases and two sets of mass characteristics. The results of the study show that these parameters have promise as criteria for predicting spin susceptibility of fighter-type aircraft in the early stages of design and development. An airplane whose $C_{n\beta,dynamic}$ and aileron-alone divergence parameters are both negative at near-stall angles of attack tends to be susceptible to spinning and an airplane with positive values for these parameters tends not to be susceptible to spinning. With a positive $C_{n\beta,dynamic}$ and a negative aileron-alone divergence parameter, an airplane may or may not be susceptible to spin depending upon whether an airplane is directionally unstable or stable at near-stall angles of attack and also upon the variation in pitching moment. The results of the study also indicate that, in general, proverse yaw appears to be preferable to adverse yaw regarding spin susceptibility.

TABLE OF CONTENTS

ILLUSTRATIONS

ILLUSTRATIONS (CONTD)

ILLUSTRATIONS (CONTD)

SYMBOLS

I_x	moment of inertia about longitudinal body axis	slug-ft^2
I_y	moment of inertia about lateral body axis	slug-ft^2
I_z	moment of inertia about normal body axis	slug-ft^2
I_{xz}	product of inertia	slug-ft^2
m	airplane mass	slugs
W	airplane weight	lb
S	wing area	ft^2
b	wing span	ft
$\bar{c}$	wing mean aerodynamic chord	ft
c.g.	center of gravity	% $\bar{c}$
ρ	air density	slugs/ft^3
q_o	dynamic pressure ($\frac{1}{2}\rho V^2$)	lb/ft^2
u, v, w	linear velocity components along the x, y, and z body axes, respectively	ft/sec
V	resultant linear velocity	ft/sec
p, q, r	airplane roll, pitch, and yaw rates about x, y, and z body axes, respectively	degrees/sec
H	altitude	ft
g	acceleration due to gravity	32.174 ft/sec^2
T	engine thrust force along x body axis	lb

SYMBOLS (CONTD)

Definition of Angles

α	angle of attack, measured between the X body axis and the projection in the X-Z plane of the relative wind vector, positive when the X axis is above the projected relative wind vector (Figure 38)	deg
β	angle of sideslip, measured between the relative wind vector and its projection in the X-Z plane, positive when the relative wind vector is to the right of the X-Z plane (Figure 38)	deg
θ	airplane pitch attitude angle, measured in a vertical plane between the X body axis and the horizontal plane, positive airplane nose up (Figure 39)	deg
ϕ	airplane roll attitude angle, measured in the Y-Z plane between the Y body axis and the horizontal plane, positive right wing down (Figure 39)	deg
ψ	airplane yaw attitude angle, measured between the initial flight direction and the projection in the horizontal plane of the X body axis, positive airplane nose right (Figure 39)	deg
δ_a	control deflection - aileron or any lateral control surface, positive direction right stick (i.e., left aileron trailing edge down)	deg
δ_H	control deflection - elevator or any horizontal control surface positive direction trailing edge down	deg

SYMBOLS (CONTD)

δ_R	control deflection - rudder, positive direction trailing edge left	deg
F_x, F_y, F_z	components of the aerodynamic forces along the x, y, z body axes, respectively	lb
L, M, N	components of the aerodynamic moments about the x, y, and z body axes, respectively	ft-lb

Aerodynamic Coefficient and Derivatives

C_N	normal force coefficient, body axis $C_N = -F_z/q_o S$	
C_y	side force coefficient, body axis $C_y = F_y/q_o S$	
C_c	chord force coefficient, body axis $C_c = -F_x/q_o S$	
C_ℓ	rolling moment coefficient $C_\ell = L/q_o Sb$	
C_m	pitching moment coefficient $C_m = M/q_o S\bar{c}$	
C_n	yawing moment coefficient $C_n = N/q_o Sb$	
$C_{y_\beta} = \frac{\partial C_y}{\partial \beta}$	derivative of side force coefficient with respect to sideslip angle	per deg
$C_{\ell_\beta} = \frac{\partial C_\ell}{\partial \beta}$	derivative of rolling moment coefficient with respect to sideslip angle	per deg

SYMBOLS (CONTD)

$C_{n_\beta} = \frac{\partial C_n}{\partial \beta}$	derivative of yawing moment coefficient with respect to sideslip angle	per deg
$C_{\ell_p} = \frac{\partial C_\ell}{\partial \left(\frac{pb}{2V}\right)}$	derivative of rolling moment coefficient with respect to roll rate	per radian
$C_{n_p} = \frac{\partial C_n}{\partial \left(\frac{pb}{2V}\right)}$	derivative of yawing moment coefficient with respect to roll rate	per radian
$C_{m_q} = \frac{\partial C_m}{\partial \left(\frac{q\bar{c}}{2V}\right)}$	derivative of pitching moment coefficient with respect to pitch rate	per radian
$C_{\ell_r} = \frac{\partial C_\ell}{\partial \left(\frac{rb}{2V}\right)}$	derivative of rolling moment coefficient with respect to yaw rate	per radian
$C_{n_r} = \frac{\partial C_n}{\partial \left(\frac{rb}{2V}\right)}$	derivative of yawing moment coefficient with respect to yaw rate	per radian
$C_{m_{\dot{\alpha}}} = \frac{\partial C_m}{\partial \left(\frac{\dot{\alpha}\bar{c}}{2V}\right)}$	derivative of pitching moment coefficient with respect to the rate of change of angle of attack	per radian
$C_{y_{\delta_a}} = \frac{\partial C_y}{\partial \delta_a}$	derivative of side force coefficient with respect to lateral control deflection	per deg
$C_{\ell_{\delta_a}} = \frac{\partial C_\ell}{\partial \delta_a}$	derivative of rolling moment coefficient with respect to lateral control deflection	per deg
$C_{n_{\delta_a}} = \frac{\partial C_n}{\partial \delta_a}$	derivative of yawing moment coefficient with respect to lateral control deflection	per deg

SYMBOLS (CONTD)

$C_{y_{\delta_R}} = \frac{\partial C_y}{\partial \delta_R}$	derivative of side force coefficient with respect to rudder deflection	per deg
$C_{\ell_{\delta_R}} = \frac{\partial C_\ell}{\partial \delta_R}$	derivative of rolling moment coefficient with respect to rudder deflection	per deg
$C_{n_{\delta_R}} = \frac{\partial C_n}{\partial \delta_R}$	derivative of yawing moment coefficient with respect to rudder deflection	per deg
$C_{c_{\delta_H}} = \frac{\partial C_c}{\partial \delta_H}$	derivative of chord wise force coefficient with respect to elevator deflection	per deg
$C_{N_{\delta_H}} = \frac{\partial C_N}{\partial \delta_H}$	derivative of normal force coefficient with respect to elevator deflection	per deg
$C_{m_{\delta_H}} = \frac{\partial C_m}{\partial \delta_H}$	derivative of pitching moment coefficient with respect to elevator deflection	per deg
$C_{n_\beta} - C_{\ell_\beta} \frac{C_{n_{\delta_a}}}{C_{\ell_{\delta_a}}}$	aileron-alone divergence parameter	per deg
$C_{n\beta,\text{dynamic}}$	$C_{n_\beta} \cos \alpha - \frac{I_z}{I_x} C_{\ell_\beta} \sin \alpha$	per deg

A dot over a symbol represents differentiation with respect to time.

SECTION I

INTRODUCTION

The purpose of this study is to determine the usefulness of existing lateral-directional divergence parameters for predicting a fighter-type airplane's spin susceptibility characteristics following departure from controlled flight. The expression "post stall gyration" is often used to denote uncontrolled motions about one or more aircraft axes following departure from controlled flight. If the post stall gyration resulting from a stall consists of an appreciable amount of yawing motion with a corresponding increase of angle of attack, the airplane can be considered spin susceptible. The type of rolling motion is also significant regarding spin susceptibility in that an increasing bank angle with time together with excursions in sideslip angle and a nose down attitude could be interpreted by a service pilot as "spin." Such an interpretation causes a pilot to apply anti-spin recovery controls or lateral control in an effort to "pick up" the down wing. If lateral control is used to pick up the down wing, adverse or proverse yaw can drive the airplane into a fully developed spin.

A degradation in lateral-directional static stability characteristics in the high angle of attack, low speed regime can and often does lead to a loss of control with subsequent "spinning" motion. An airplane with poor lateral-directional stability characteristics at near-stall angles of attack could have a high degree of spin susceptibility following departure from controlled flight. Consequently, it is desirable to establish a correlation between lateral-directional

SECTION I

INTRODUCTION

The purpose of this study is to determine the usefulness of existing lateral-directional divergence parameters for predicting a fighter-type airplane's spin susceptibility characteristics following departure from controlled flight. The expression "post stall gyration" is often used to denote uncontrolled motions about one or more aircraft axes following departure from controlled flight. If the post stall gyration resulting from a stall consists of an appreciable amount of yawing motion with a corresponding increase of angle of attack, the airplane can be considered spin susceptible. The type of rolling motion is also significant regarding spin susceptibility in that an increasing bank angle with time together with excursions in sideslip angle and a nose down attitude could be interpreted by a service pilot as "spin." Such an interpretation causes a pilot to apply anti-spin recovery controls or lateral control in an effort to "pick up" the down wing. If lateral control is used to pick up the down wing, adverse or proverse yaw can drive the airplane into a fully developed spin.

A degradation in lateral-directional static stability characteristics in the high angle of attack, low speed regime can and often does lead to a loss of control with subsequent "spinning" motion. An airplane with poor lateral-directional stability characteristics at near-stall angles of attack could have a high degree of spin susceptibility following departure from controlled flight. Consequently, it is desirable to establish a correlation between lateral-directional

static stability and spin susceptibility, preferably in the form of criteria utilizing static aerodynamic data, since these kind of data are obtained early during the initial design stages. If spin susceptibility is investigated early in the design and development stage, design changes can be made which will produce satisfactory high angle of attack lateral-directional stability characteristics and thus minimize spin susceptibility.

Certain parameters involving only lateral-directional static aerodynamic data are studied for the purpose of establishing these parameters as criteria for determining spin susceptibility during design evaluation of fighter-type airplanes. These parameters are known as the "$C_{n\beta,dynamic}$" criterion and the "aileron-alone divergence" parameter.

As discussed in References 1 and 2, the parameter $C_{n\beta,dynamic}$ is generally a primary factor in determining the undamped natural frequency of the Dutch roll mode and has been shown to correlate with directional divergence of inertially slender configurations. Further, it was shown for the study presented in Reference 1 that the expression $C_{n\beta,dynamic} < 0$ is an approximate criterion for divergence in the form of lateral-directional oscillatory instability. The parameter $C_{n\beta,dynamic}$ is defined herein as

$$C_{n\beta,dynamic} = C_{n\beta} \cos \alpha - \frac{I_z}{I_x} C_{\ell\beta} \sin \alpha \qquad (1)$$

The aileron-alone divergence parameter relates to divergence characteristics when lateral control alone is applied and is defined herein as

SECTION II

GENERAL METHOD OF ANALYSIS

The motion of an airplane entering the high angle of attack, low speed (Mach number less than 0.50) flight regime is analyzed in six degrees of freedom utilizing a digital computer. The equations of motion are included in Appendix I as well as diagrams (Figures 38 and 39) defining the reference axes, angles of attack and sideslip, and attitude angles.

The static and dynamic aerodynamic data (in coefficient form) used as a base for the studies discussed in this report are presented in Appendix II. The basic aerodynamic characteristics are representative of a fighter-type airplane considered to be relatively spin resistant when flown at low speed to angles of attack near the stall angle of attack. Changes to these basic data are made and involve the directional stability derivative (C_{n_β}), the effective dihedral (C_{ℓ_β}), and pitching moment. Figures 40, 41, and 45 in Appendix II and Table I show these changes. The directional stability derivative and effective dihedral are used to define $C_{n_\beta, \text{dynamic}}$ and the aileron-alone divergence parameter. The motion of the airplane is first computed utilizing the basic data and then recomputed with variations in directional stability and effective dihedral characteristics.

TABLE I

AERODYNAMIC CASES

Case	Changes to Basic Aerodynamic Data
A (Basic)	
B	$C_{n\beta}$ unstable for $\alpha > 20.6°$
C	$C_{\ell\beta}$ positive for $20° < \alpha < 27.5°$
D	$C_{\ell\beta}$ positive for $20° < \alpha < 27.5°$ $C_{n\beta}$ unstable for $\alpha > 20.6°$

The definition of $C_{n\beta,dynamic}$ also includes the yaw to roll moment of inertia ratio, I_z/I_x. Two sets of mass characteristics (Table II) are used in the analyses to determine their effect on spin susceptibility. The weight is concentrated chiefly along the fuselage for both airplanes.

The thrust required initially to trim the airplane is maintained during the entire maneuver. Engine gyroscopic effects are neglected in the equations of motion for accelerations.

TABLE II

MASS CHARACTERISTICS AND INERTIAL PARAMETERS

	Airplane 1	Airplane 2
Weight (lb)	38,790	10,910
s (ft^2)	538	170
b (ft)	38.4	25.25
c (ft)	16.04	6.73
Moments of Inertia:		
Ix (slug-ft^2)	25,850	1,700
Iy (slug-ft^2)	122,800	29,500
Iz (slug-ft^2)	140,900	30,100
Ixz (slug-ft^2)	2,600	0
Iz/Ix	5.45	17.7

SECTION III

$C_{n\beta,\ dynamic}$ PARAMETER FOR PREDICTING SPIN SUSCEPTIBILITY

1. METHOD OF ANALYSIS

Four aerodynamic cases are considered (Table I and Appendix II) for determining the usefulness of $C_{n\beta,dynamic}$ as a criterion for predicting spin susceptibility.

The airplane is flown to high angles of attack from a 1-g wings-level trimmed flight condition at an altitude of 30,000 feet by applying a horizontal control surface deflection. The control surface is deflected over a time interval which produces a deflection rate of 10 degrees per second to a maximum deflection of minus 21 degrees (stick back) which is held throughout the maneuver. At the same time, a sideslip angle increase is obtained from an initial input of 2.5 degrees in sideslip angle. Lateral and directional control surface deflections are not applied.

2. RESULTS OF ANALYSIS, AIRPLANE 1

The results of the six degree of freedom analyses for a fighter-type airplane whose yaw to roll moment of inertia ratio, I_z/I_x, equals 5.45 (airplane 1) is presented in Figures 1 through 13. Figure 1 shows the time histories of sideslip angle for the four cases studied. The case which produces an abrupt directional divergence and therefore is considered spin susceptible is indicated by the curve labeled D. Figures 2 and 12 show that the beginning of the abrupt divergence occurs at an angle of attack of about 24.5 degrees (2.5 seconds), where $C_{n\beta,dynamic}$ first becomes a relatively large negative value (Figure 3). Figure 3 shows that $C_{n\beta,dynamic}$ is always positive for the three cases (A, B, and C) which display rather well-behaved motion following departure

from controlled flight while the value of $C_{n\beta,dynamic}$ for case D is about -0.003 per degree at and immediately following departure from controlled flight.

The remaining figures (Figures 4 through 13) show time histories of rates, angles of attack, and orientation angles. The motion or post stall gyration displayed by the divergent case (case D) is seen to be quite severe in comparison to the motion indicated for cases A, B, and C. The roll angle time history (Figure 11) for case D shows that the airplane rolls to the right through 180 degrees in about 5.5 seconds and through 360 degrees in about 8 seconds. In contrast, cases A, B, and C show relatively small changes in roll angle with time. Note that case C shows a mild, continuous roll to the left (Figure 10) because of the negative sideslip angle with time (Figure 1). Pitch angle or attitude (Figure 9) is seen to be oscillatory for case D as well as yaw angle (Figure 12). Note that at 180 degrees of roll the airplane attitude is about 50 degrees nose down and at 360 degrees of roll about 65 degrees nose up. Figure 12 shows that for case D the airplane experiences abrupt changes in yaw angle and will spin, yawing through one turn in about 25 seconds, if no recovery control is applied. A pilot can be expected to become quite confused and disoriented because of this motion, that is, the combination of severe rolling, pitching, and yawing motion; and the probability of applying the improper recovery controls while in a post stall gyration is considered high. Consequently, case D is considered to be spin susceptible from this standpoint also.

The importance to spin susceptibility of effective dihedral,

whether positive or negative, is indicated when comparing the two $C_{n\beta,dynamic}$ curves for case B and case D (Figure 3). The variation of the directional stability derivative ($C_{n\beta}$) with angle of attack used for both of these cases is unstable for angles of attack above 20.6 degrees. However, case B represents positive effective dihedral ($-C_{\ell\beta}$) at all angles of attack while case D represents slightly negative effective dihedral ($+C_{\ell\beta}$) for angles of attack between 20 and 27.5 degrees. In the first case, positive effective dihedral compensates for the negative directional stability thus producing reasonably well-behaved motion at these angles of attack.

Comparison of the two $C_{n\beta,dynamic}$ curves for cases A and C further illustrates the importance of positive effective dihedral at near-stall angles of attack. In both of these cases, the variation of the directional stability derivative with angle of attack is stable up to an angle of attack of 37.5 degrees while the variation of effective dihedral with angle of attack for cases A and C is the same as for cases B and D respectively. A large decrease in $C_{n\beta,dynamic}$, beginning at about an angle of attack of 14 degrees, is shown for the case C curve. The computed motion is well-behaved for this case but the initial variation of sideslip angle, particularly over the first six seconds, is greater than for case A (Figure 1). In addition, changes in yaw angle are considerably greater for case C as shown in Figures 12 and 13. Although the motion is not considered spin susceptible motion, it does illustrate the influence of effective dihedral; that is, negative effective dihedral at near-stall angles of attack can degrade the beneficial effect of positive directional stability.

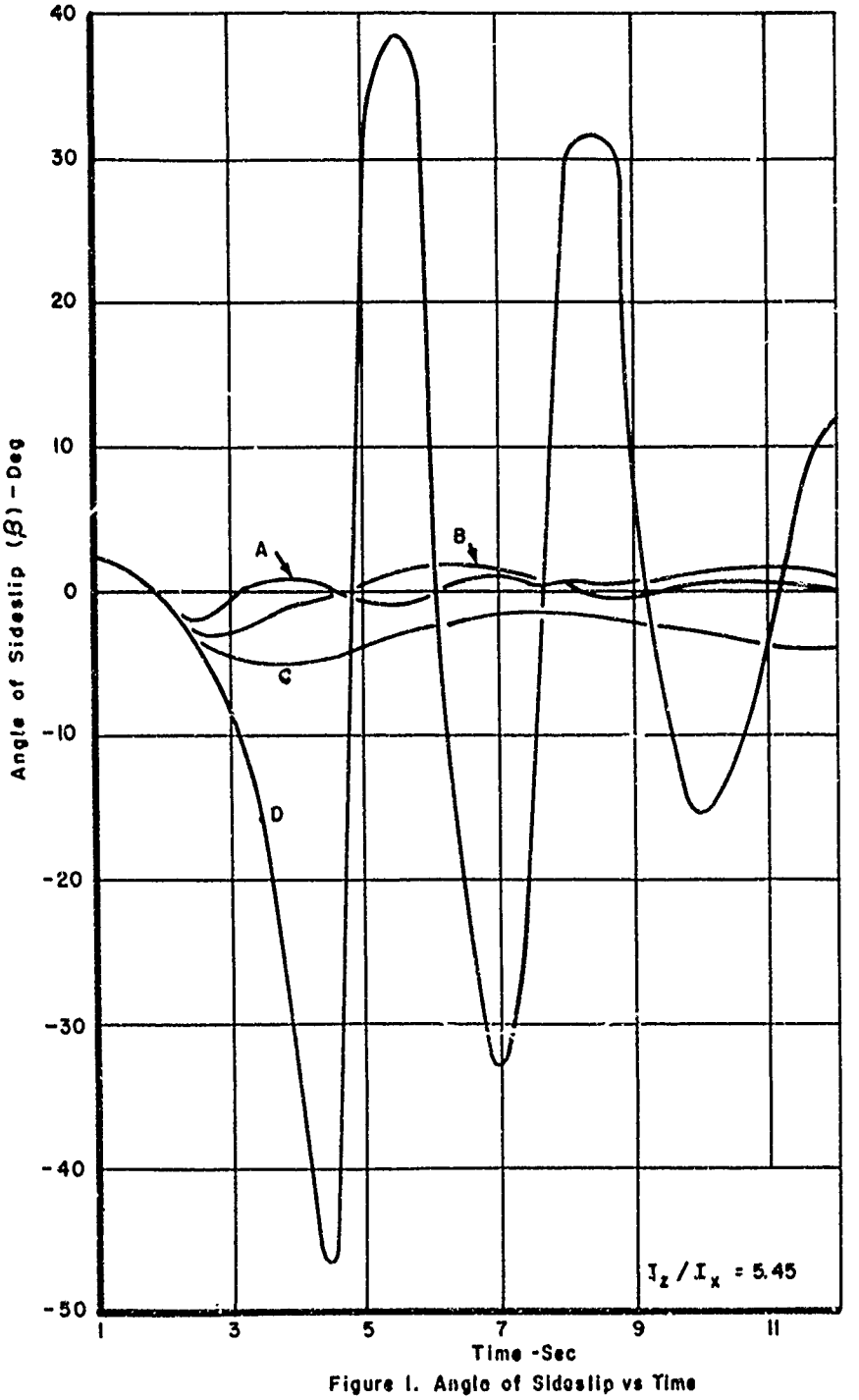

Figure 1. Angle of Sideslip vs Time

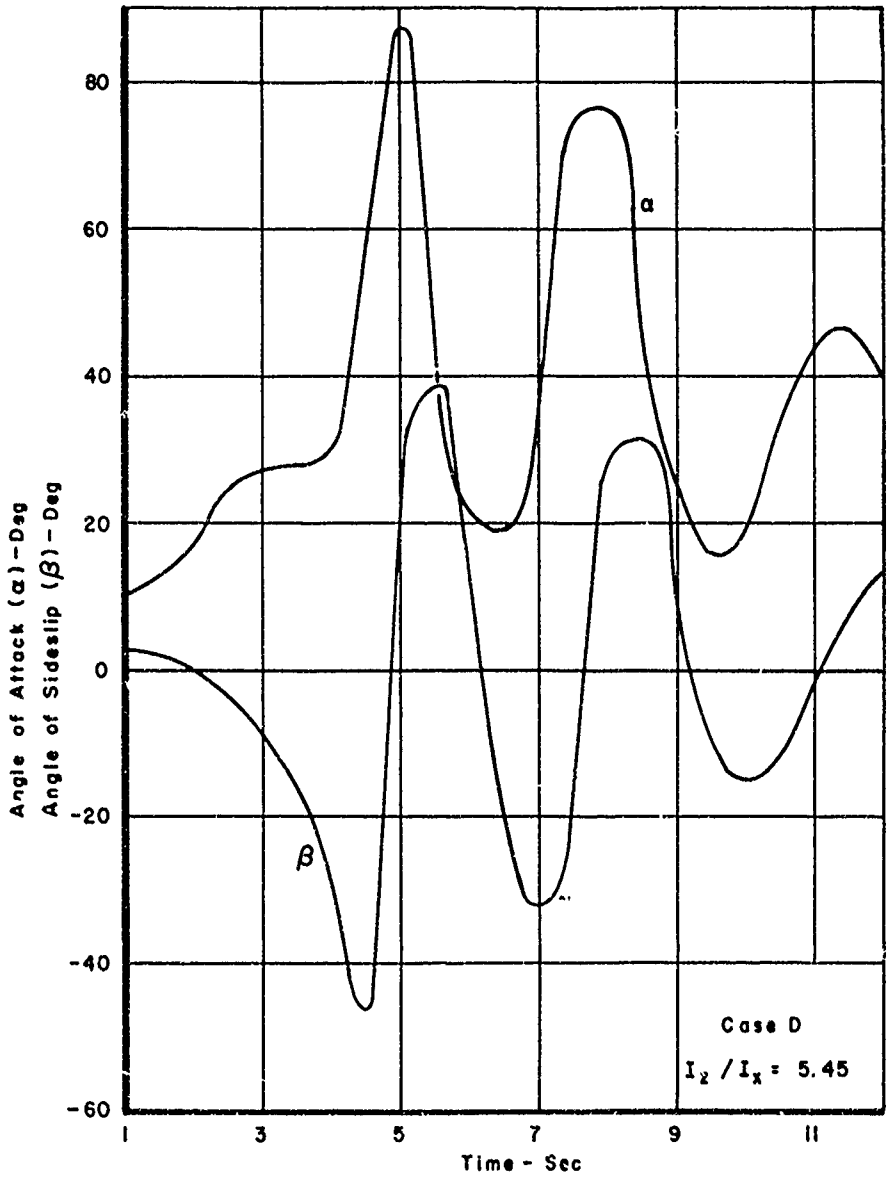

Figure 2. Angle of Attack, Sideslip vs Time

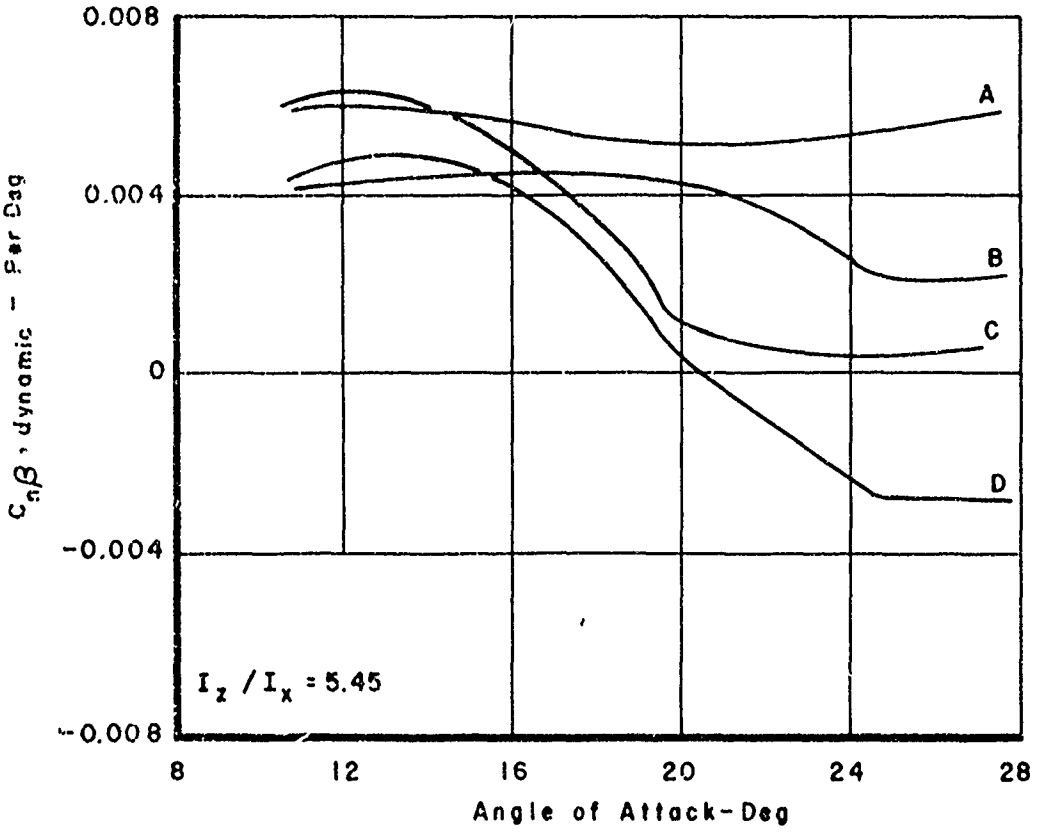

Figure 3. $C_{n\beta}$, dynamic vs Angle of Attack

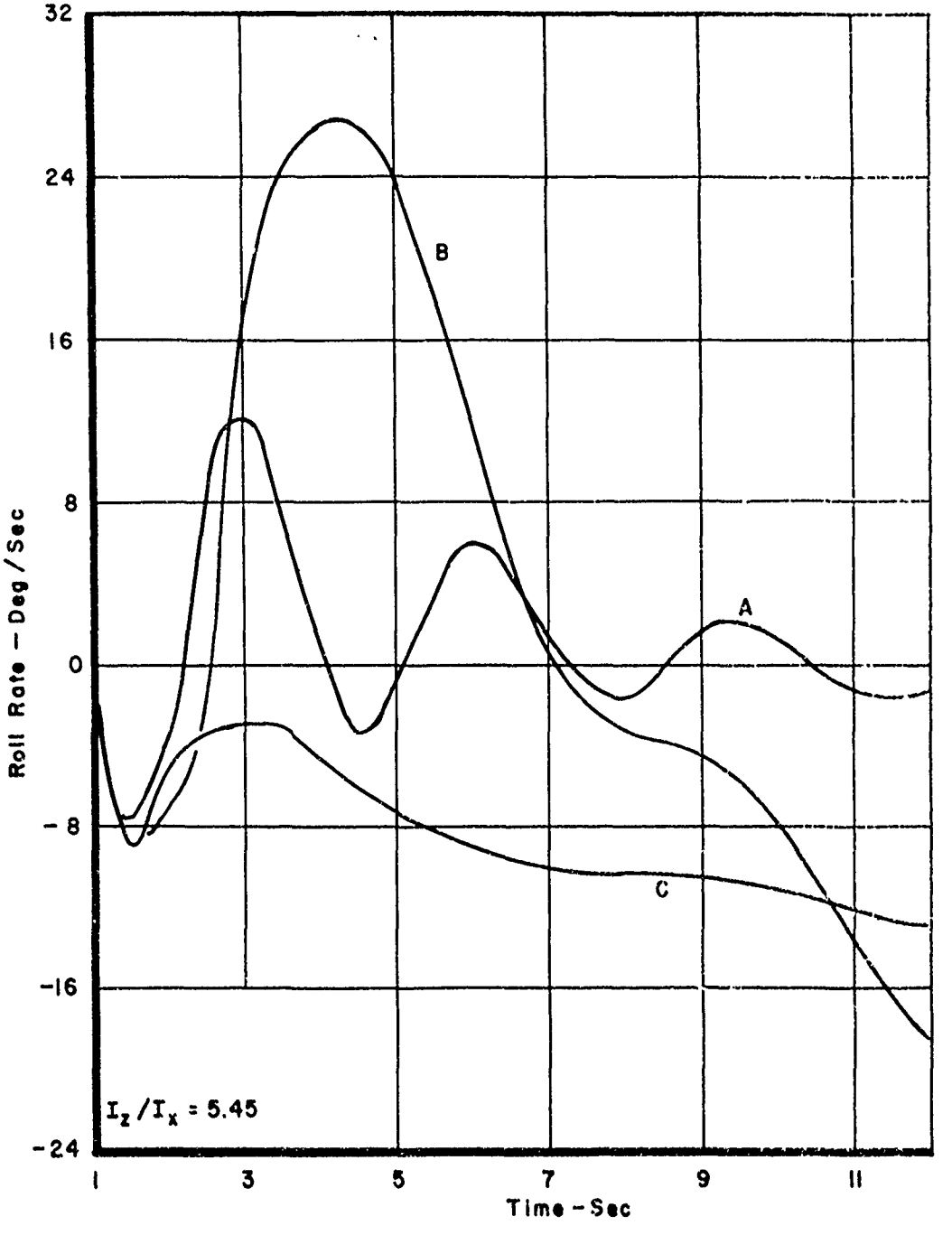

Figure 4. Roll Rate vs Time

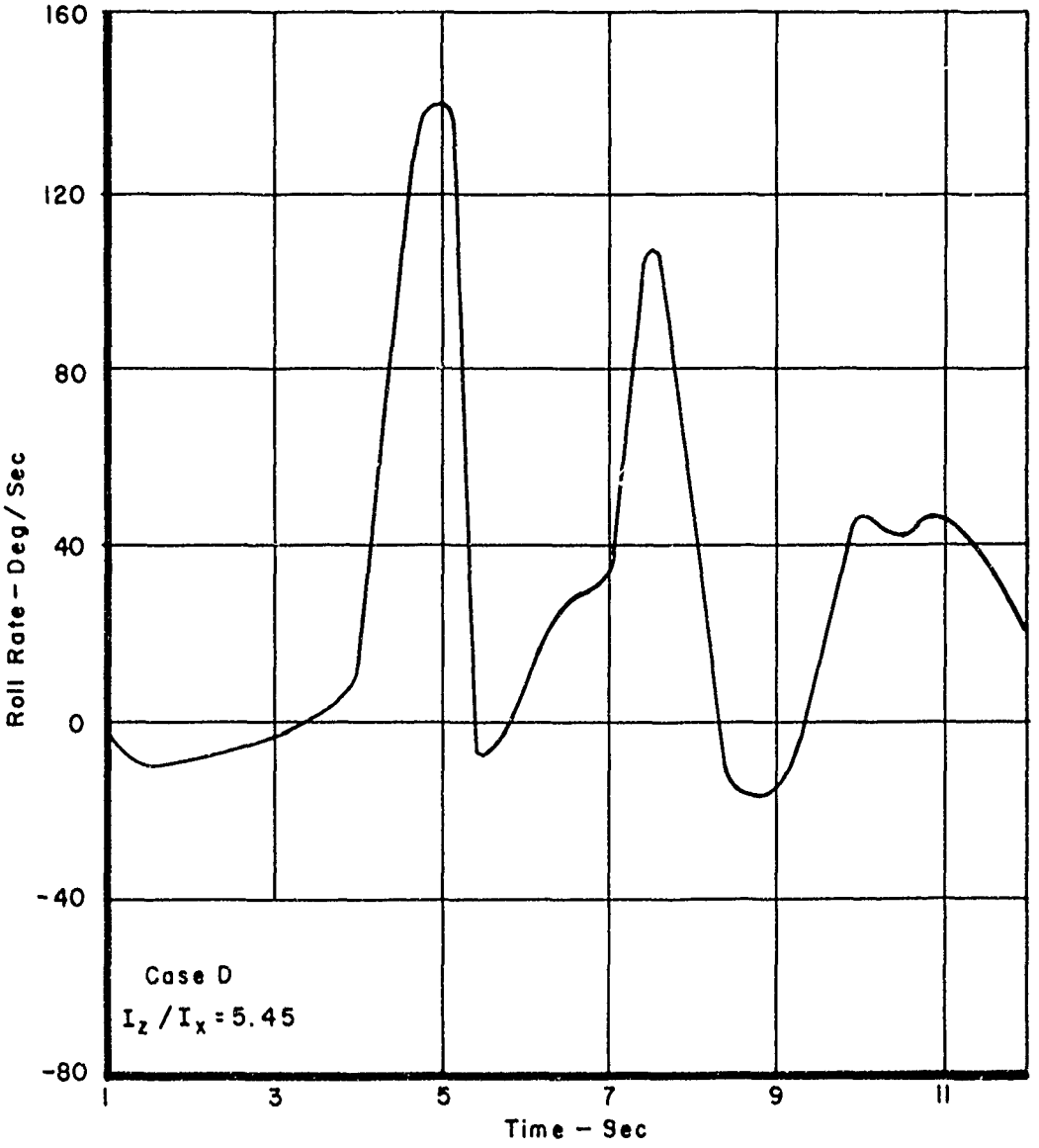

Figure 5. Roll Rate vs Time

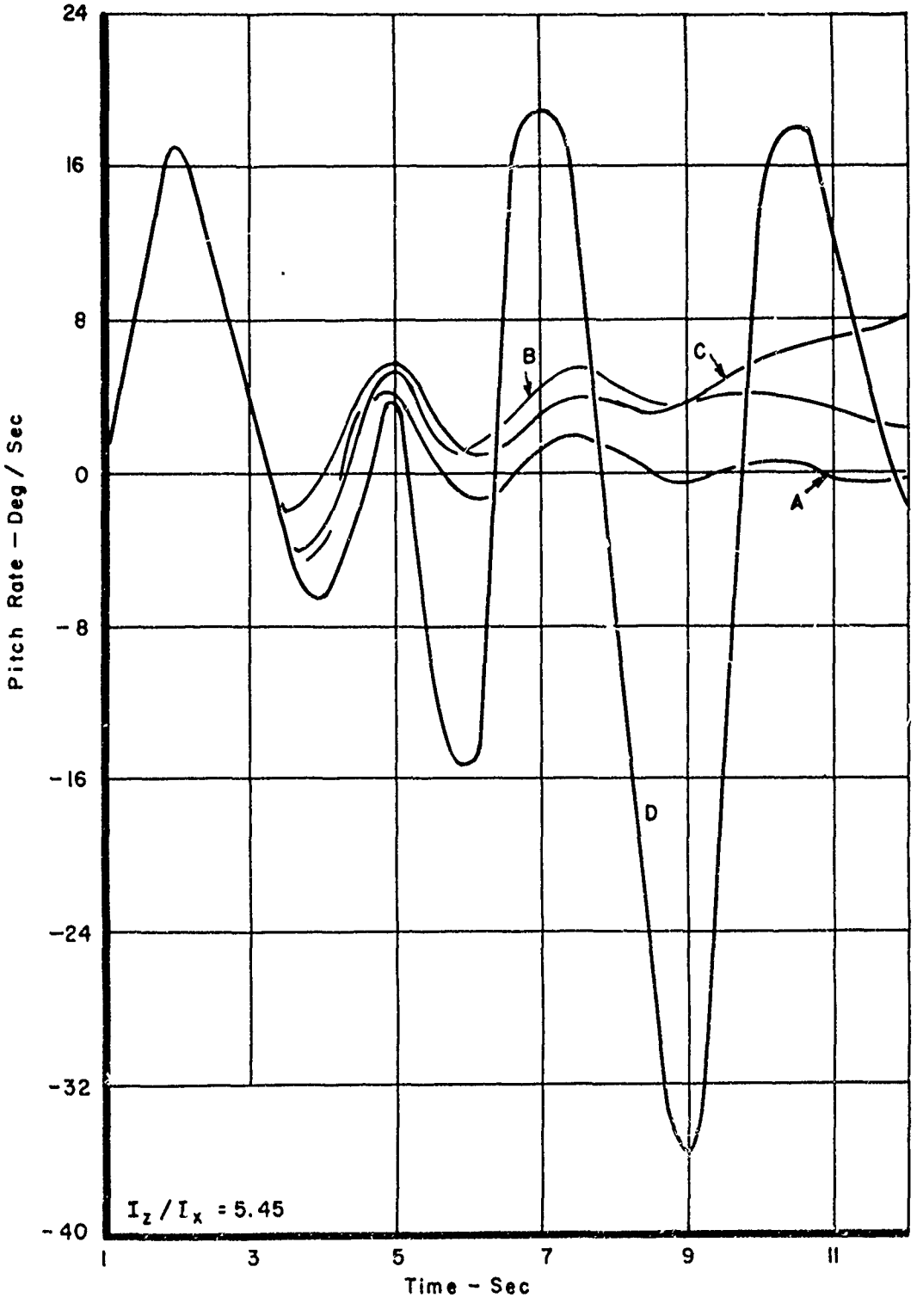

Figure 6. Pitch Rate vs Time

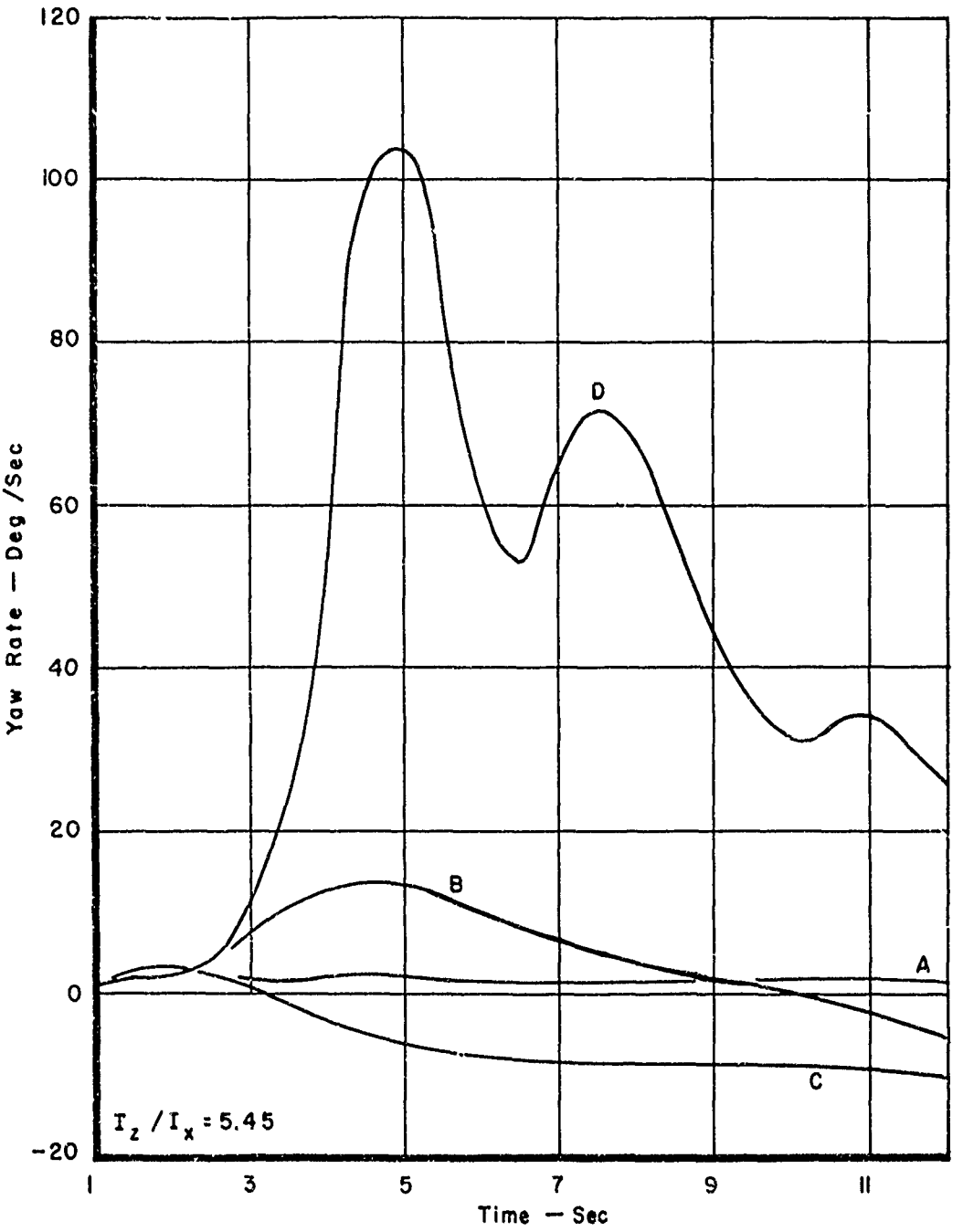

Figure 7. Yaw Rate vs Time

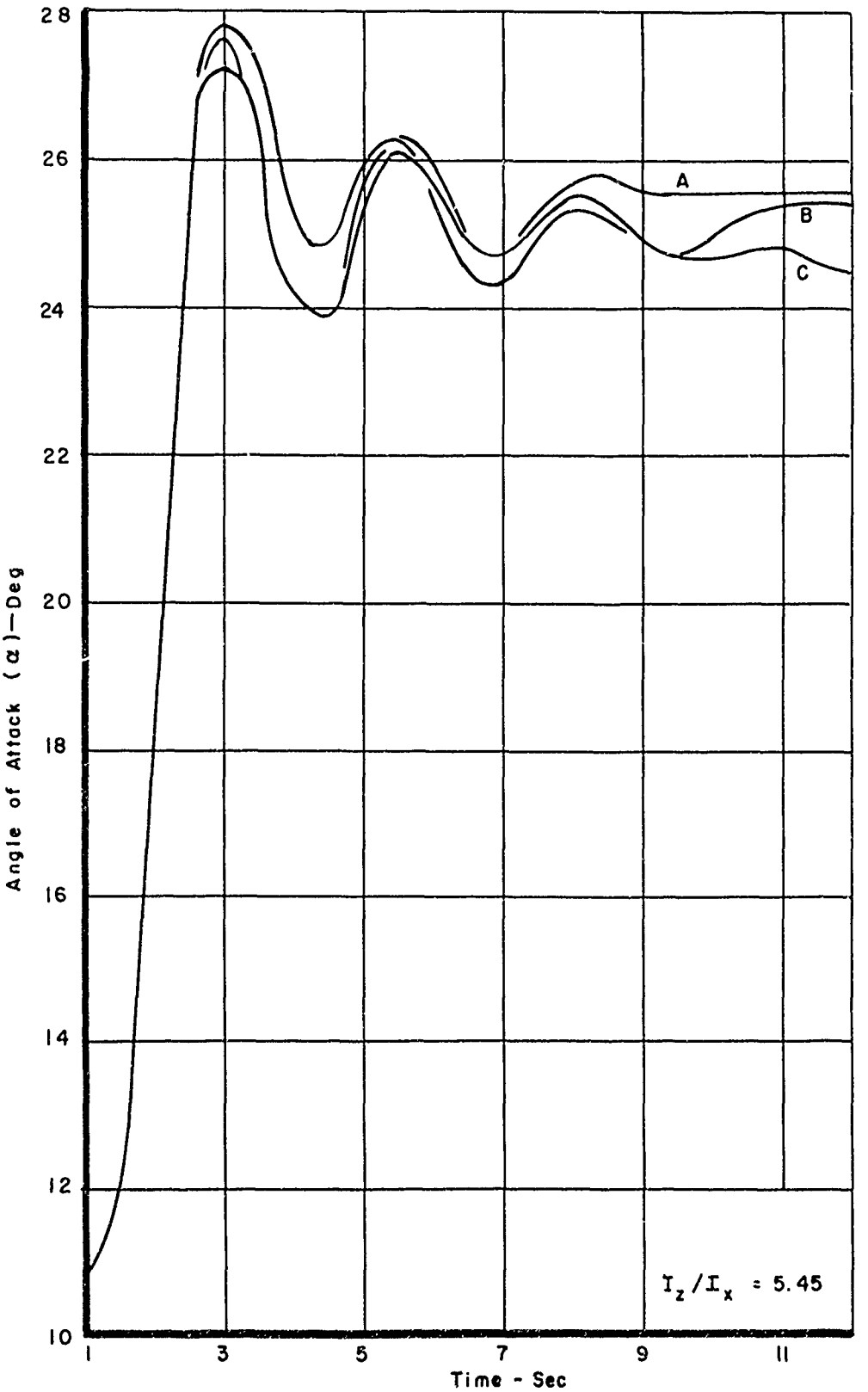

Figure 8. Angle of Attack vs Time

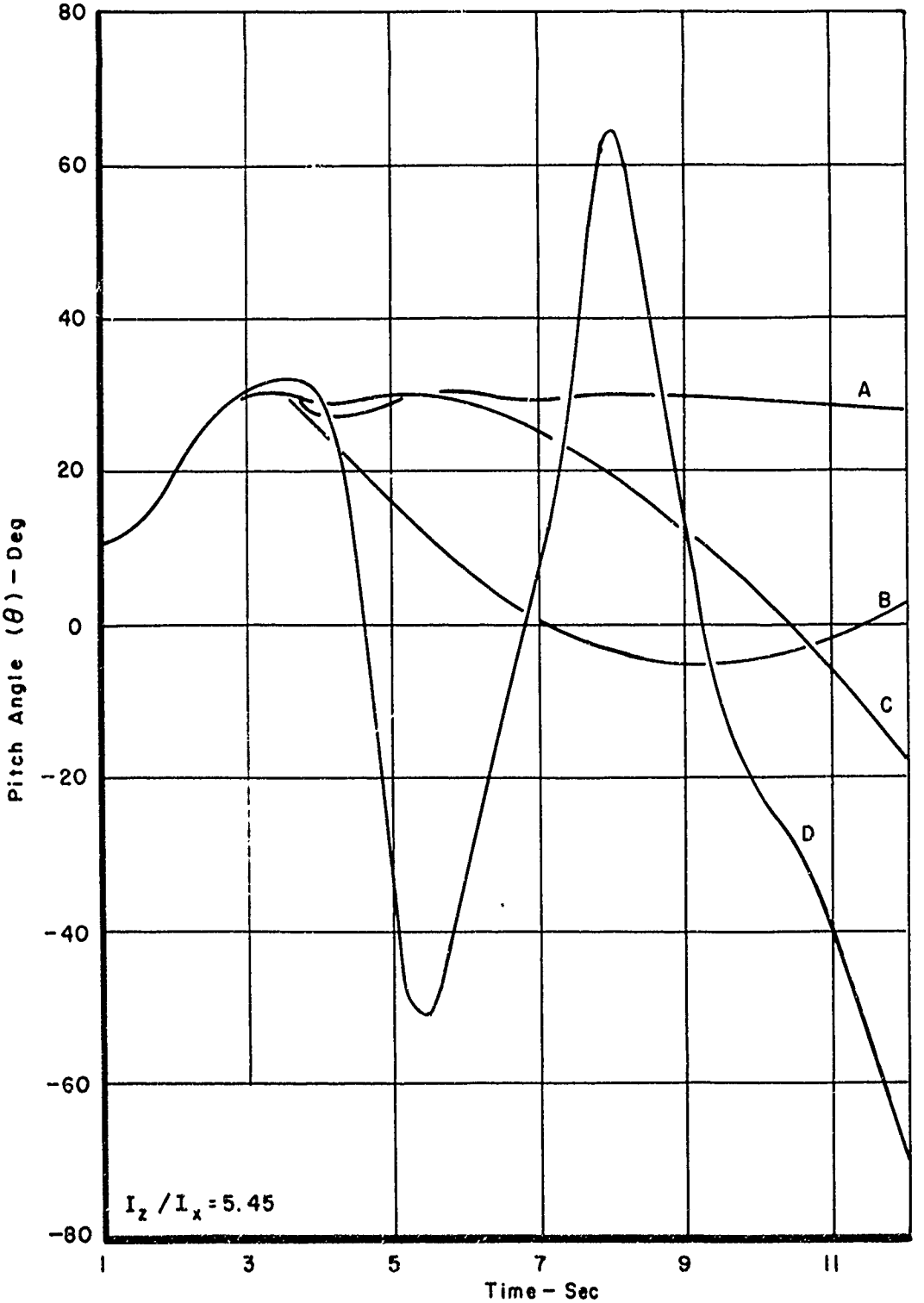

Figure 9. Pitch Angle vs Time

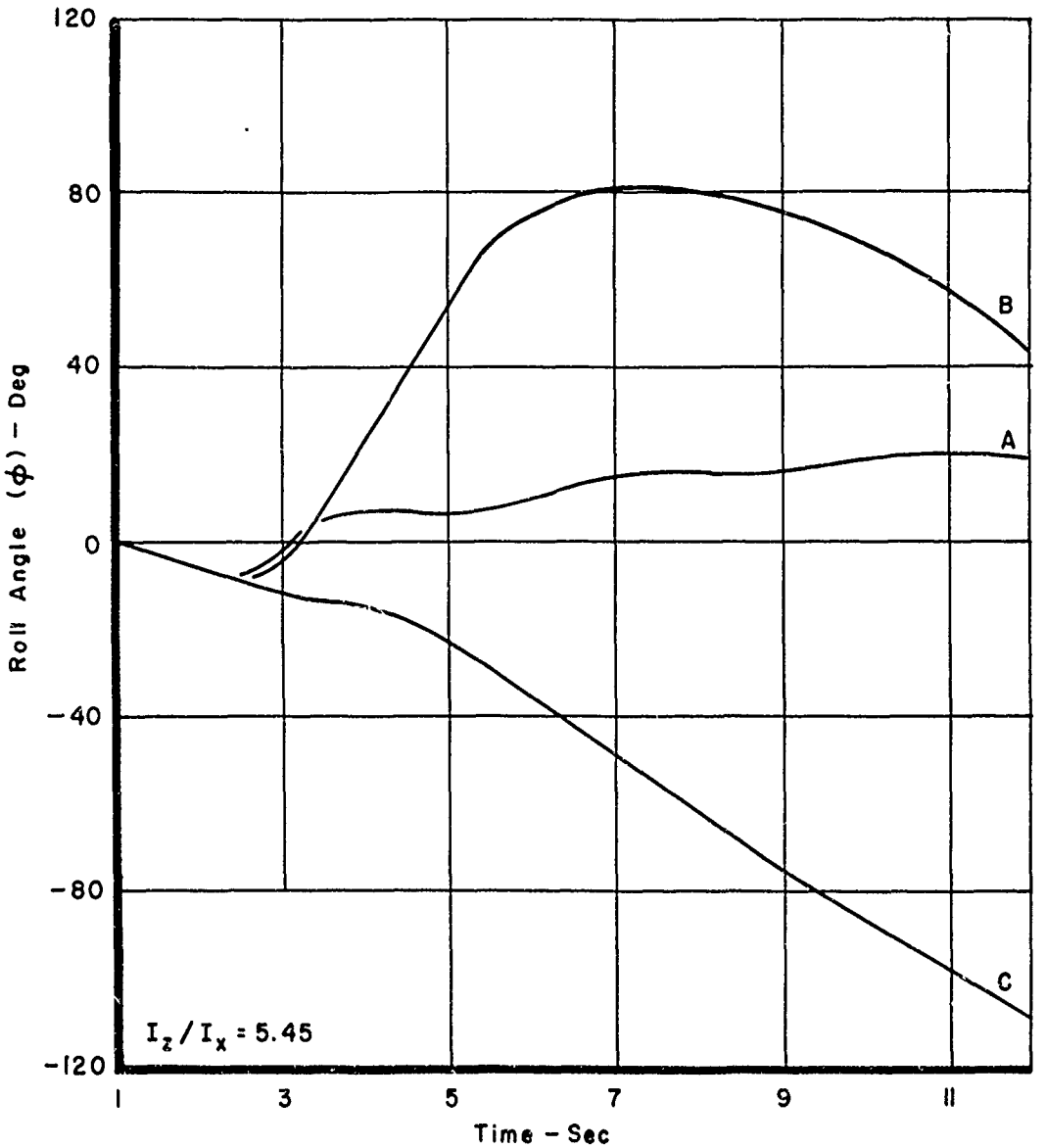

Figure 10. Roll Angle vs Time

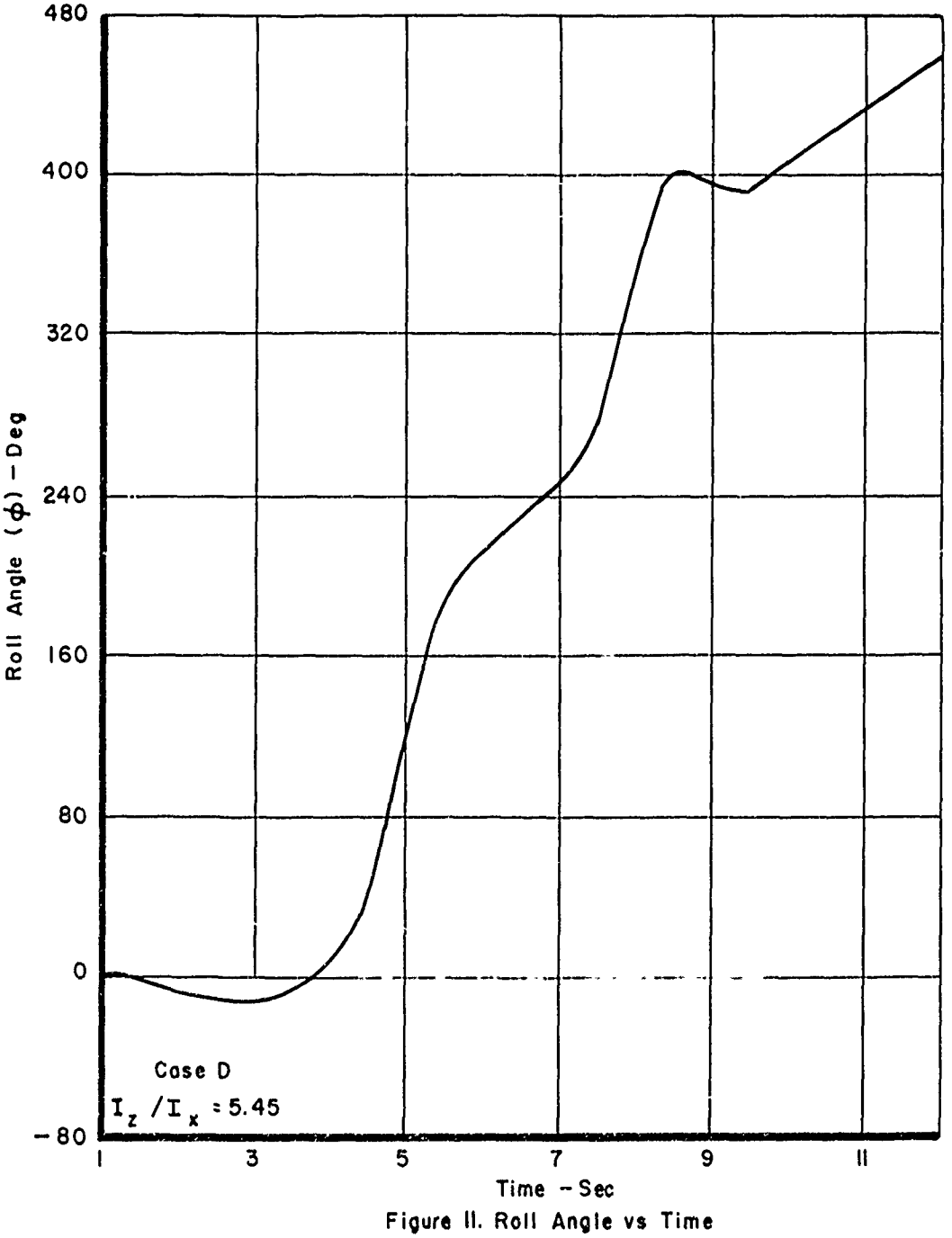

Figure II. Roll Angle vs Time

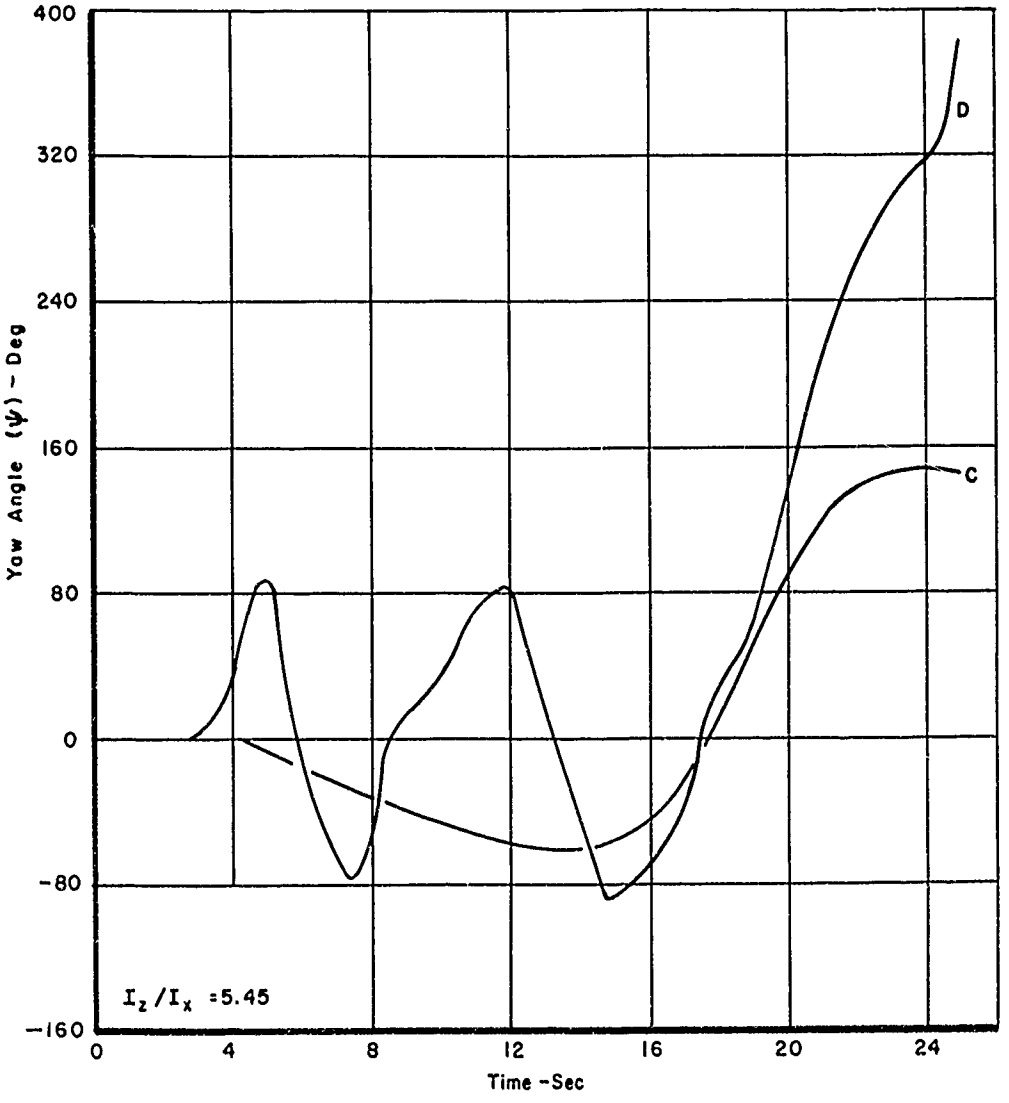

Figure 12. Yaw Angle vs Time

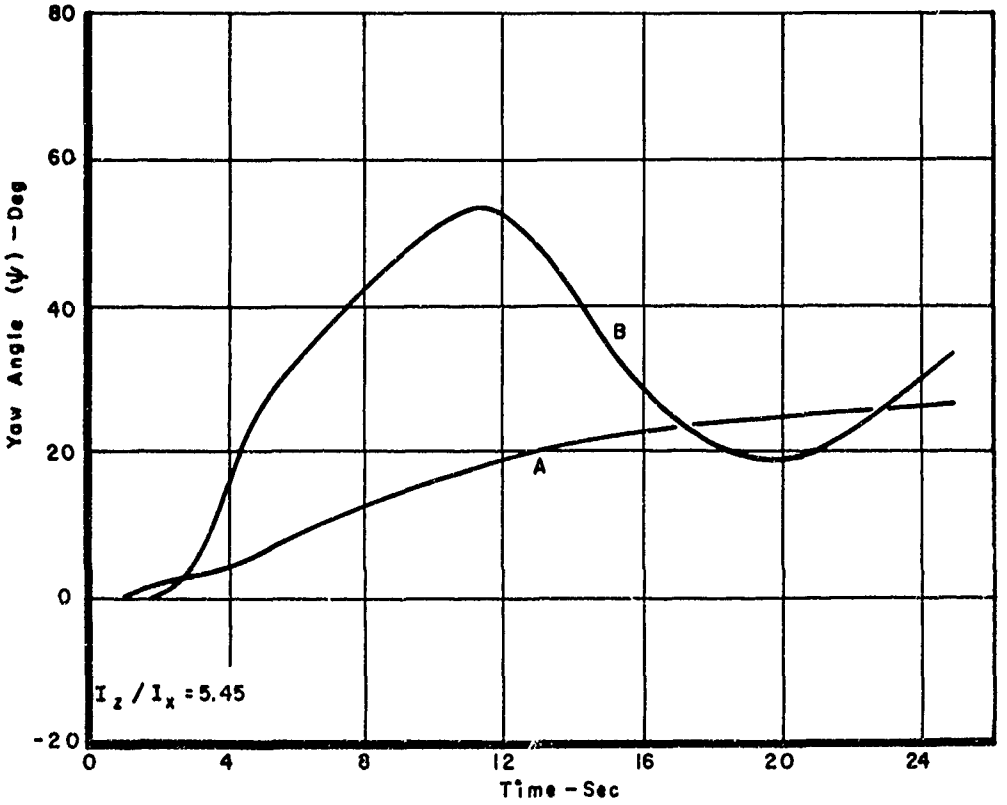

Figure 13 Yaw Angle vs Time

3. RESULTS OF ANALYSIS, AIRPLANE 2

A similar analysis was conducted on an airplane whose I_z/I_x equals 17.7 (airplane 2) for the same four cases. The same general conclusions can be drawn regarding the use of $C_{n\beta,dynamic}$ to predict spin susceptibility and the importance of effective dihedral (Figures 14 through 25). Case D is considered to be spin susceptible because of the rapid increase of sideslip angle (Figure 14) at near-stall angles of attack together with an appreciable yaw rate (Figure 20) and a corresponding increase in angle of attack (Figure 15). Figure 16 shows that the parameter $C_{n\beta,dynamic}$ is a large negative value at an angle of attack of 25.7 degrees where an abrupt divergence occurs (6.0 seconds). However, there are significant differences in the computed motion between airplanes 1 and 2. The time histories of sideslip and yaw angle for case D show a "gradual" divergence over the first 5 seconds and then an abrupt divergence in sideslip to about 20 degrees in the next 1.5 seconds (Figures 15 and 25). Airplane 1 begins an abrupt divergence within 1.5 seconds and initially peaks to approximately 45 degrees in the next 2.0 seconds (Figure 2). This abrupt divergence occurs at an angle of attack of approximately 24.5 degrees (at 2.5 seconds) while the abrupt divergence for airplane 2 occurs at an angle of attack of about 25.7 degrees (at 6.0 seconds). The motion is in general less oscillatory and less severe for airplane 2. A full turn in yaw was not achieved and the change in roll angle did not exceed 360° for the first 12 seconds. Nevertheless, the post stall gyration shown in Figures 14 through 25 for case D can be considered conducive to spin.

Figure 16 shows $C_{n\beta,dynamic}$ plotted versus angle of attack. The

curve for case C indicates a negative $C_{n\beta,dynamic}$ over a small range of angle of attack. The corresponding time history of sideslip angle (Figure 14) shows an increase in sideslip initially peaking to about 3 degrees and then rapidly diminishing. This further illustrates the fact that $C_{n\beta,dynamic}$ will be in the order of -0.003 per degree when a directional divergence occurs at near-stall angles of attack as indicated by the curve for case D and the corresponding time history of sideslip angle. It should also be noted that for the same case (i.e., case C) the peak magnitude in sideslip angle is less, by about 2 degrees, for airplane 2,as compared to airplane 1 (Figure 1). In fact, the sideslip excursions for airplane 2 are of smaller magnitude and well damped as compared to the sideslip excursions for airplane 1.

It is worth noting again that for the case where directional divergence occurs (case D) the variation of the directional stability derivative with angle of attack is unstable for angles of attack above 20.6 degrees. Based on this, an airplane would be expected to experience a directional divergence at an angle of attack close to 20.6 degrees. However, under dynamic flight conditions the divergence for airplane 1 occurs at 24.5 degrees and at 25.7 degrees for airplane 2.

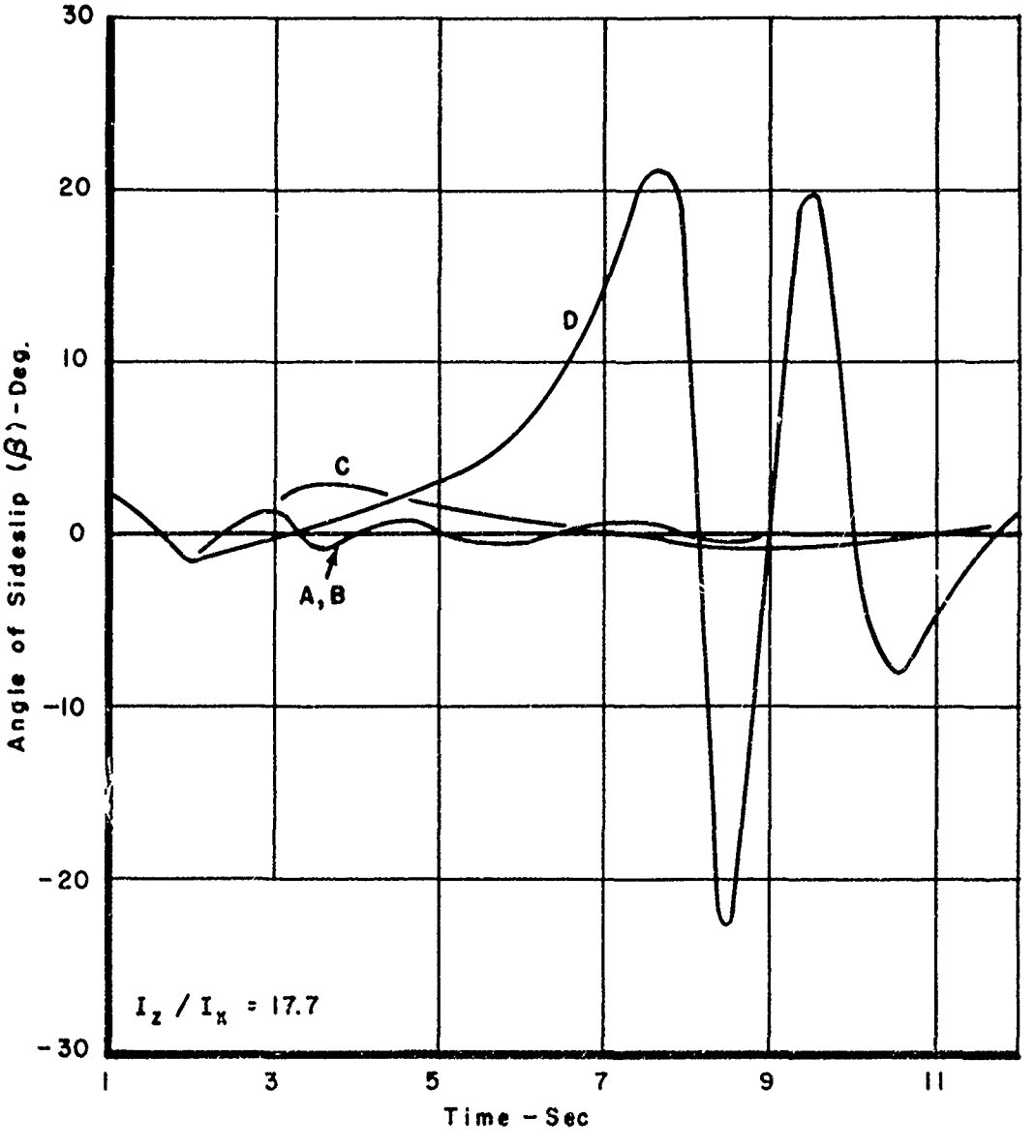

Figure 14. Angle of Sideslip vs Time

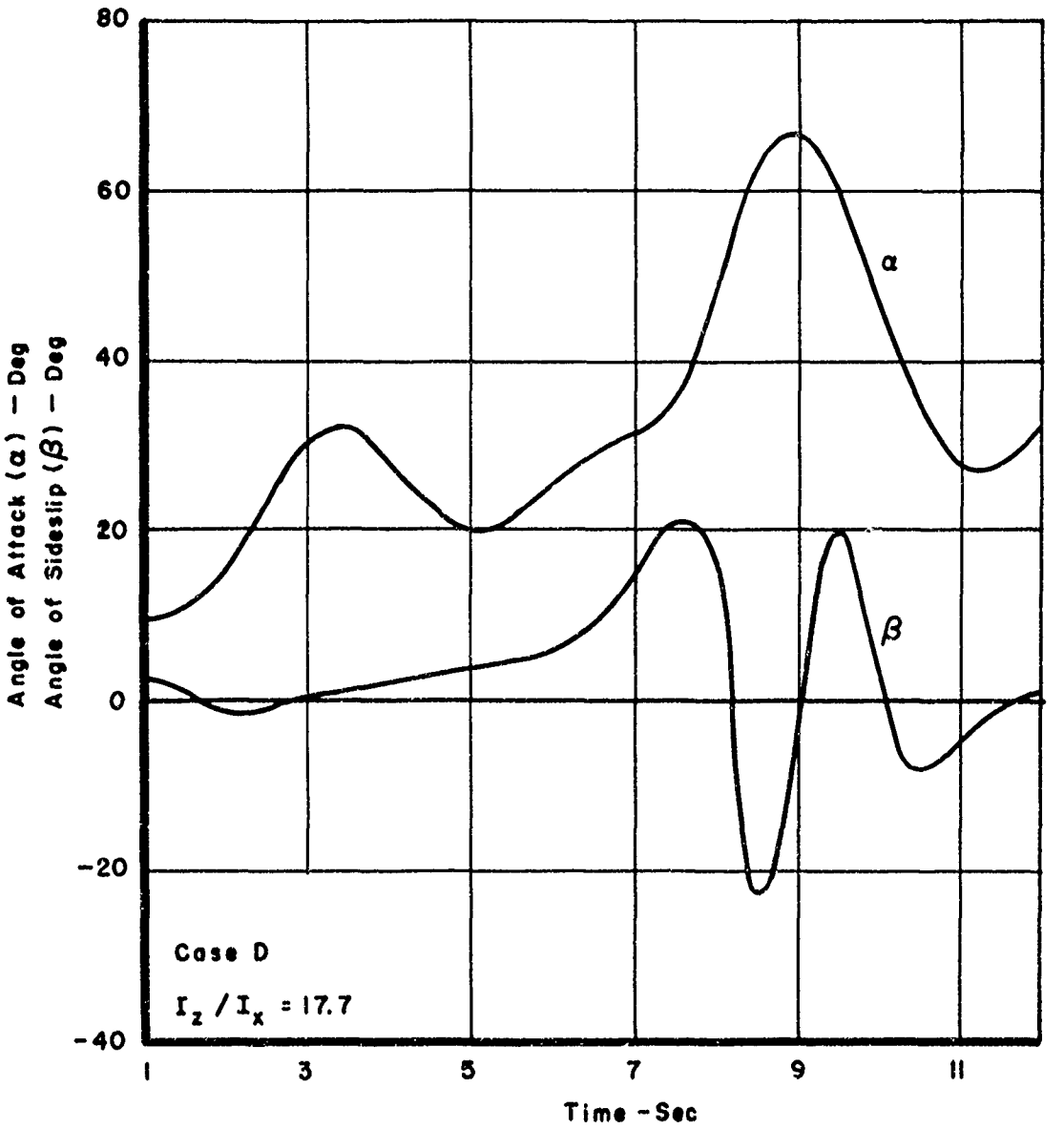

Figure 15. Angle of Attack, Sideslip vs Time

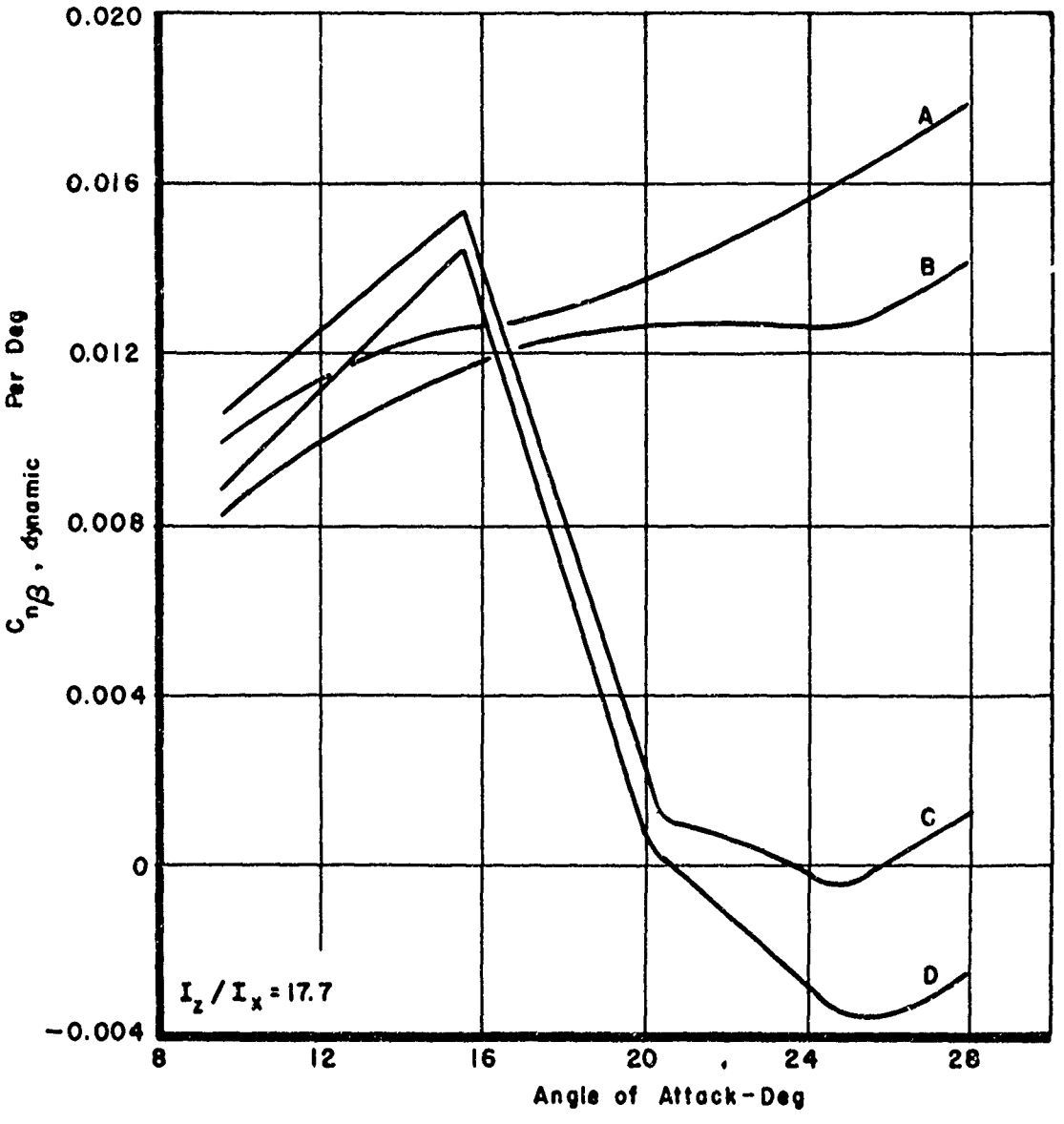

Figure 16. $C_{n_\beta, \text{dynamic}}$ vs Angle of Attack

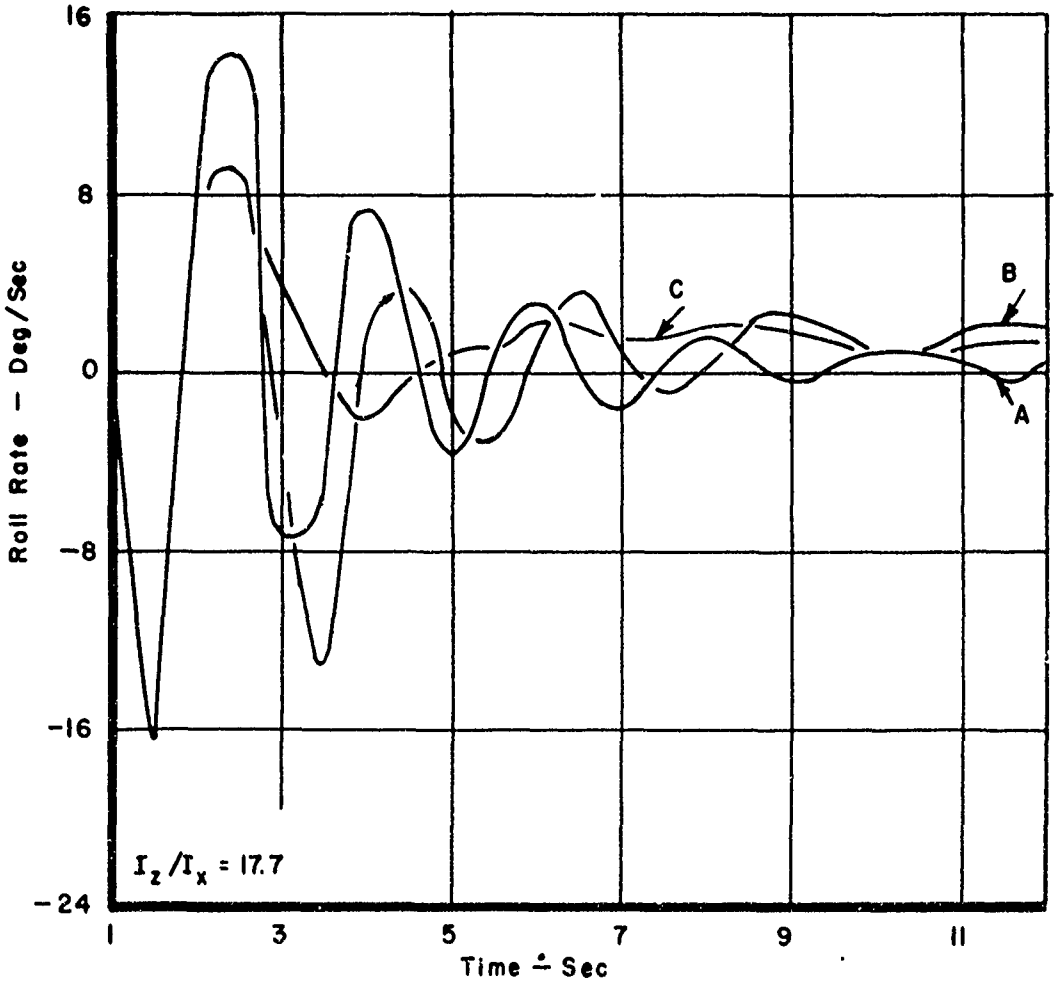

Figure 17. Roll Rate vs Time

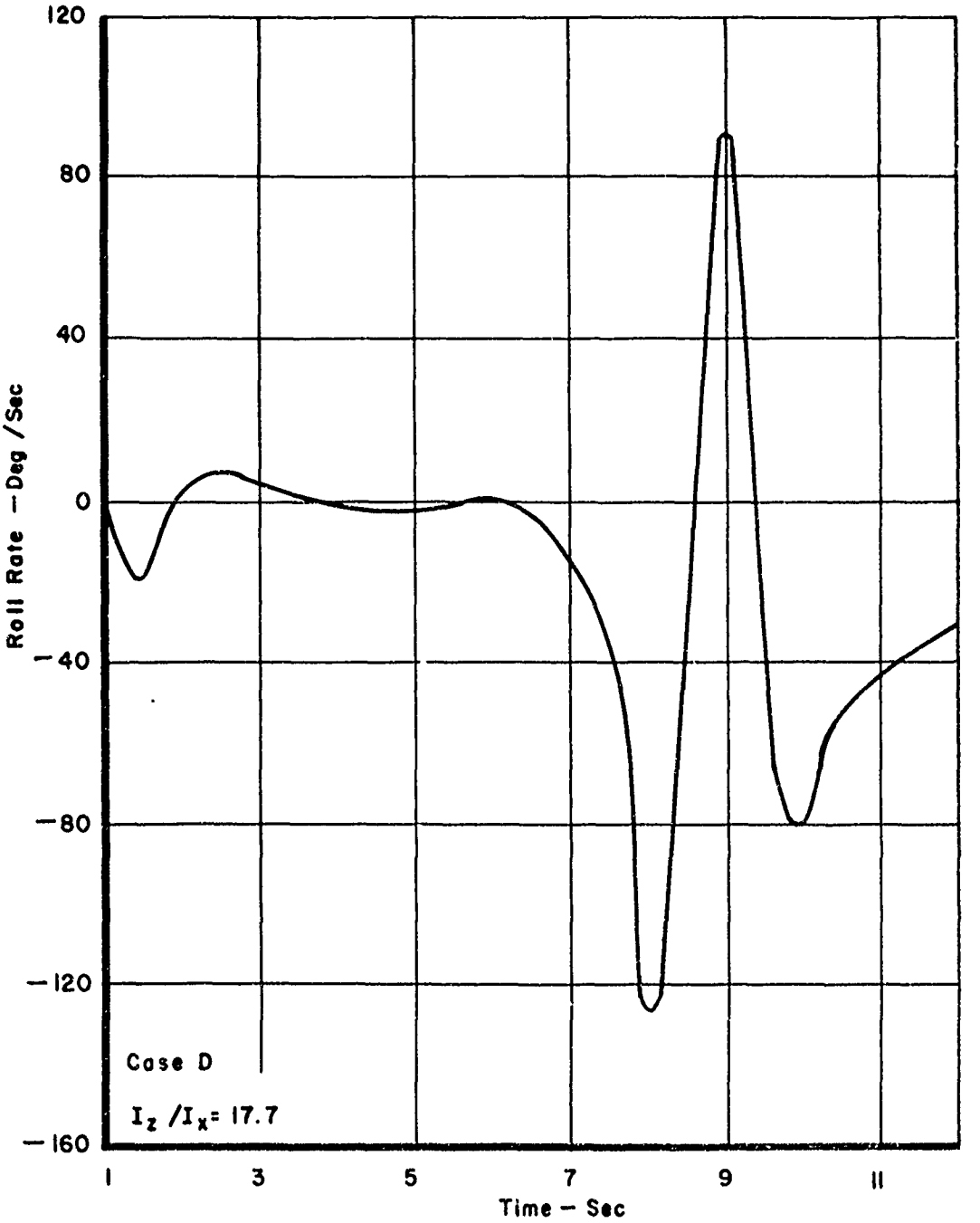

Figure 18. Roll Rate vs Time

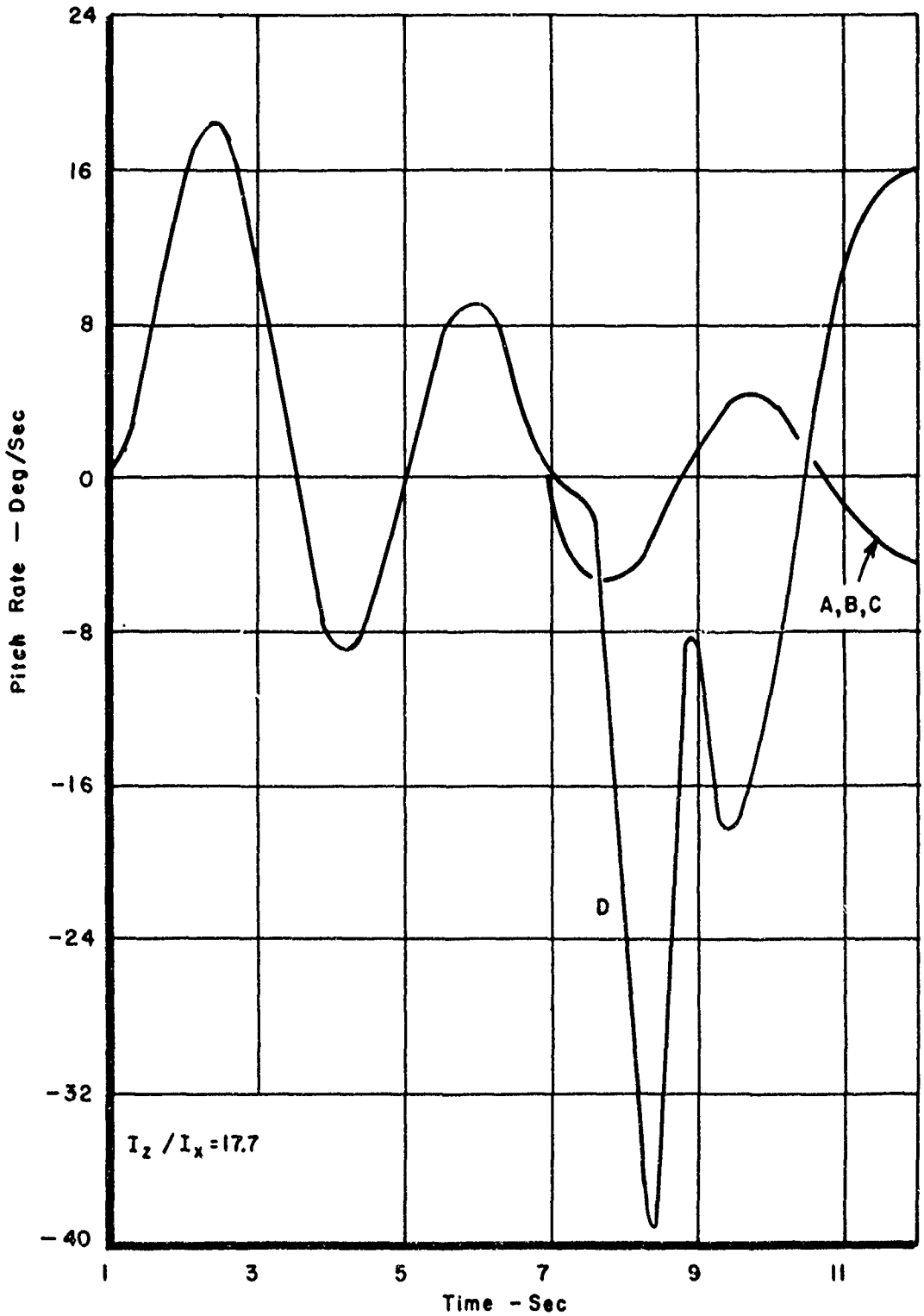

Figure 19 Pitch Rate vs Time

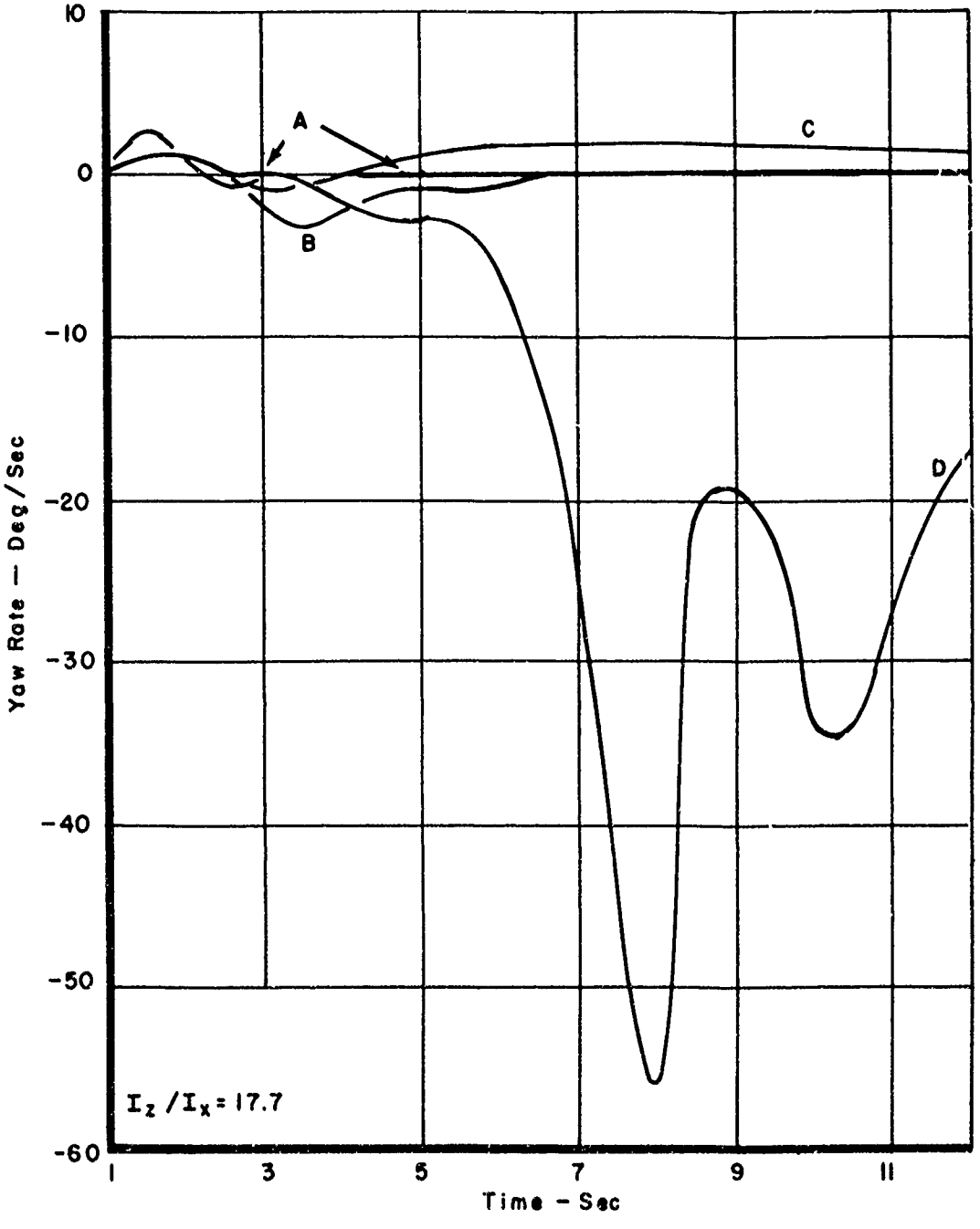

Figure 20. Yaw Rate vs Time

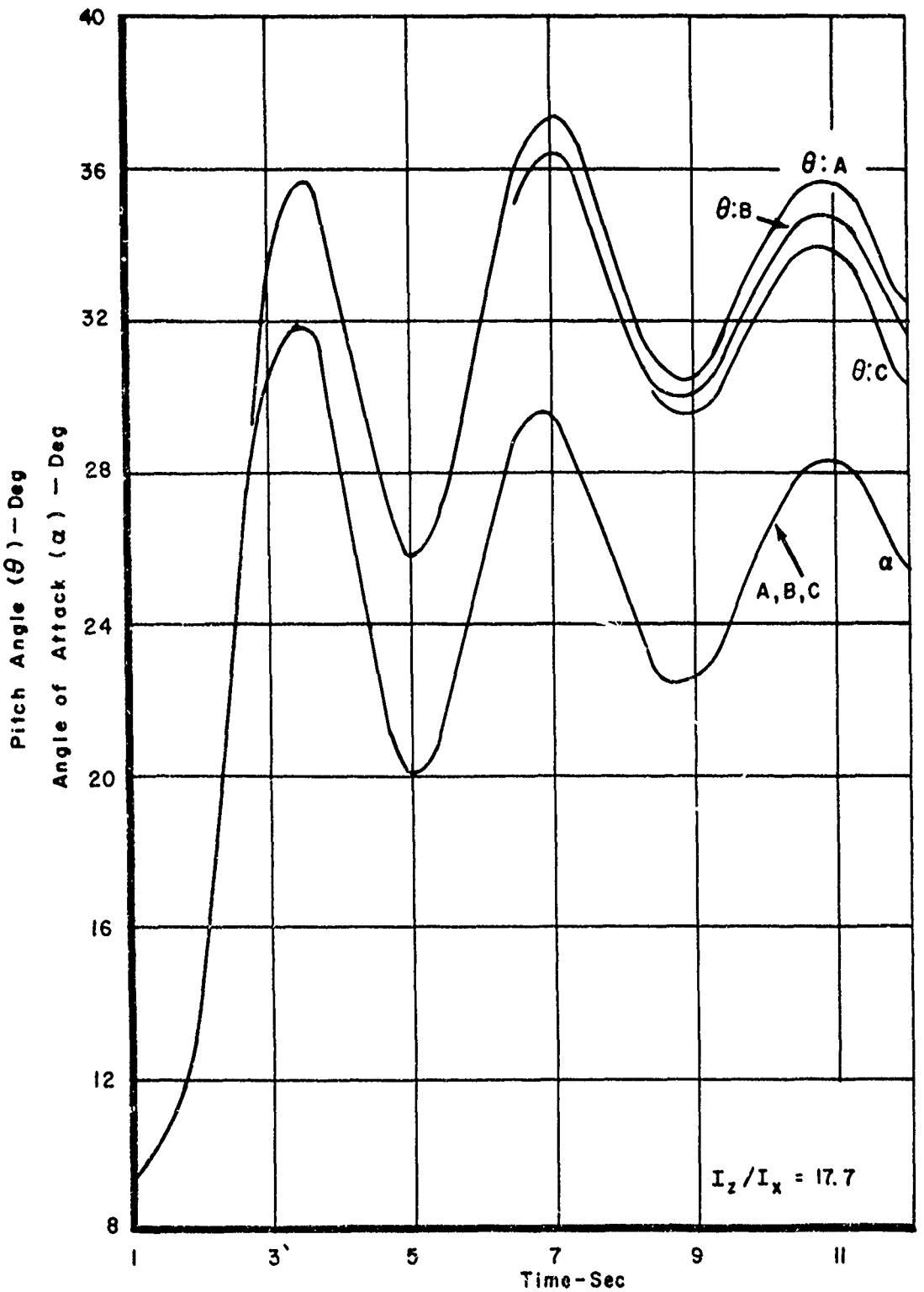

Figure 21. Angle of Attack, Pitch Angle vs Time

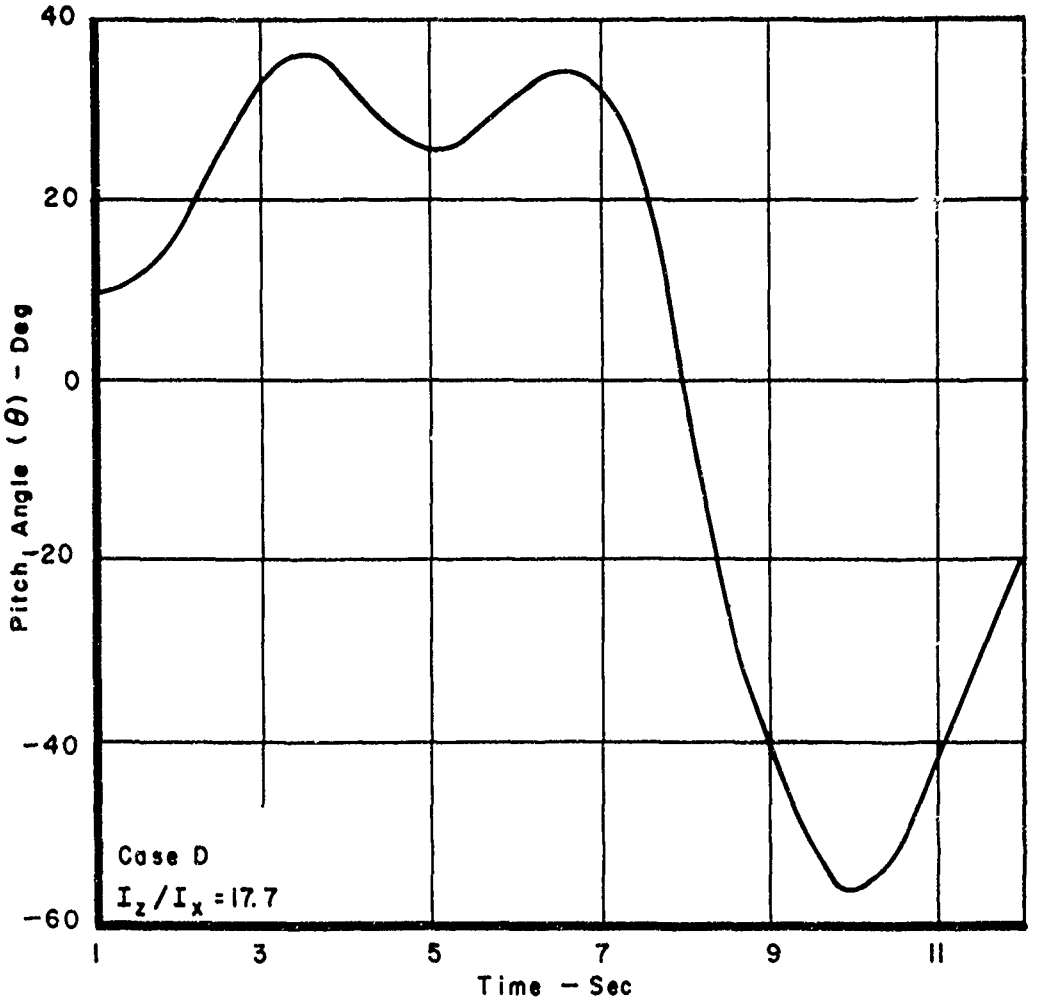

Figure 22. Pitch Angle vs Time

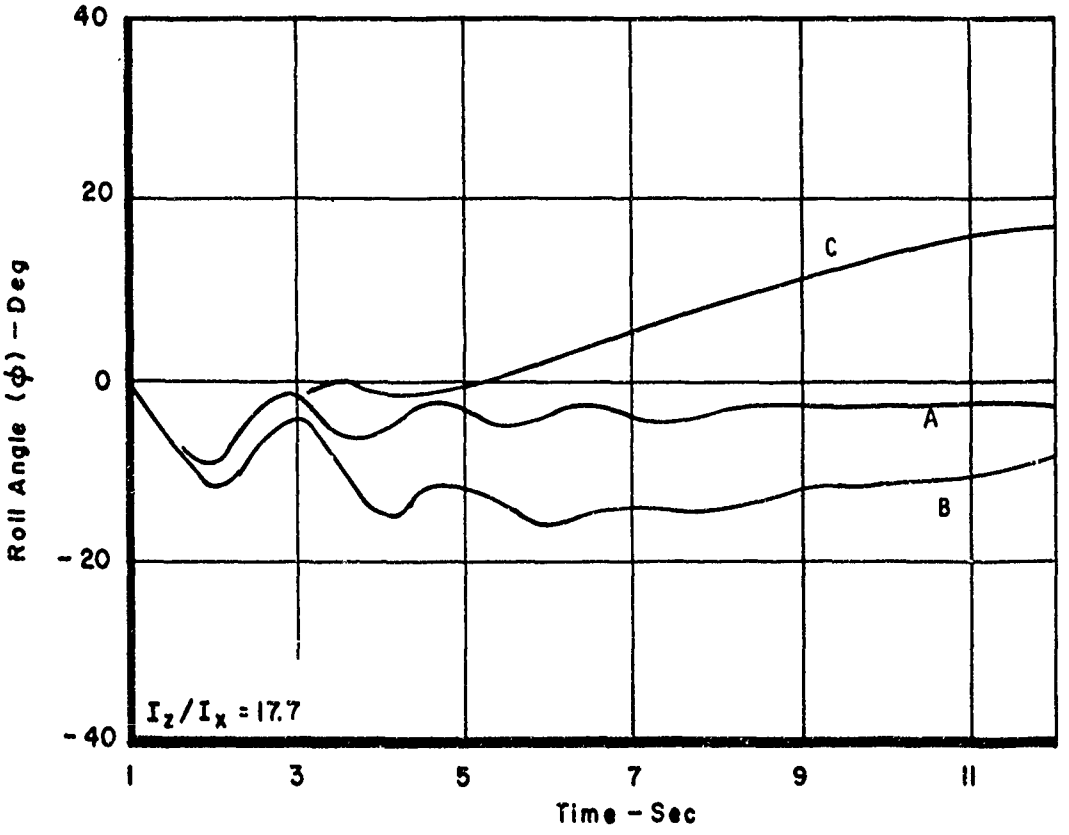

Figure 23. Roll Angle vs Time

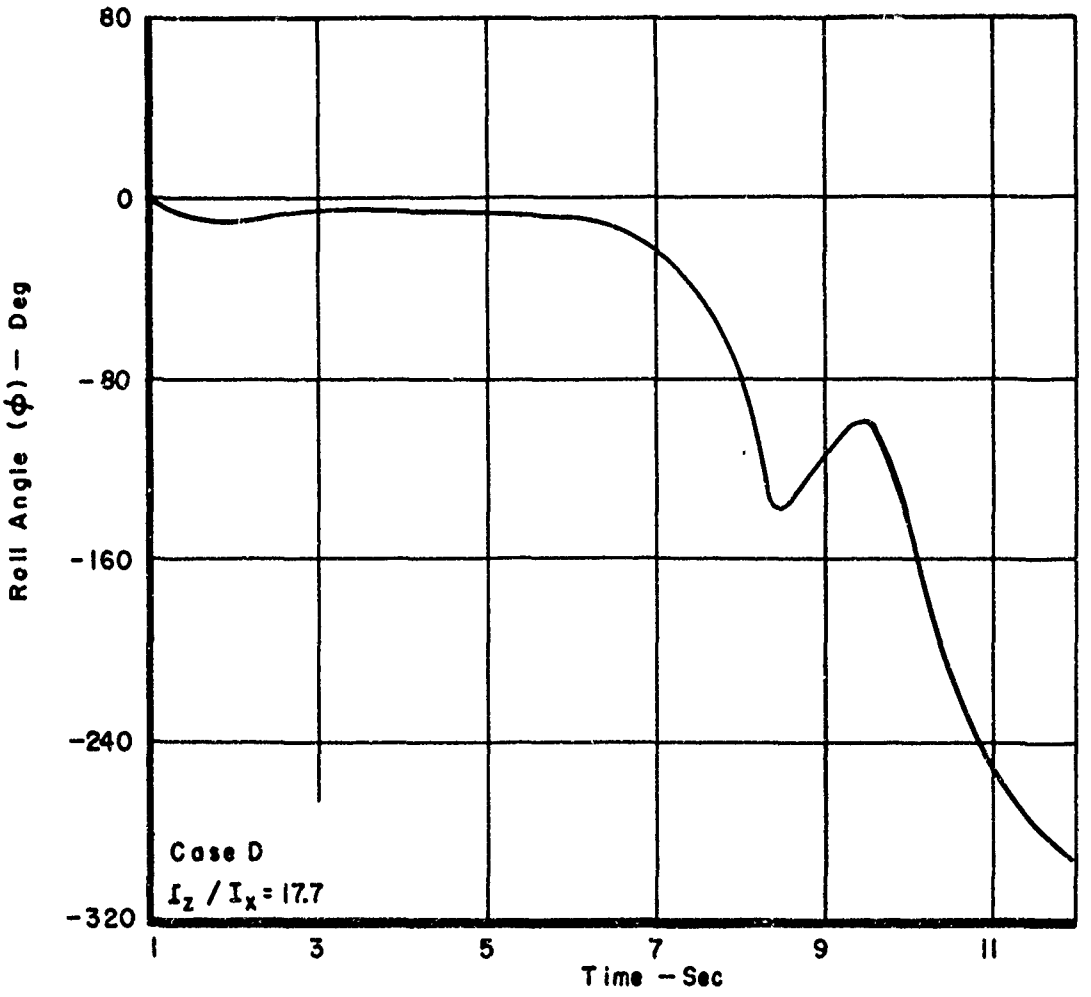

Figure 24. Roll Angle vs Time

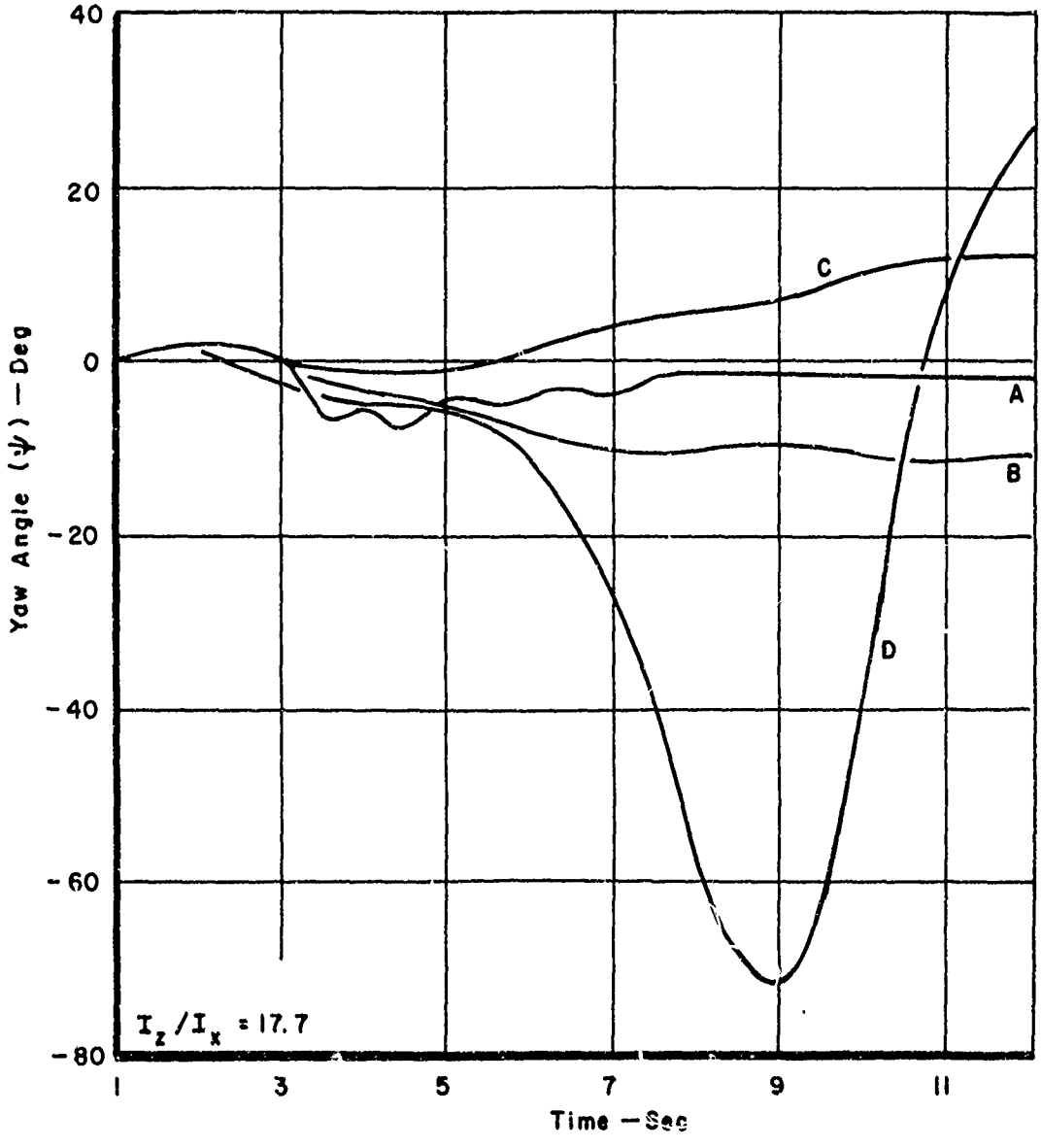

Figure 25. Yaw Angle vs Time

SECTION IV

AILERON-LONE DIVERGENCE PARAMETER FOR PREDICTING SPIN SUSCEPTIBILITY

1. METHOD OF ANALYSIS

The six degree of freedom analyses is repeated for the four aerodynamic cases and the two sets of mass characteristics listed in Tables I and II, respectively. In addition, the effect of pitching moment on spin susceptibility is investigated.

The airplane is initially trimmed at angles of attack of 22, 23, 24, 25, 27, and 30 degrees at an altitude of 30,000 feet. At each angle of attack and for each case, a lateral control surface deflection (δ_a) of 30 degrees (right stick) is applied at a rate of 20 degrees per second and maintained. The effects of both adverse and proverse yaw due to lateral control deflection (Appendix II, Figure 47) on spin susceptibility is considered for each aerodynamic case and at each angle of attack as is the effect of pitching moment (Appendix II, Figure 45).

Now, depending upon the aerodynamic case (A, B, C, or D), each angle of attack represents a degree of lateral-directional stability or instability. Since the values of $C_{n\beta,dynamic}$ and the aileron-alone divergence parameter are functions of angle of attack, the values of these parameters at the initial trim angles of attack are used to determine their utility as criteria for predicting spin susceptibility.

2. RESULTS OF ANALYSIS, AIRPLANE 1

Case D: An example of the motion obtained for airplane 1, case D, following a lateral control deflection, is shown in Figures 26 through 29. Although these time histories represent the effect of lateral control input at an initial trim angle of attack of 27 degrees and adverse yaw, this type of motion is representative for angles of attack above 23 degrees, for proverse yaw as well as adverse yaw, and regardless of pitching moment

characteristics.

Figures 26 through 29 represent a steep left oscillatory spin which completes about 5.8 turns in 40 seconds (Figure 28). The airplane initially diverges in yaw to the left at about 3 seconds and in roll at about 3 seconds. Note that the roll divergence is opposite to the roll command (right stick), in the same direction as the yaw, and that when the airplane completes about one roll to the left and begins oscillating (Figure 29) the motion consists primarily of yaw.

The values of $C_{n\beta,dynamic}$ and the aileron-alone divergence parameter at the trim angles of attack investigated for all four cases are shown in Figures 30 and 31. Figure 30 represents adverse yaw and Figure 31 represents proverse yaw. The case D points are shown in the lower left hand quadrant (negative $C_{n\beta,dynamic}$ and aileron-alone divergence parameter) and are identified for each trim angle of attack.

Referring to Figure 30, at angles of attack above 23 degrees, spins are obtained following a lateral control input and as previously noted the motion is similar to that shown in Figures 26 through 29. At 23 degrees angle of attack, the airplane has a strong tendency to spin to the left but will not sustain large average values of angle of attack and yaw rates. At 22 degrees angle of attack following a lateral control input the airplane pitches nose down and exhibits severe oscillations about all three axes with no significant increase in angle of attack or yaw rate.

In general, the area within the dashed lines shown in Figure 30 represents a region of spin susceptibility with case D lateral-directional stability characteristics. Furthermore, there is no significant difference due to the variation in pitching moment shown in Figure 45.

Case B: Case B points with adverse yaw are shown in the lower right hand quadrant of Figure 30. Unlike Case D, Case B represents an airplane

with appreciable positive effective dihedral at near-stall angles of attack (Figure 41). Both cases are directionally unstable at near-stall angles of attack.

An airplane with case B lateral-directional stability characteristics will not be spin susceptible below 27 degrees angle of attack with the basic pitching moment. However, with decreased longitudinal stability the case B airplane will readily spin at angles of attack below 27 degrees. The motion is similar to that shown in Figures 26 through 29 but the spin is less oscillatory and quickly stabilizes.

Dashed lines are shown originating from the 22 and 27 degree angle of attack points. The area bounded by the horizontal dashed lines at 22 and 27 degrees angle of attack and by the vertical dashed line represents a region of spin susceptibility dependent upon the variation in pitching moment. At an angle of attack of 27 and 30 degrees, the airplane is spin susceptible regardless of the variation in pitching moment.

It appears that appreciable values of positive effective dihedral will compensate to some extent for a lack of directional stability at near-stall angles of attack. As pointed out earlier, the only difference between cases D and B is that the latter case represents an airplane with appreciable positive effective dihedral at near-stall angles of attack. However, the variation in pitching moment is important and can become an overriding factor particularly at the lower angles of attack (22 through 25 degrees). At the higher angles of attack (27 and 30 degrees) and with the directional stability characteristics of case B (i.e., increasing instability with angle of attack), the degree of directional instability is the primary factor regarding spin susceptibility.

Case C: All but one of the case C points with adverse yaw are shown

in the upper right hand quadrant of Figure 30. Case C represents a directionally stable airplane up to 37.5 degrees angle of attack and very little effective dihedral at near-stall angles of attack, ranging from slightly negative to slightly positive.

The motion exhibited by case C with adverse yaw is primarily a rolling motion with no tendency to spin and the variation in pitching moment shown in Figure 45 has no significant effect on the motion. Apparently the directionally stable case C airplane is not particularly bothered by poor effective dihedral characteristics within the constraints of this analysis.

Case A: The case A points with adverse yaw are shown in the lower right hand quadrant of Figure 30. The motion following lateral control inputs at any of the trim angles of attack is primarily roll, like case C, and again the variation in pitching moment has no significant effect. However, sideslip angle buildup is less, and consequently the number of rolls in a given time interval is generally less for case A. Case A represents an airplane whose lateral-directional stability characteristics are considered excellent at near-stall angles of attack.

It is of interest to compare the results obtained between cases A and B. Both cases have the same positive effective dihedral characteristics but, as noted previously, case B represents a directionally unstable airplane at near-stall angles of attack. It is apparent that if an airplane is to have satisfactory high angle of attack characteristics, that is, not spin susceptible at near-stall angles of attack, a requirement for maintaining directional stability at these angles of attack is essential. If this is not possible, then maintaining an appreciable amount of positive effective dihedral at near-stall angles of attack is absolutely essential.

Figure 31 shows the results of the analyses for all four cases with proverse yaw. A region of spin susceptibility is identified for case D which is independent of the variation in pitching moment. Cases A, B, and C are shown in the upper right hand quadrant. The motion exhibited for these three cases with proverse yaw is well-behaved with no tendency to spin, regardless of the variation in pitching moment. In general, proverse yaw appears to be preferable to adverse yaw regarding spin susceptibility except for an airplane whose lateral-directional stability characteristics are like Case D.

3. RESULTS OF ANALYSIS, AIRPLANE 2

Case D: Figures 32 through 35 show an example of the motion obtained for airplane 2, case D, and represent the effect of lateral control input at an initial trim angle of attack of 27 degrees, adverse yaw, and the basic pitching moment.

The steep left spin is similar to that obtained with airplane 1, case D. However, it is not as oscillatory, and stabilizes sooner. The airplane completes about one roll to the left, after which the motion consists primarily of yaw and about 4.6 turns are completed in 40 seconds.

The values of $C_{n\beta,dynamic}$ and the aileron-alone divergence parameter at the trim angles of attack are shown in Figures 36 and 37 for adverse and proverse yaw respectively. Like airplane 1, the case D points are in the lower left hand quadrant.

Referring to Figure 36, at angles of attack above 24 degrees the airplane is spin susceptible, and at 23 degrees the airplane motion shows no angle of attack or yaw rate increase. At 22 degrees angle of attack, there is no tendency to spin. The area within the dashed lines indicate a region of spin susceptibility for case D which is independent of the variation in pitching moment.

The difference between airplanes 1 and 2 is that the latter indicates a region of spin susceptibility beginning at a slightly higher angle of attack or alternatively, at a higher negative value of the aileron-alone divergence parameter. With proverse yaw, a comparison between Figures 31 and 37 show the same trend. However, both airplanes indicate a minimum negative value for $C_{n\beta,dynamic}$ of about 0.0016 per degree for adverse or proverse yaw. Regarding the effects of adverse and proverse yaw on airplane 2, Figure 37 shows that, with proverse yaw, the region of spin susceptibility starts at 25 degrees angle of attack with a value of approximately -0.0031 per degree for the aileron-alone divergence parameter.

The remaining cases for airplane 2, proverse as well as adverse yaw, indicate no tendency to spin, regardless of the variation in longitudinal stability. Regions of spin susceptibility for airplane 2 are identified only for case D. Since the primary difference between airplanes 1 and 2 is the inertial characteristics, it appears that an airplane with a large value of I_z/I_x will be less susceptible to spin at near-stall angles of attack than an airplane with a low value of I_z/I_x (Reference 4).

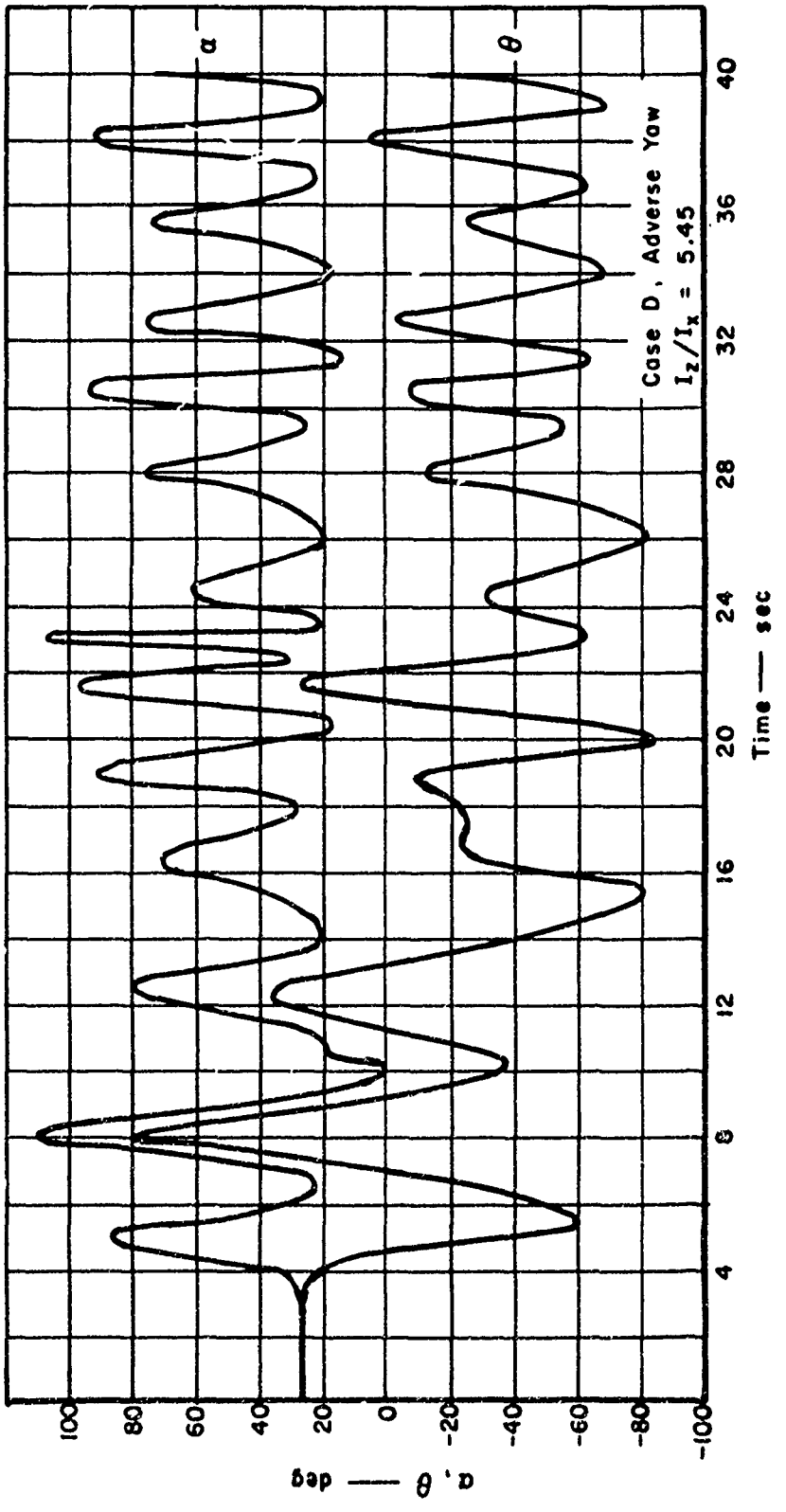

Figure 26. Angle of Attack, Pitch Angle vs Time

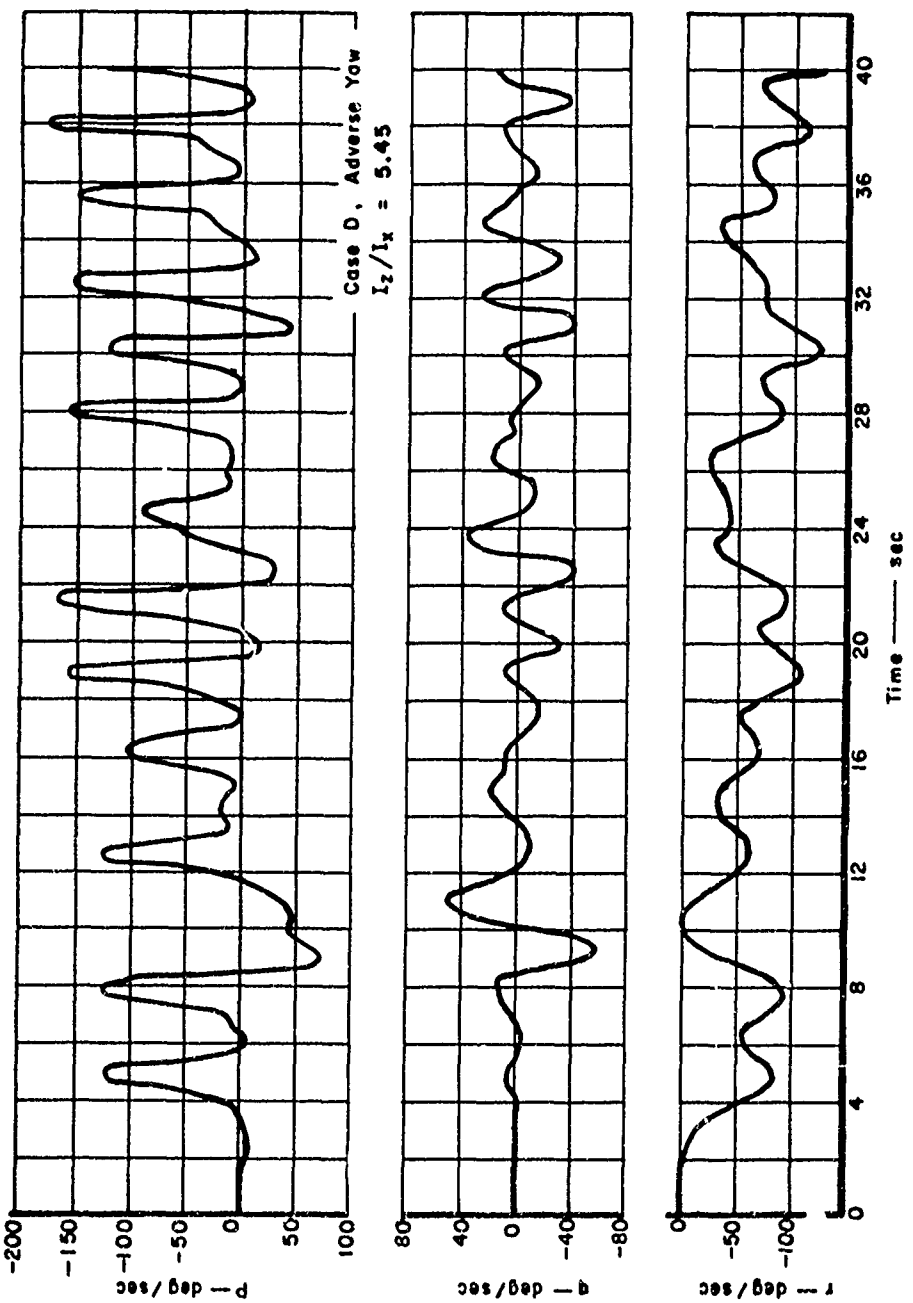

Figure 27. Roll, Pitch, Yaw Rates vs Time

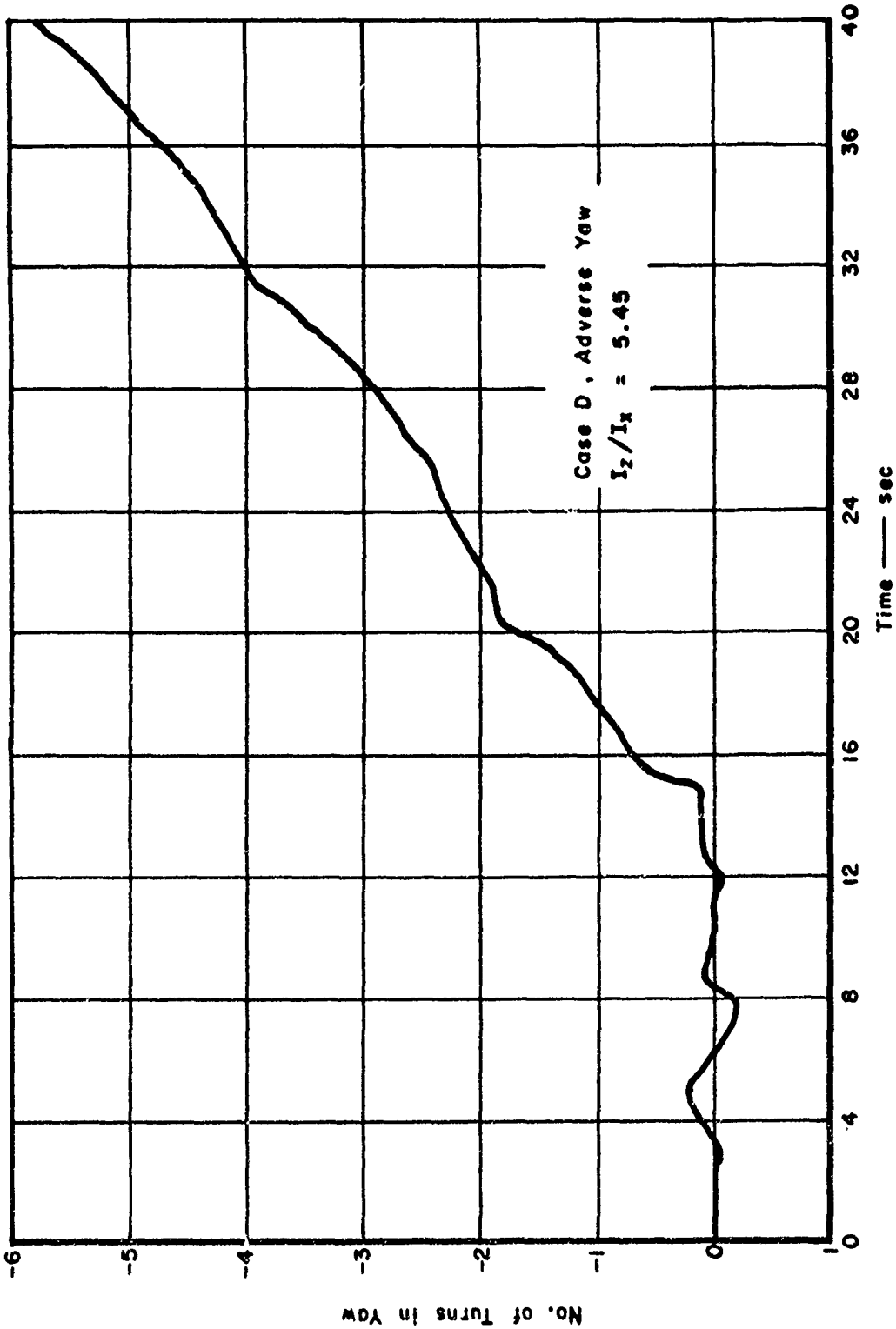

Figure 28. Number of Turns in Yaw vs Time

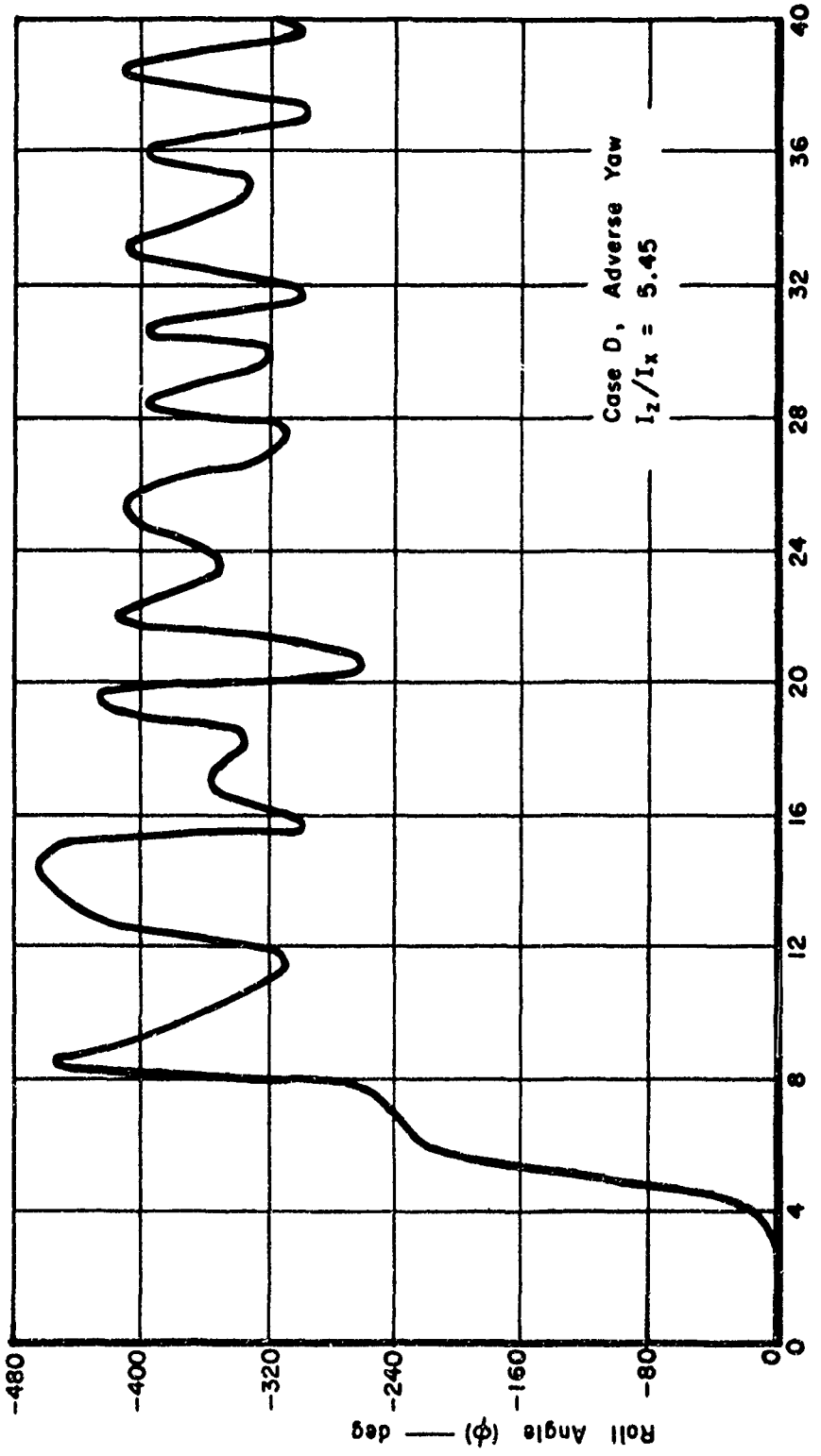

Figure 29. Roll Angle vs Time

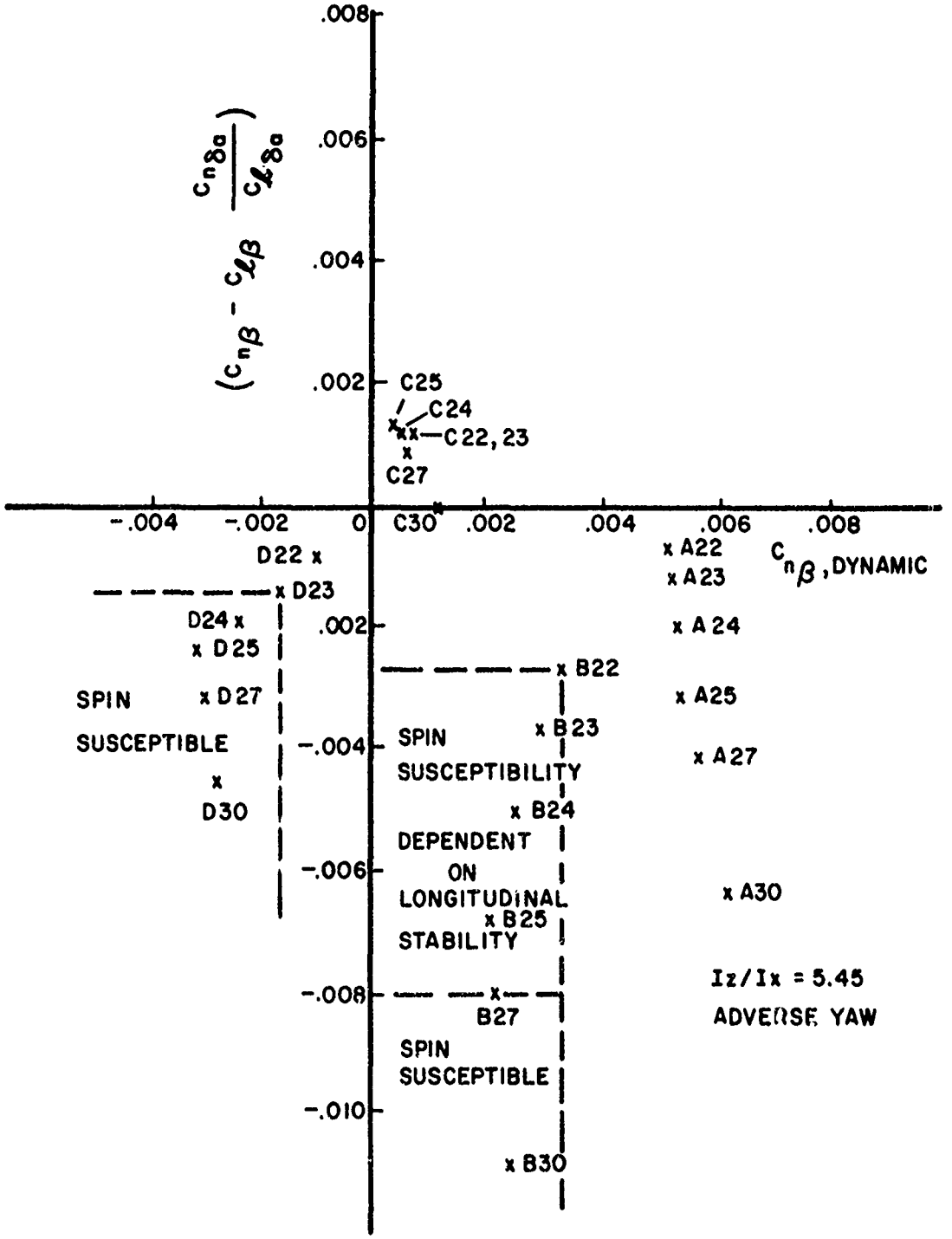

Figure 30. $C_{n\beta,\ dynamic}$ vs Aileron-Alone Divergence Parameter, Adverse Yaw-Airplane 1

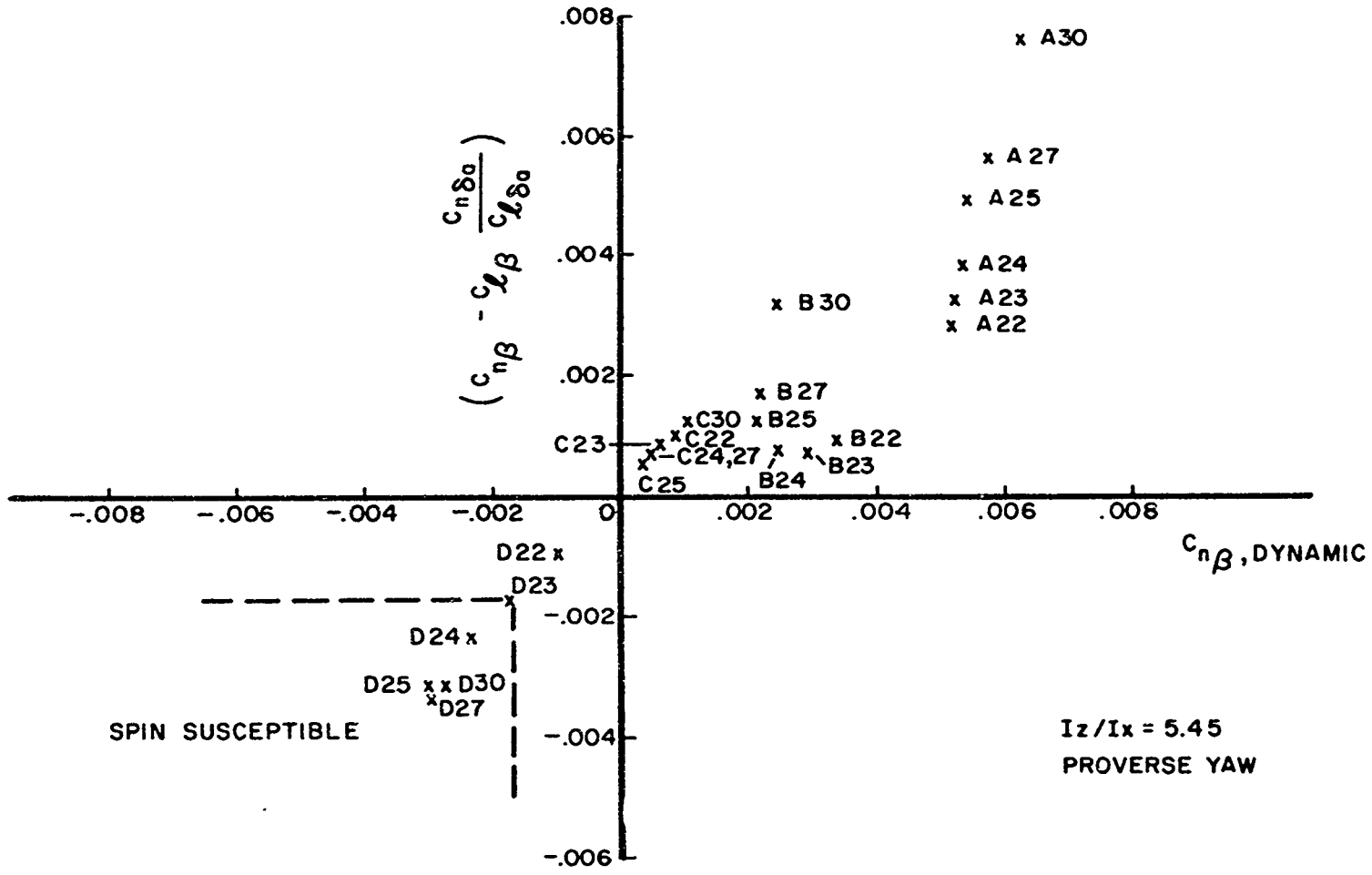

Figure 31. $C_{n\beta dynamic}$ vs Aileron-Alone Divergence Parameter, Proverse Yaw - Airplane 1

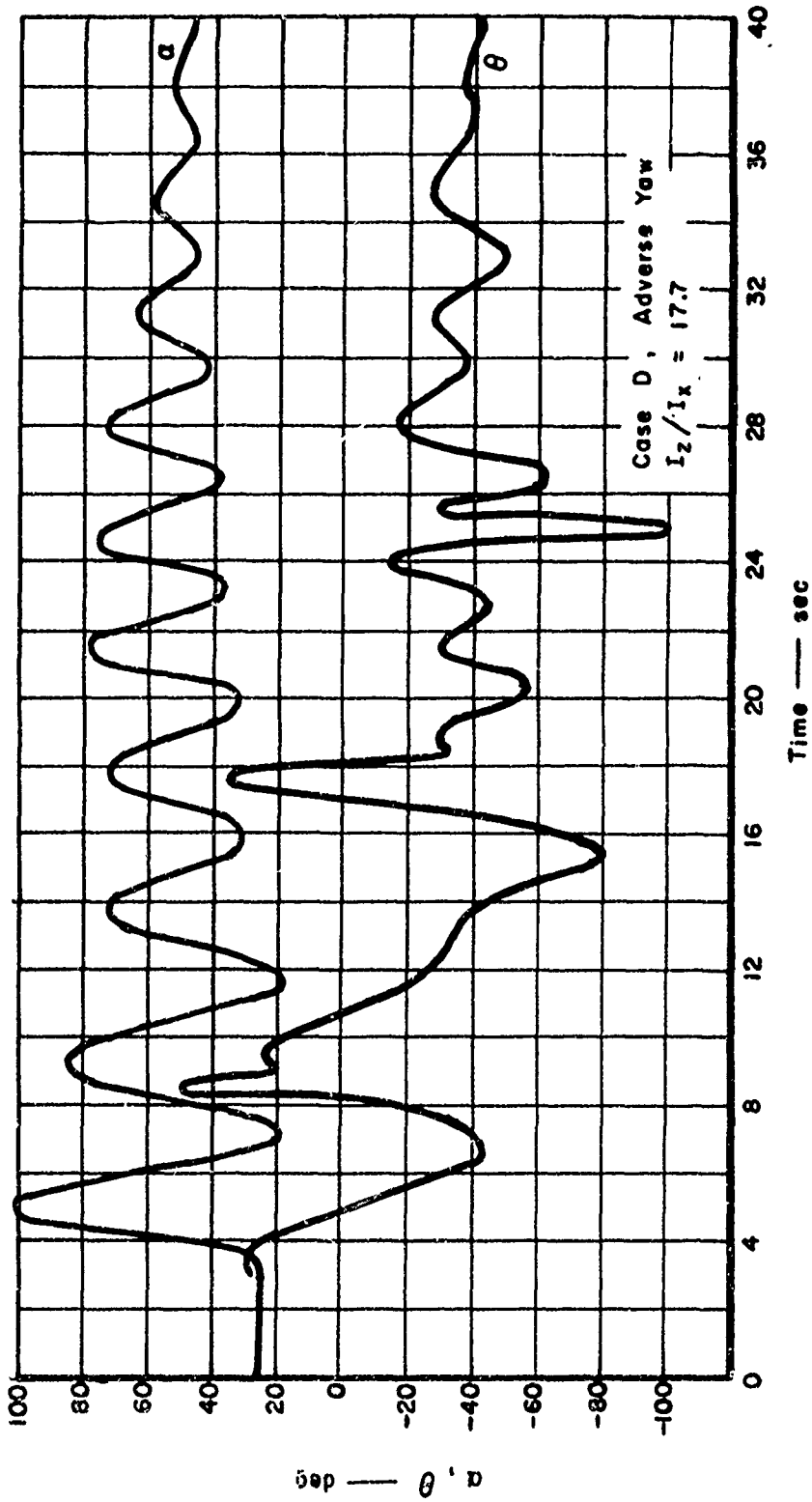

Figure 32. Angle of Attack, Pitch Angle vs Time

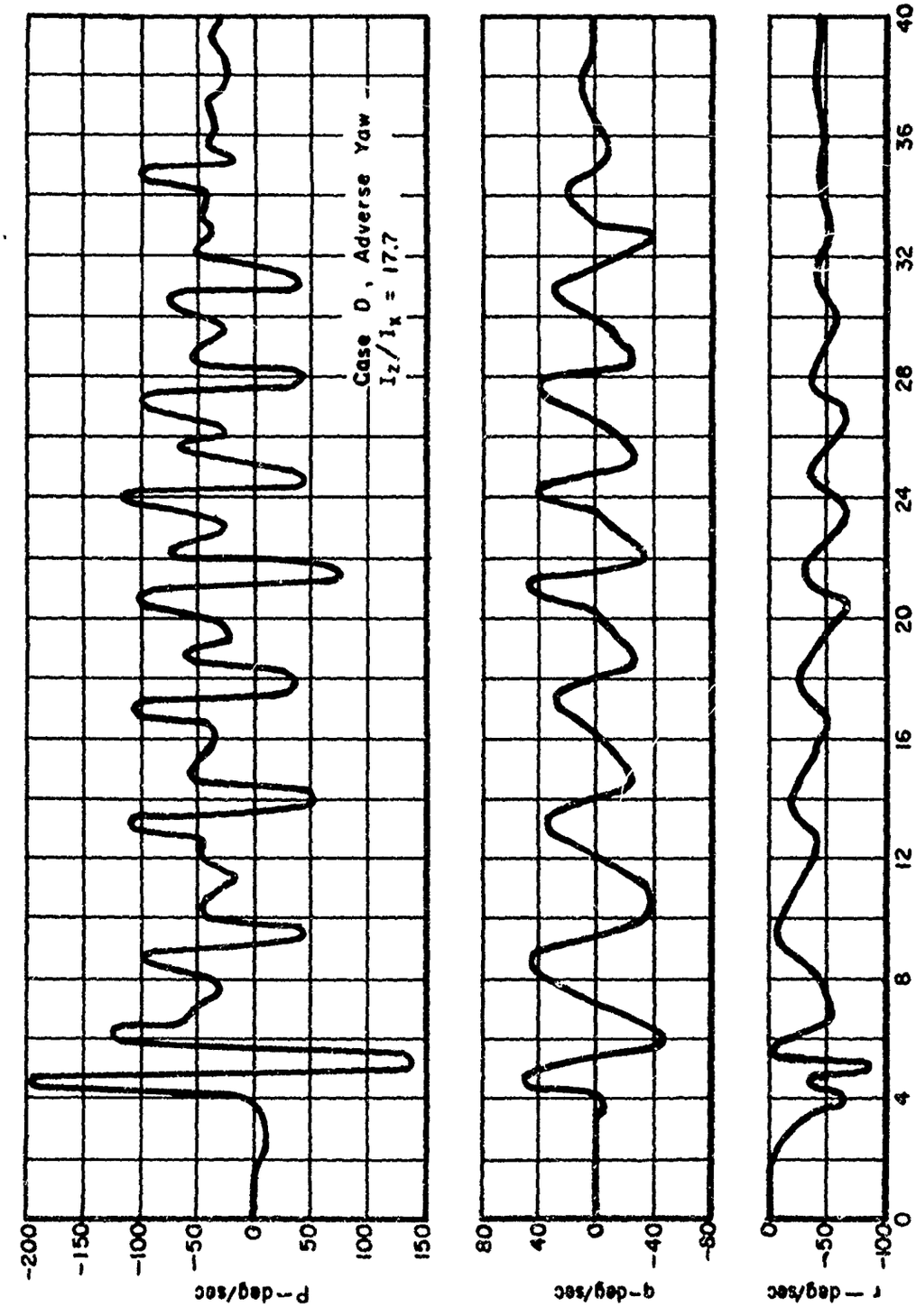

Figure 33. Roll, Pitch, Yaw Rates vs Time

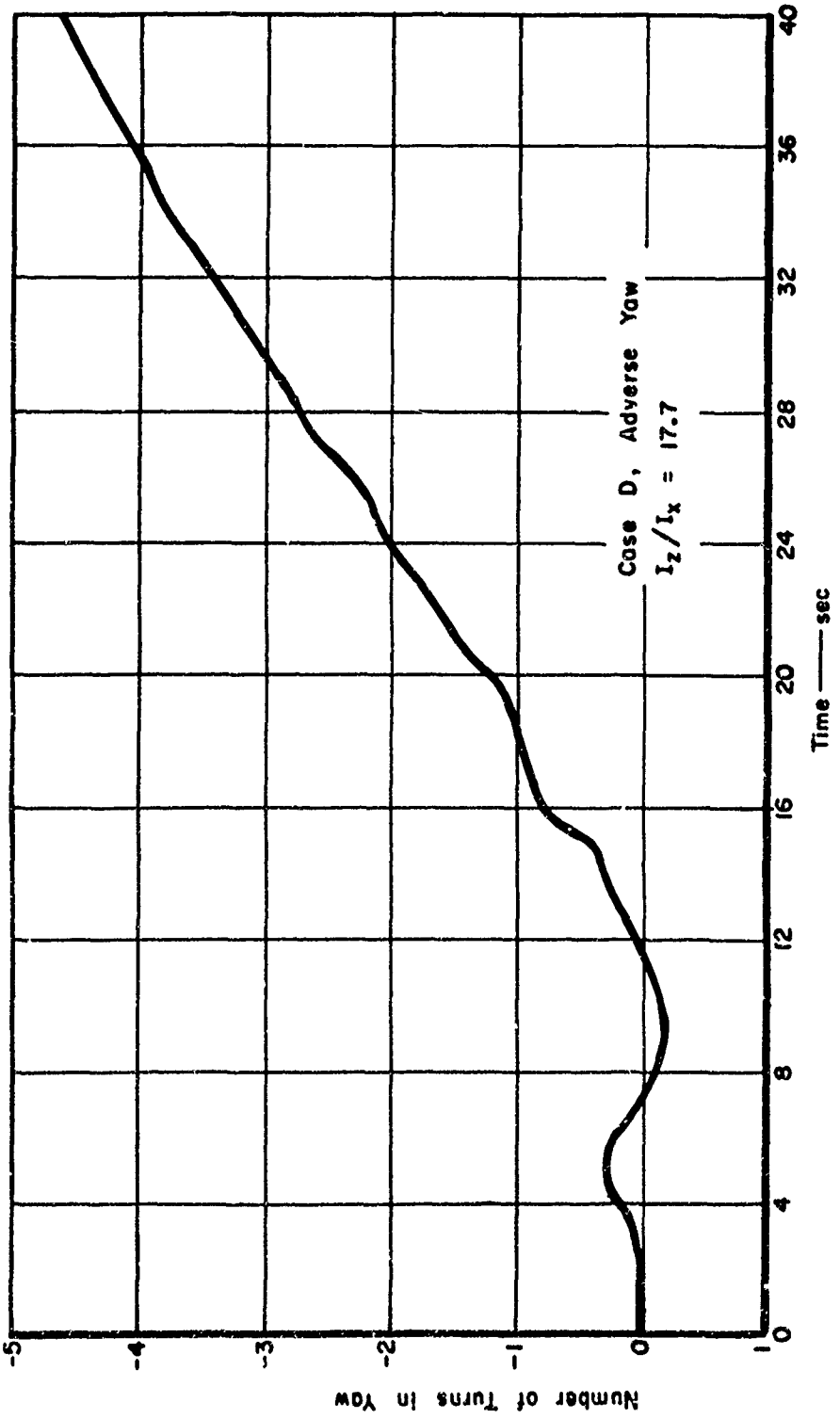

Figure 34. Number of Turns in Yaw vs Time

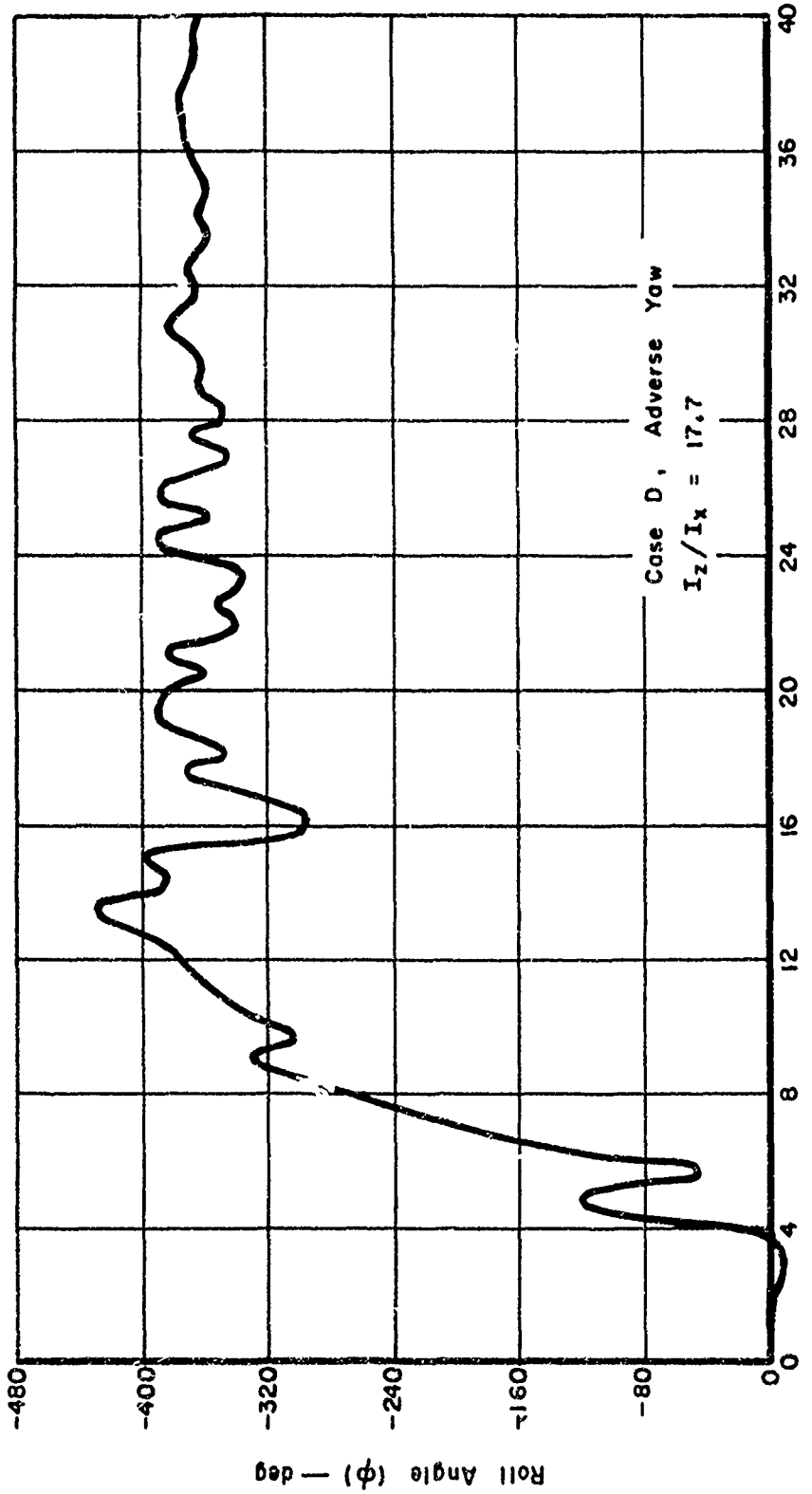

Figure 35. Roll Angle vs Time

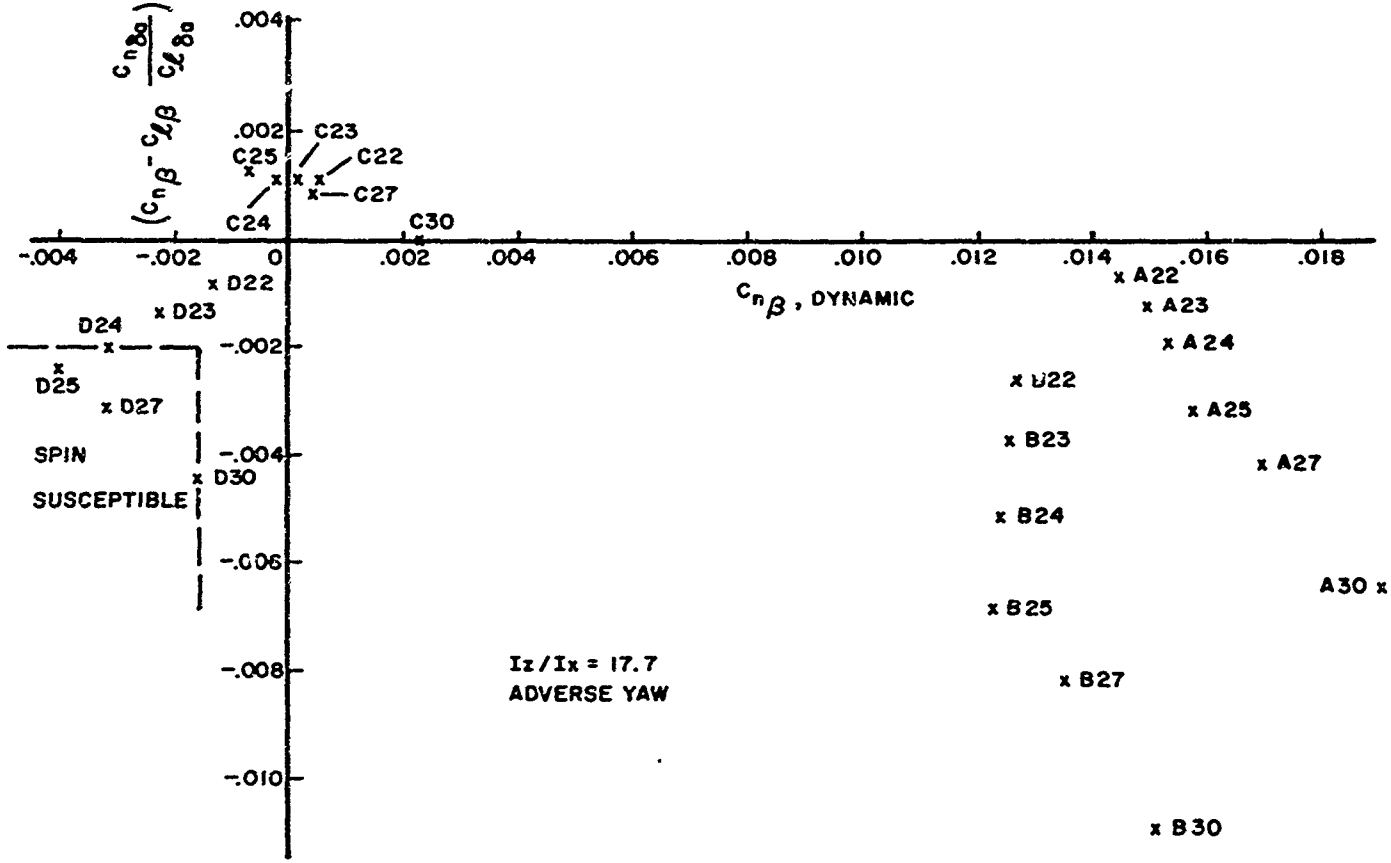

Figure 36. $C_{n\beta,\ dynamic}$ vs Aileron-Alone Divergence Parameter, Adverse Yaw- Airplane 2

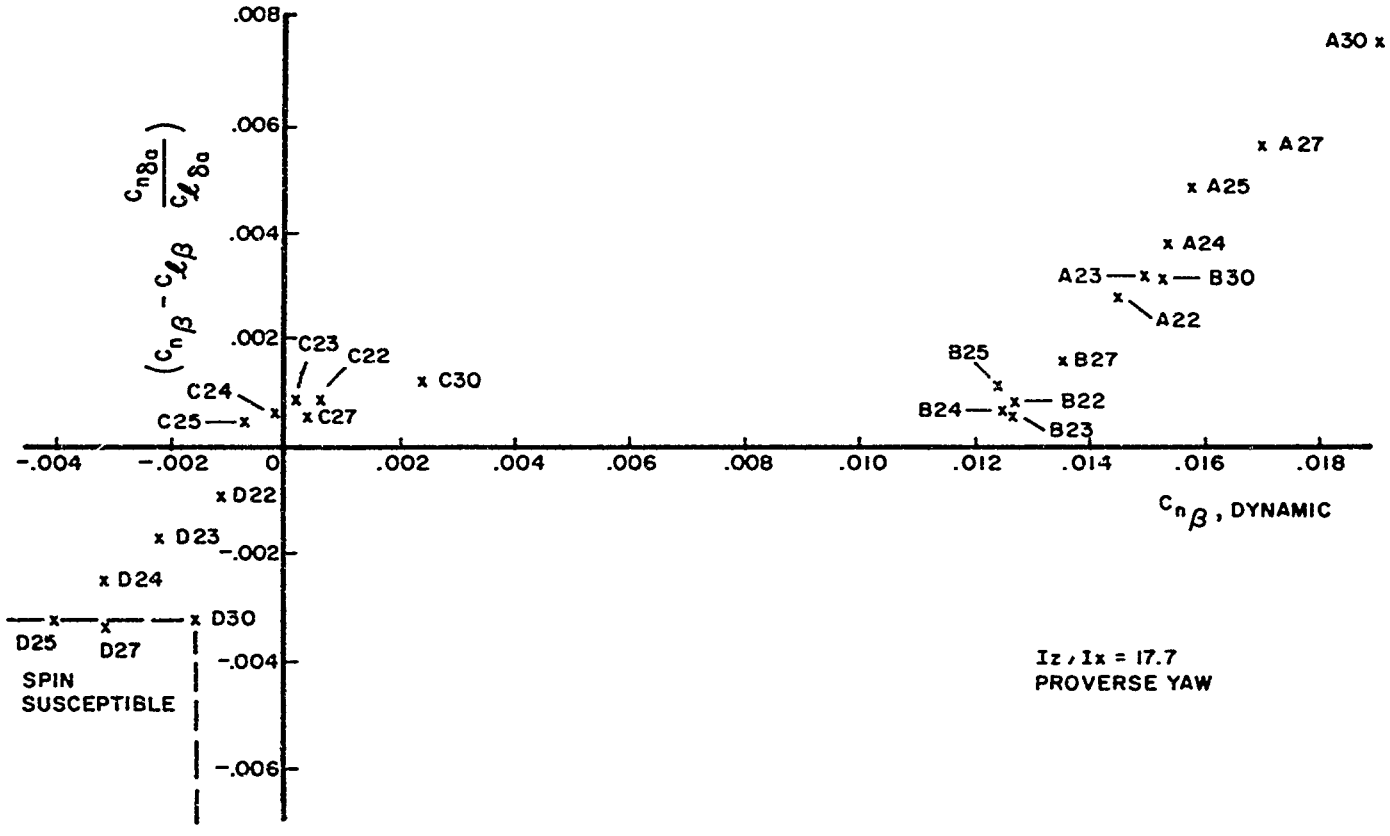

Figure 37. $C_{n\beta,\ dynamic}$ vs Aileron-Alone Divergence Parameter, Proverse Yaw- Airplane 2

SECTION V

SUMMARY AND CONCLUSIONS

It is felt that the $C_{n\beta,dynamic}$ and aileron-alone divergence parameters, as criteria for predicting spin susceptibility, show considerable promise. However, this study deals with specific cases and, although these cases are considered representative of current fighter-type airplanes, the results presented herein are not conclusive proof of the criteria. An airplane with poor lateral-directional stability characteristics, such as case D, tends to be spin susceptible once the post stall gyration is entered. When the post stall gyration is entered without the use of lateral control input, $C_{n\beta,dynamic}$ will be a relatively large negative value and remain so at near-stall angles of attack. In general, if $C_{n\beta,dynamic}$ is positive an airplane tends not to be susceptible to spinning.

The aileron-alone divergence parameter is negative for airplanes whose lateral-directional characteristics are conducive to spin (case D) regardless of the variation in pitching moment used in this study and whether or not adverse or proverse yaw is present. With lateral control input at near-stall angles of attack and case D lateral-directional stability characteristics, regions of spin susceptibility are identified whose boundaries are negative values of $C_{n\beta,dynamic}$ and negative values of the aileron-alone divergence parameter. An airplane will be spin susceptible when its $C_{n\beta,dynamic}$ and aileron-alone divergence parameters fall in these regions.

With case B lateral-directional characteristics (i.e., appreciable positive effective dihedral but directional instability at near-stall angles of attack), a region of spin susceptibility is identified for airplane I with adverse yaw which is dependent upon the variation in pitching

moment at the lower trim angles of attack investigated. At the higher trim angles of attack (27 and 30 degrees), that is, at large negative values of the aileron-alone divergence parameter, airplane 1 with case B lateral-directional characteristics will be spin susceptible regardless of the variation in pitching moment. Airplane 2 with case B lateral-directional characteristics and adverse yaw indicates no tendency to spin with either variation in pitching moment. It is concluded that for an airplane whose $C_{n\beta,dynamic}$ and aileron-alone divergence parameters fall in the spin susceptible region for case B (Figure 30), further analyses are needed to definitely determine spin susceptibility or nonsusceptibility. Until this is established, points that fall in this region should be considered as an indication of spin susceptibility. Points that fall outside the spin susceptible region in the lower right hand quadrant (e.g., case A for airplane 1 and cases A and B for airplane 2) indicate nonsusceptibility to spinning.

In general, proverse yaw appears to be preferable to adverse yaw, regarding spin susceptibility. Proverse yaw due to lateral control deflection on airplane 1 eliminated the region of spin susceptibility for case B and reduced the region of spin susceptibility for airplane 2, case D. An airplane whose $C_{n\beta,dynamic}$ and aileron-alone divergence parameters are both positive will not be spin susceptible.

The results of this study also indicate that airplanes with large values of the yaw to roll moment of inertia ratio are less susceptible to spins than airplanes with low values of I_Z/I_X. The regions of spin susceptibility begin at larger negative values of the aileron-alone divergence parameter, and directional divergence is delayed to higher angles of attack. Furthermore, regions of spin susceptibility for airplane 2 were found only for case D with adverse and proverse yaw.

APPENDIX I

EQUATIONS OF MOTION AND ASSOCIATED EXPRESSIONS

The six degree of freedom differential equations of motion referred to a body axis system and associated expressions are as follows:

Force Equations

$$\dot{u} = -g\sin\theta - \frac{qw}{57.3} + \frac{rv}{57.3} - \frac{Sq_0}{m}\left(C_c + C_{c\delta_H}\cdot\delta_H\right) + \frac{T}{m}$$

$$\dot{v} = g\cos\theta\sin\phi - \frac{ru}{57.3} + \frac{pw}{57.3} + \frac{Sq_0}{m}\left(C_{y\beta}\cdot\beta + C_{y\delta_R}\cdot\delta_R + C_{y\delta_a}\cdot\delta_a\right)$$

$$\dot{w} = g\cos\theta\cos\phi + \frac{qu}{57.3} - \frac{pv}{57.3} - \frac{Sq_0}{m}\left(C_N + C_{N\delta_H}\cdot\delta_H\right)$$

Moment Equations

$$\dot{p} = \left(\frac{I_{xz}}{I_x}\right)\dot{r} + \left(\frac{I_{xz}}{57.3\,I_x}\right)pq + \left(\frac{I_y - I_z}{57.3\,I_x}\right)qr + \frac{57.3\,Sbq_0}{I_x}\left(C_{l\beta}\cdot\beta + C_{l\delta_a}\cdot\delta_a + C_{l\delta_R}\cdot\delta_R\right) + \frac{Sb^2q_0}{2VI_x}\left(C_{lp}\cdot p + C_{lr}\cdot r\right)$$

$$\dot{q} = \left(\frac{I_{xz}}{57.3\,I_y}\right)r^2 - \left(\frac{I_{xz}}{57.3\,I_y}\right)p^2 + \left(\frac{I_z - I_x}{57.3\,I_y}\right)pr + \frac{57.3\,S\bar{c}\,q_0}{I_y}\left(C_m + C_{m\delta_H}\cdot\delta_H\right) + \frac{S\bar{c}^2q_0}{2VI_y}\left(C_{mq}\cdot q + C_{m\dot{\alpha}}\cdot\dot{\alpha}\right)$$

$$\dot{r} = \left(\frac{I_{xz}}{I_z}\right)\dot{p} - \left(\frac{I_{xz}}{57.3\,I_z}\right)qr + \left(\frac{I_x - I_y}{57.3\,I_z}\right)pq + \frac{57.3\,Sbq_0}{I_z}\left(C_{n\beta}\cdot\beta + C_{n\delta_R}\cdot\delta_R + C_{n\delta_a}\cdot\delta_a\right) + \frac{Sb^2q_0}{2VI_z}\left(C_{nr}\cdot r + C_{np}\cdot p\right)$$

Attitude Equations

$$\dot{\theta} = q\cos\phi - r\sin\phi$$

$$\dot{\phi} = p + \dot{\psi}\sin\theta$$

$$\dot{\psi} = \frac{r\cos\phi + q\sin\phi}{\cos\theta}$$

Altitude Equation

$$\dot{h} = u\sin\theta - v\cos\theta\sin\phi - w\cos\theta\cos\phi$$

Linear Acceleration & Velocity Equations

$$\dot{V} = \frac{u\dot{u} + v\dot{v} + w\dot{w}}{V}$$

$$V = \left(u^2 + v^2 + w^2\right)^{1/2}$$

Rate of Change of Angle of Attack

$$\dot{\alpha} = 57.3\left(\frac{\dot{w}\cos\alpha - \dot{u}\sin\alpha}{V\cos\beta}\right)$$

Rate of Change of Sideslip Angle

$$\dot{\beta} = 57.3\left(\frac{\dot{v} - \dot{V}\sin\beta}{V\cos\beta}\right)$$

Derivation of Equations for Rate of Change of Angle of Attack and Sideslip :

From Figure 38

$$u = V\cos\beta\cos\alpha \tag{1}$$

$$v = V\sin\beta \tag{2}$$

$$w = V\cos\beta\sin\alpha \tag{3}$$

Differentiating (2) gives,

$$\frac{dv}{dt} = \dot{v} = \dot{V}\sin\beta + V\dot{\beta}\cos\beta \tag{4}$$

Solving for $\dot{\beta}$ yields,

$$\dot{\beta} = \frac{\dot{v} - \dot{V}\sin\beta}{V\cos\beta} \tag{5}$$

From Equation 1,

$$V\cos\beta = \frac{u}{\cos\alpha} \tag{6}$$

Substituting 6 into 3 gives,

$$w = \frac{u}{\cos\alpha}\sin\alpha$$

or

$$w\cos\alpha = u\sin\alpha \tag{7}$$

Differentiating 7 and solving for $\dot{\alpha}$,

$$\dot{w}\cos\alpha - w\dot{\alpha}\sin\alpha = \dot{u}\sin\alpha + u\dot{\alpha}\cos\alpha$$

$$\dot{\alpha}(w\sin\alpha + u\cos\alpha) = \dot{w}\cos\alpha - \dot{u}\sin\alpha$$

$$\dot{\alpha} = \frac{\dot{w}\cos\alpha - \dot{u}\sin\alpha}{w\sin\alpha + u\cos\alpha} \tag{8}$$

Now, $$w \sin\alpha = V \cos\beta \sin^2\alpha$$

$$u \cos\alpha = V \cos\beta \cos^2\alpha$$

$$\therefore \quad w \sin\alpha + u \cos\alpha = V \cos\beta (\sin^2\alpha + \cos^2\alpha)$$

$$= V \cos\beta$$

Consequently,

$$\dot{\alpha} = \frac{\dot{w} \cos\alpha - \dot{u} \sin\alpha}{V \cos\beta} \tag{9}$$

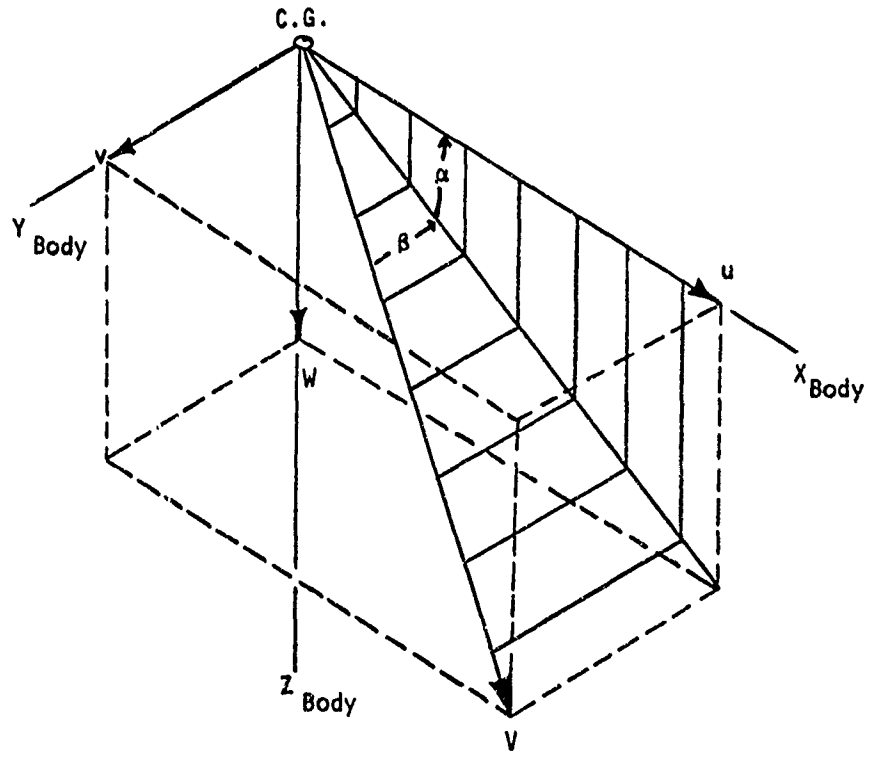

Figure 38. Reference Axes, Angle of Attack, and Angle of Sideslip Definition

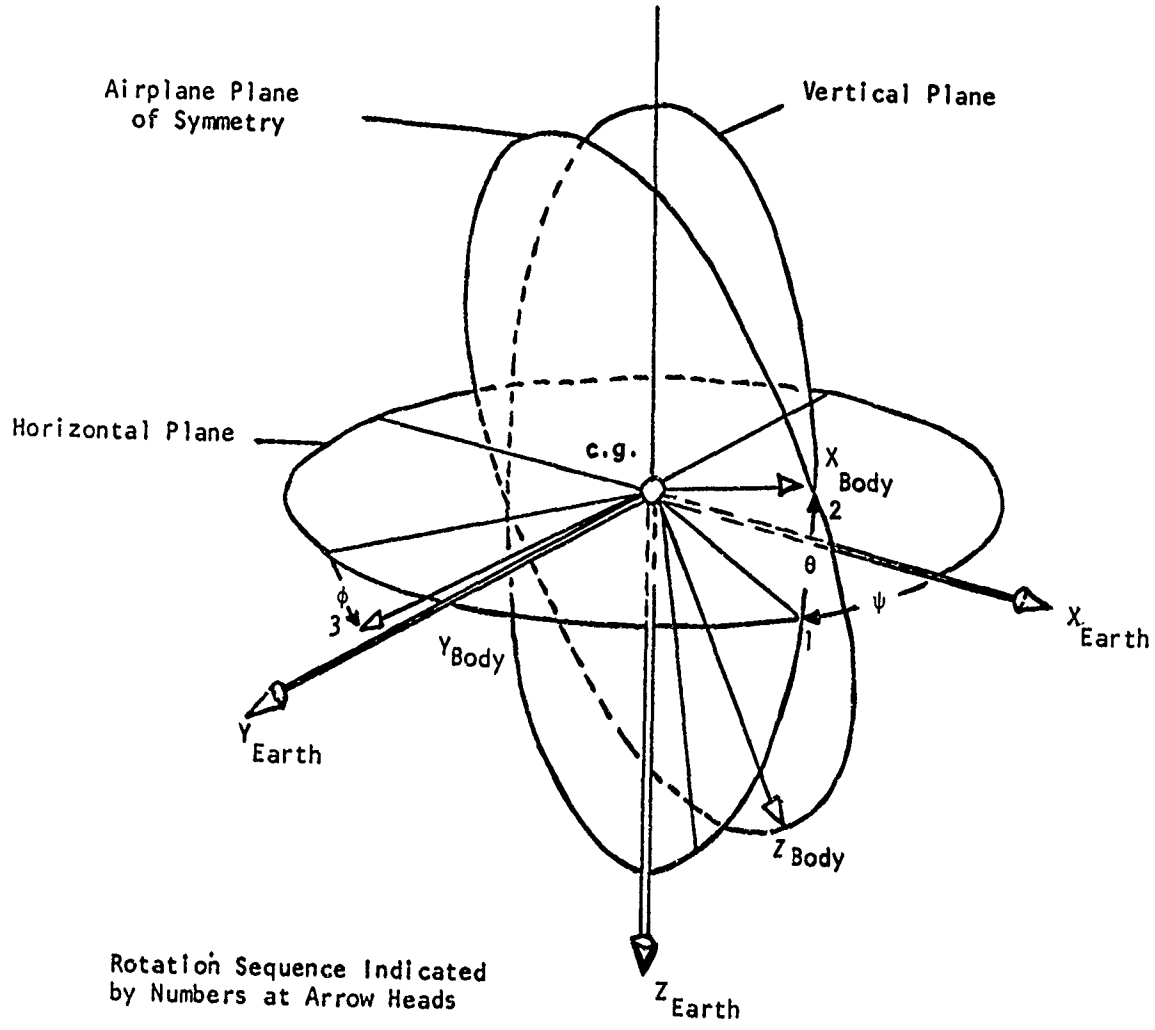

Figure 39. Attitude Angle Definition and Rotation Sequence

APPENDIX II

AERODYNAMIC DATA

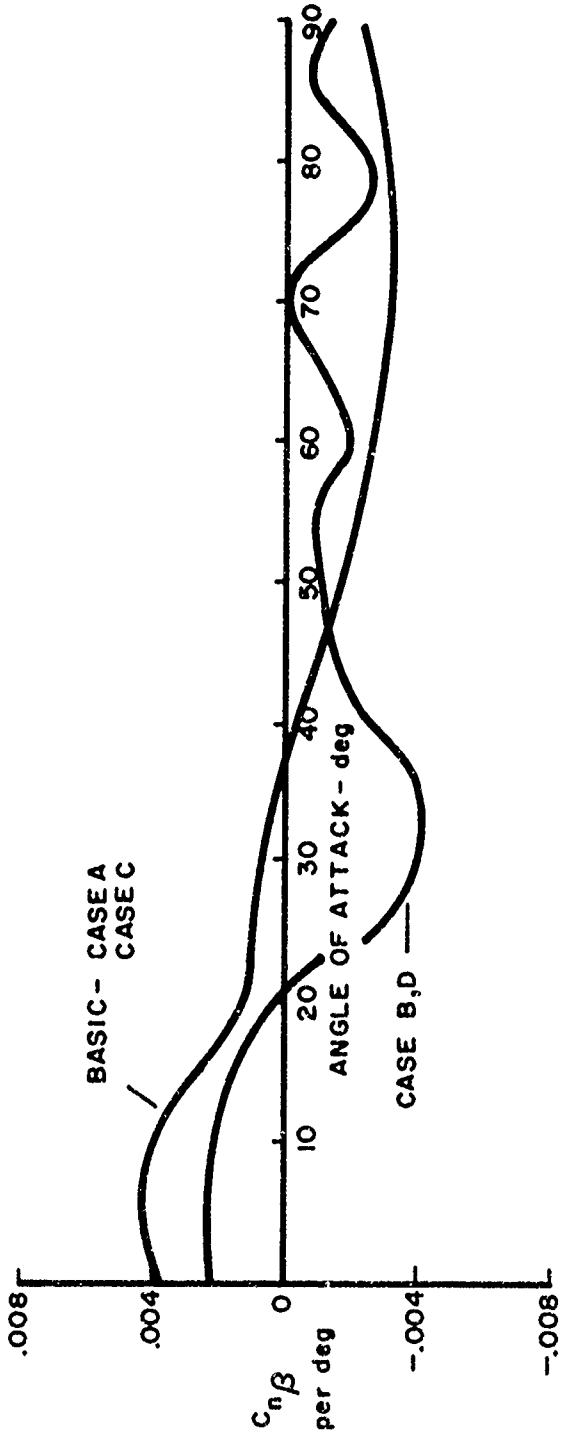

Figure 40. Variation In Yawing Moment Coefficient Due to Sideslip Angle With Angle of Attack

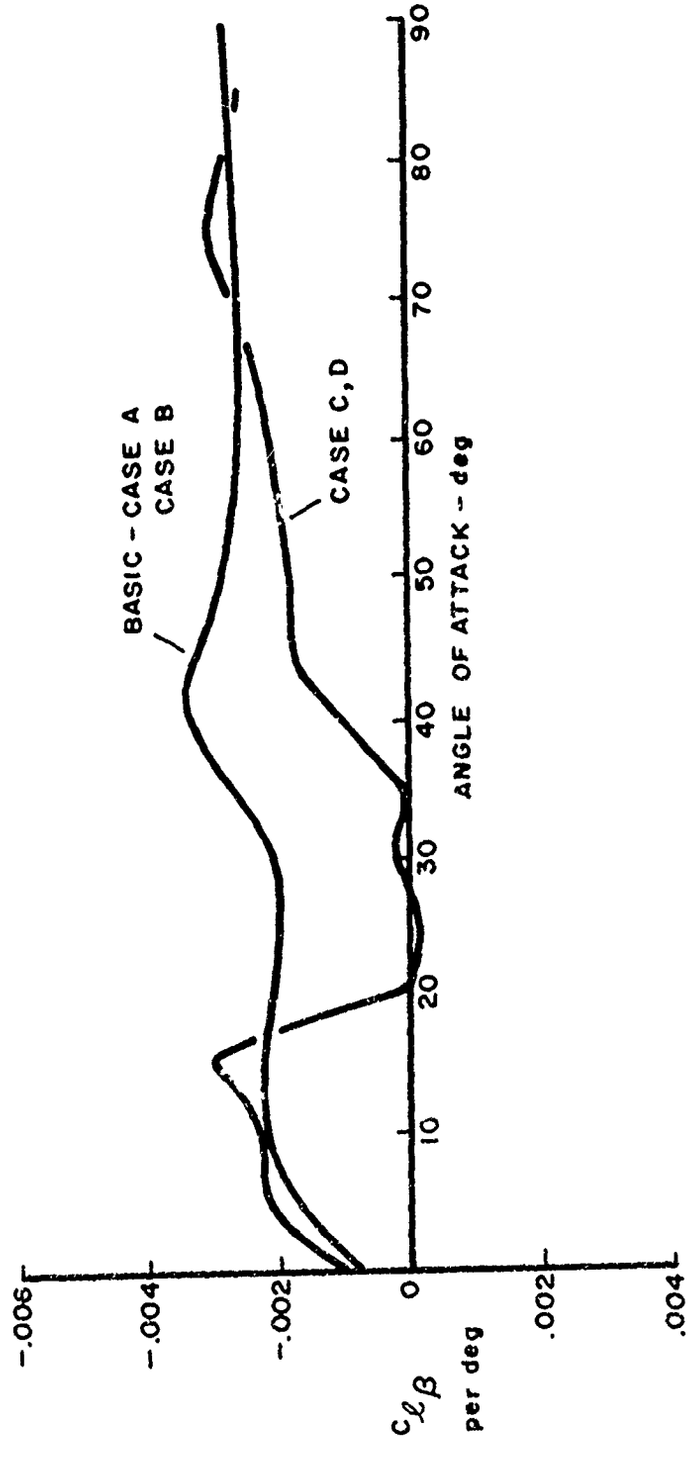

Figure 41. Variation In Rolling Moment Coefficient Due To Sideslip Angle With Angle Of Attack

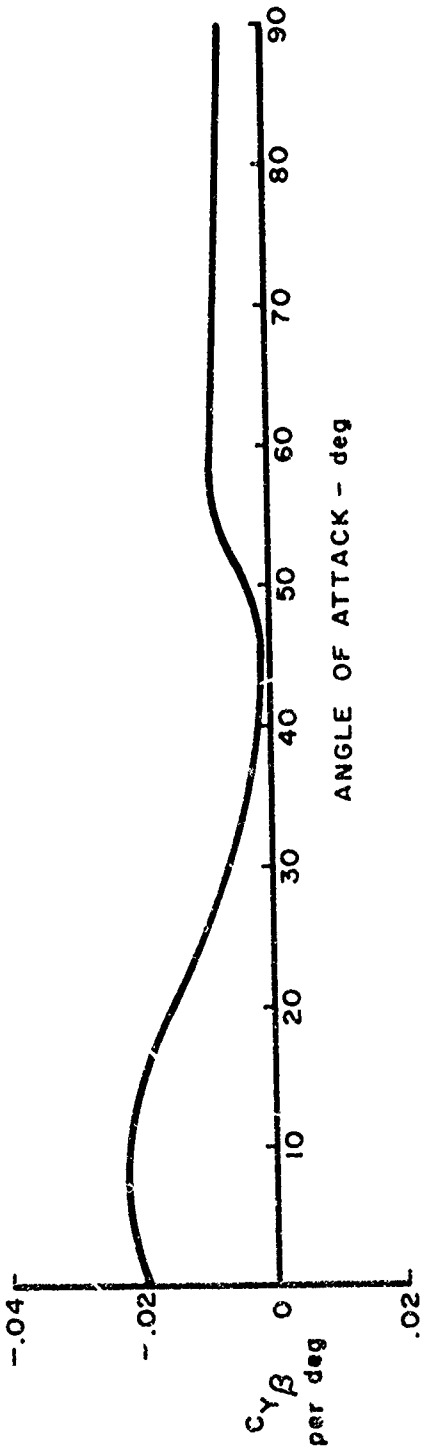

Figure 34. Variation In Side Force Coefficient Due To Sideslip Angle With Angle Of Attack

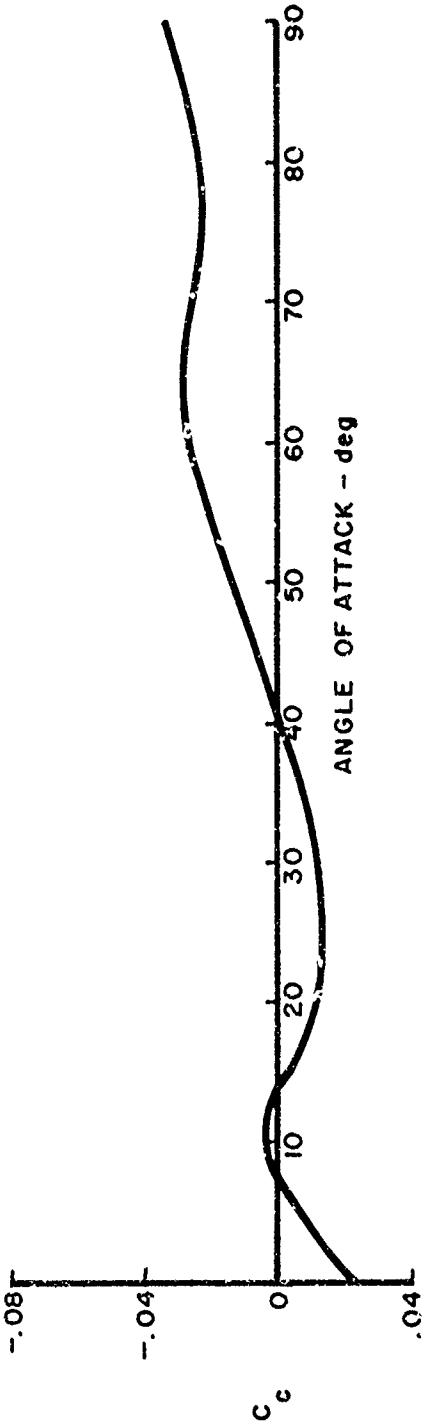

Figure 43. Variation Of Chord Force Coefficient With Angle Of Attack

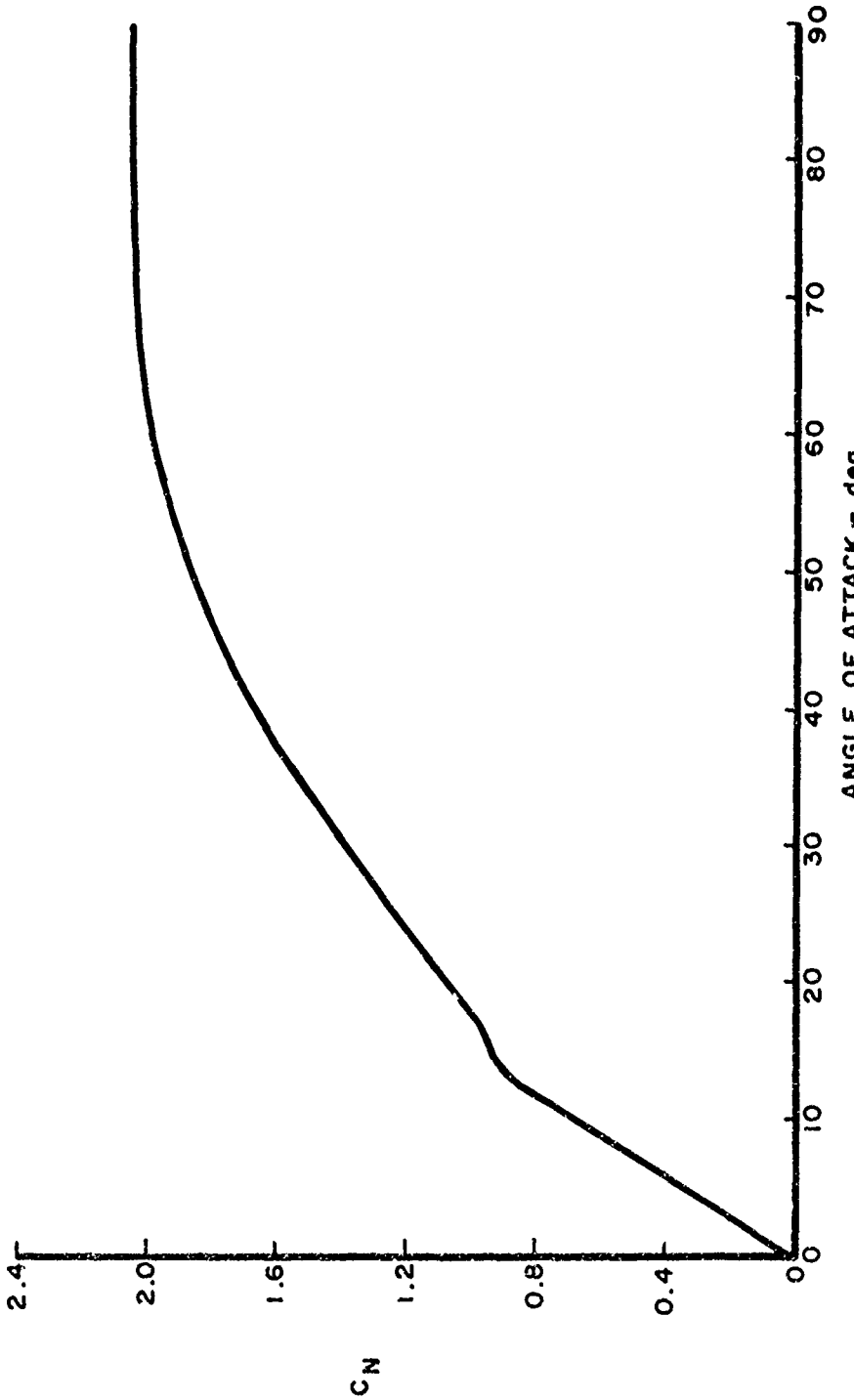

Figure 44. Variation Of Normal Force Coefficient With Angle Of Attack

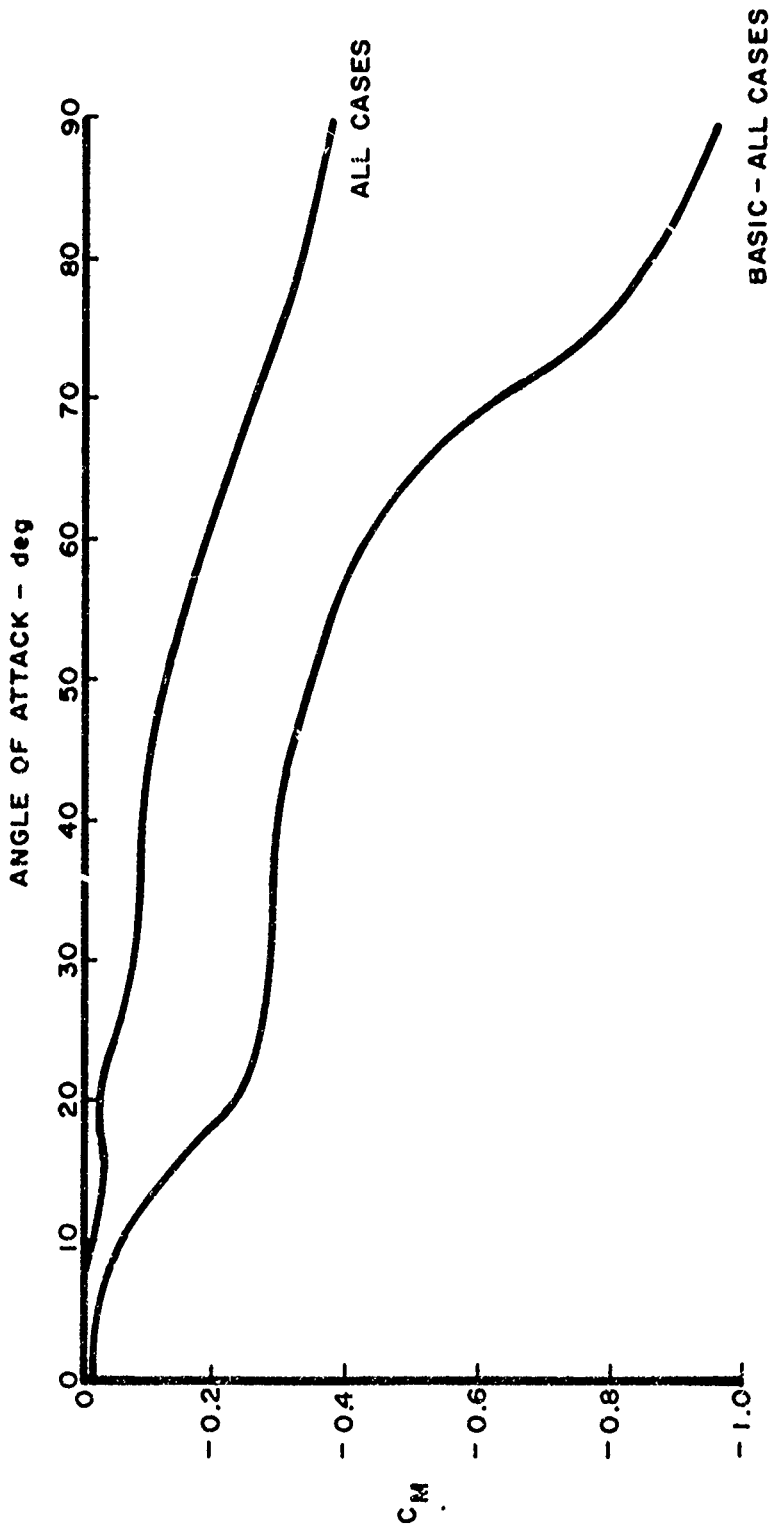

Figure 45. Variation Of Pitching Moment Coefficient With Angle of Attack

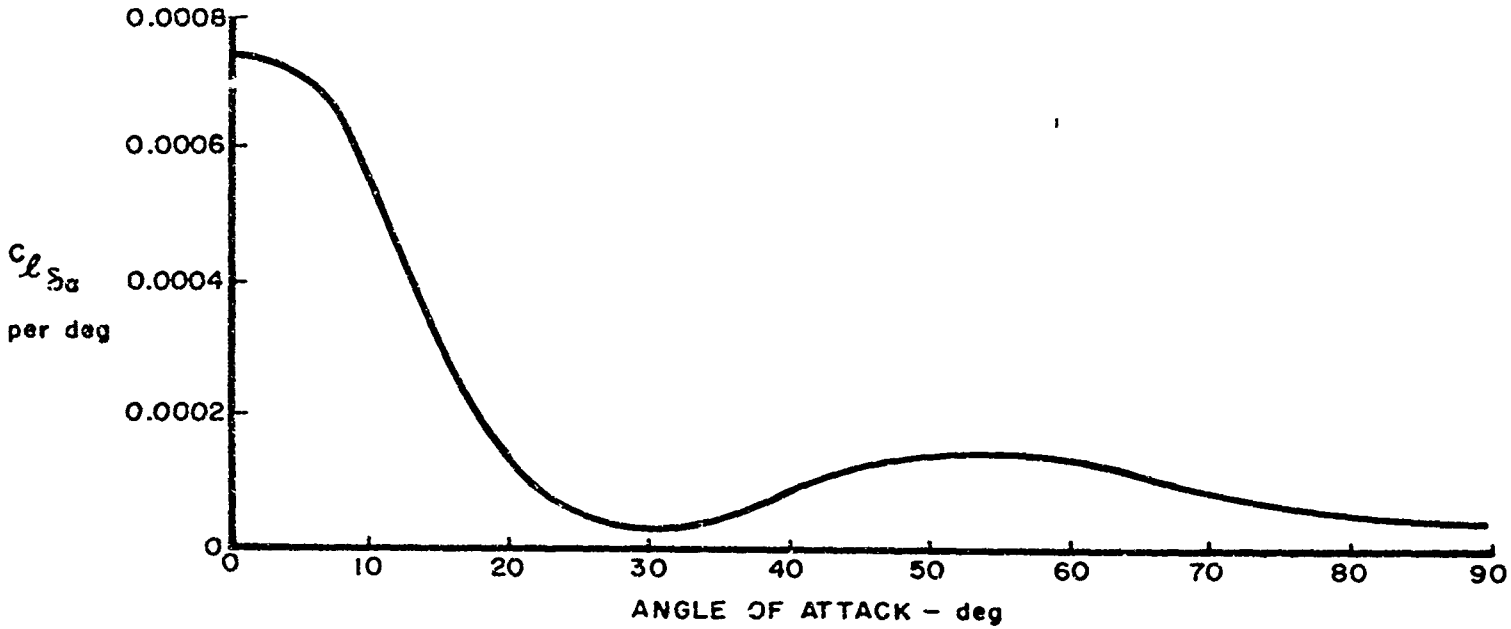

Figure 46. Variation In Rolling Moment Coefficient Due To Aileron Deflection With Angle of Attack

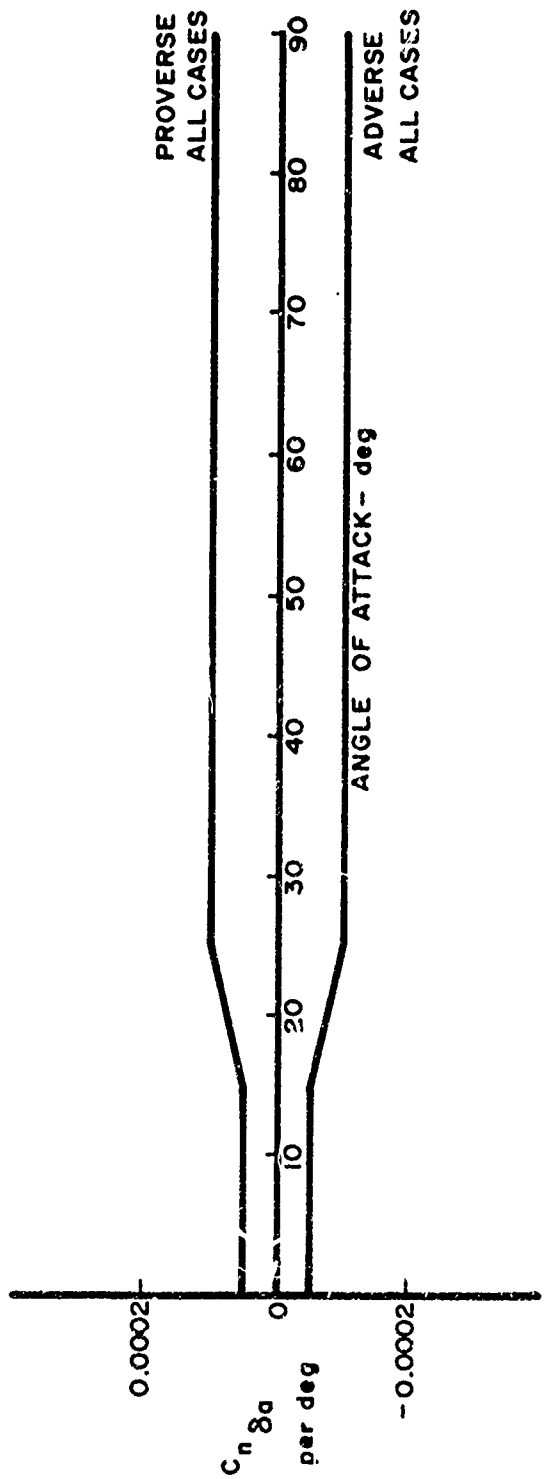

Figure 47. Variation In Yawing Moment Coefficient Due To Aileron Deflection With Angle Of Attack

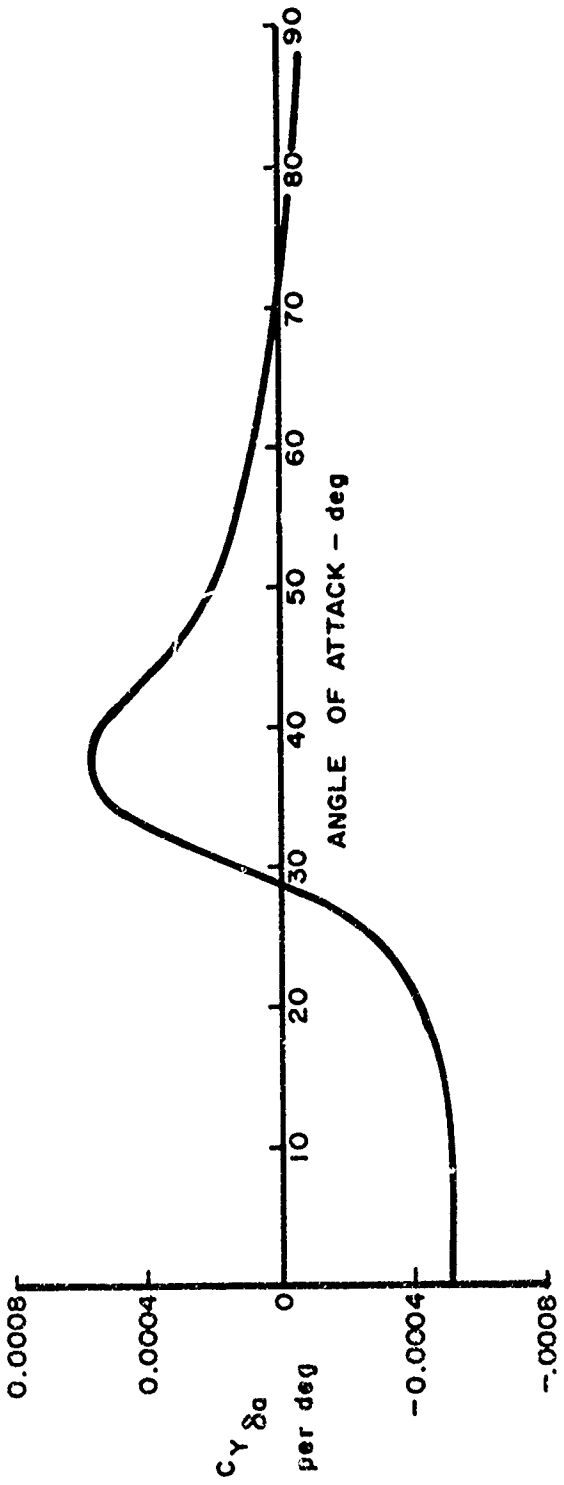

Figure 48. Variation In Side Force Coefficient Due To Aileron Deflection With Angle Of Attack

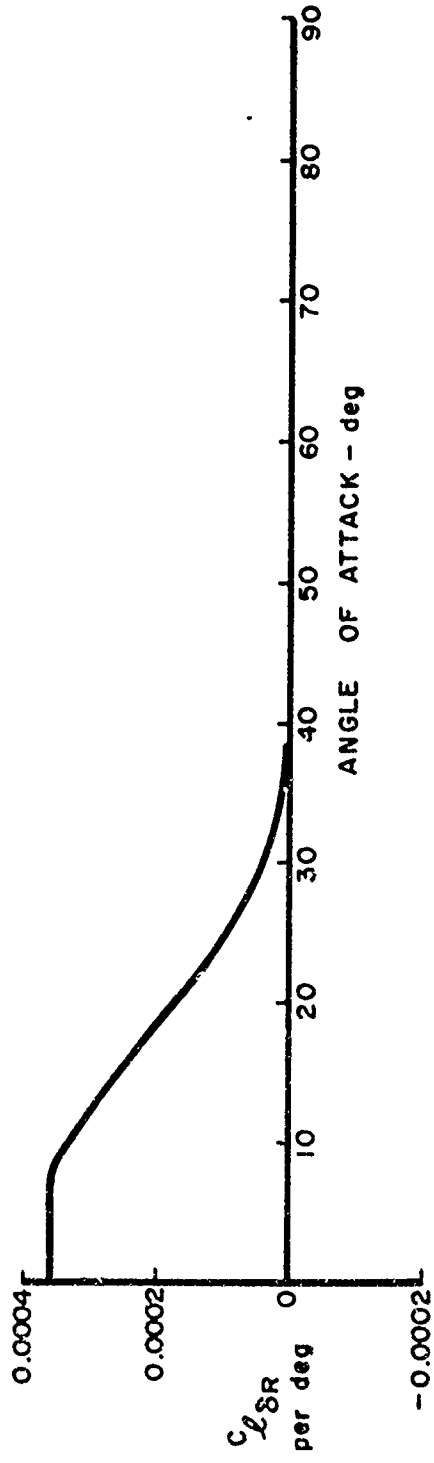

Figure 49. Variation In Rolling Moment Coefficient Due To Rudder Deflection With Angle Of Attack

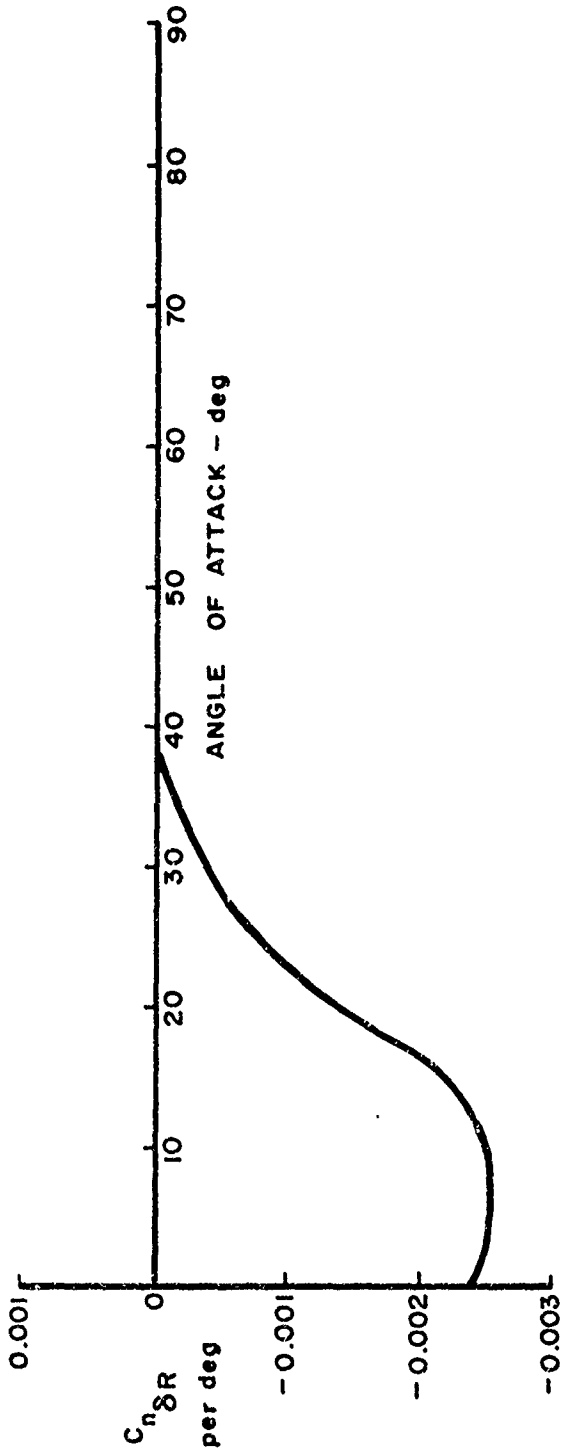

Figure 50. Variation In Yawing Moment Coefficient Due To Rudder Deflection With Angle Of Attack

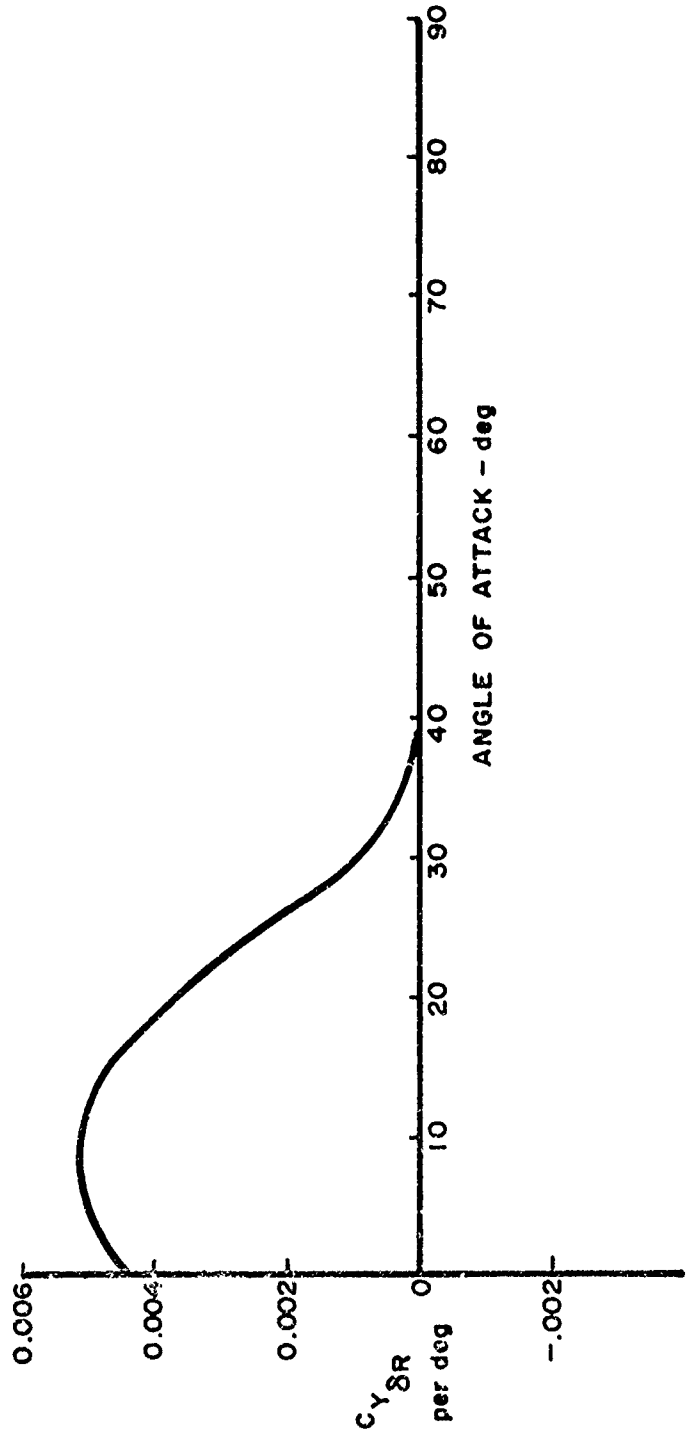

Figure 51. Variation In Side Force Coefficient Due To Rudder Deflection With Angle Of Attack

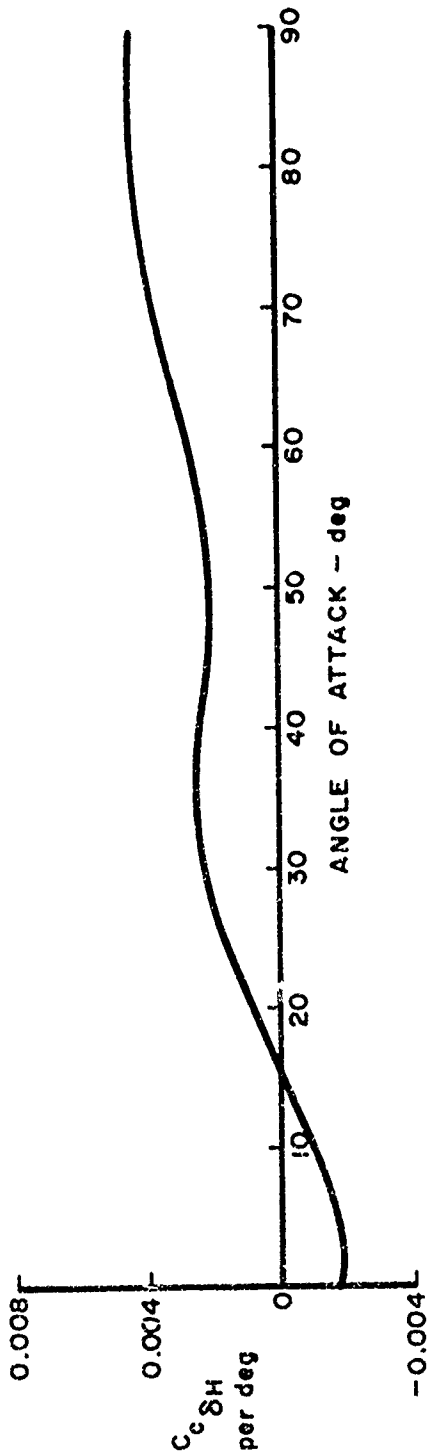

Figure 52. Variation In Chord Force Coefficient Due To Elevator Deflection With Angle Of Attack

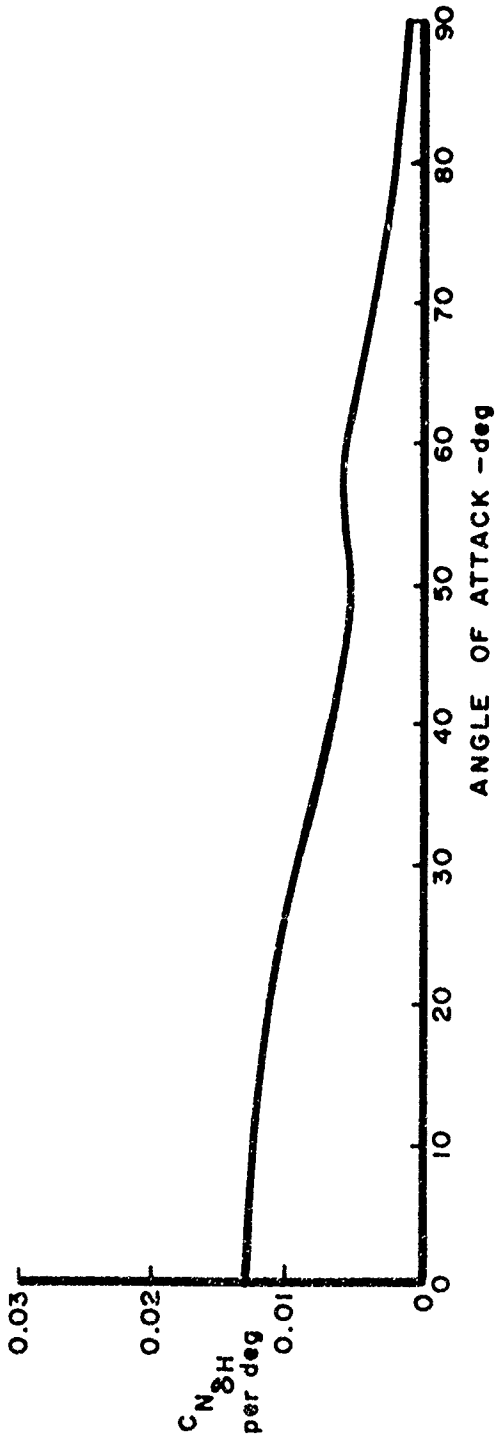

Figure 53. Variation In Normal Force Coefficient Due To Elevator Deflection With Angle Of Attack

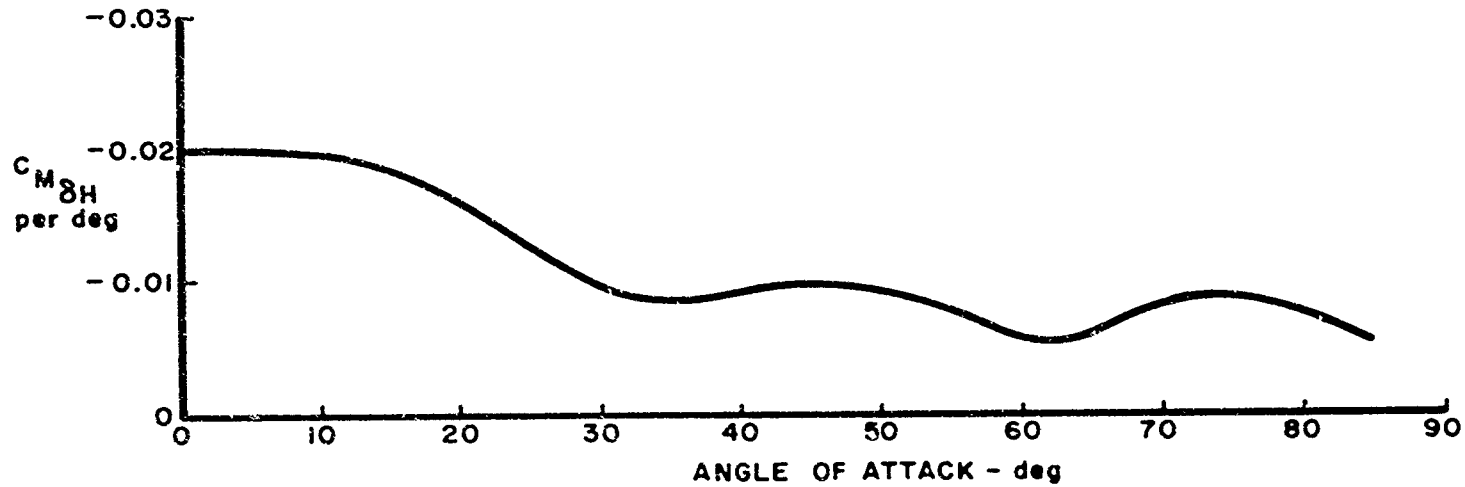

Figure 54. Variation In Pitching Moment Coefficient Due To Elevator Deflection With Angle of Attack

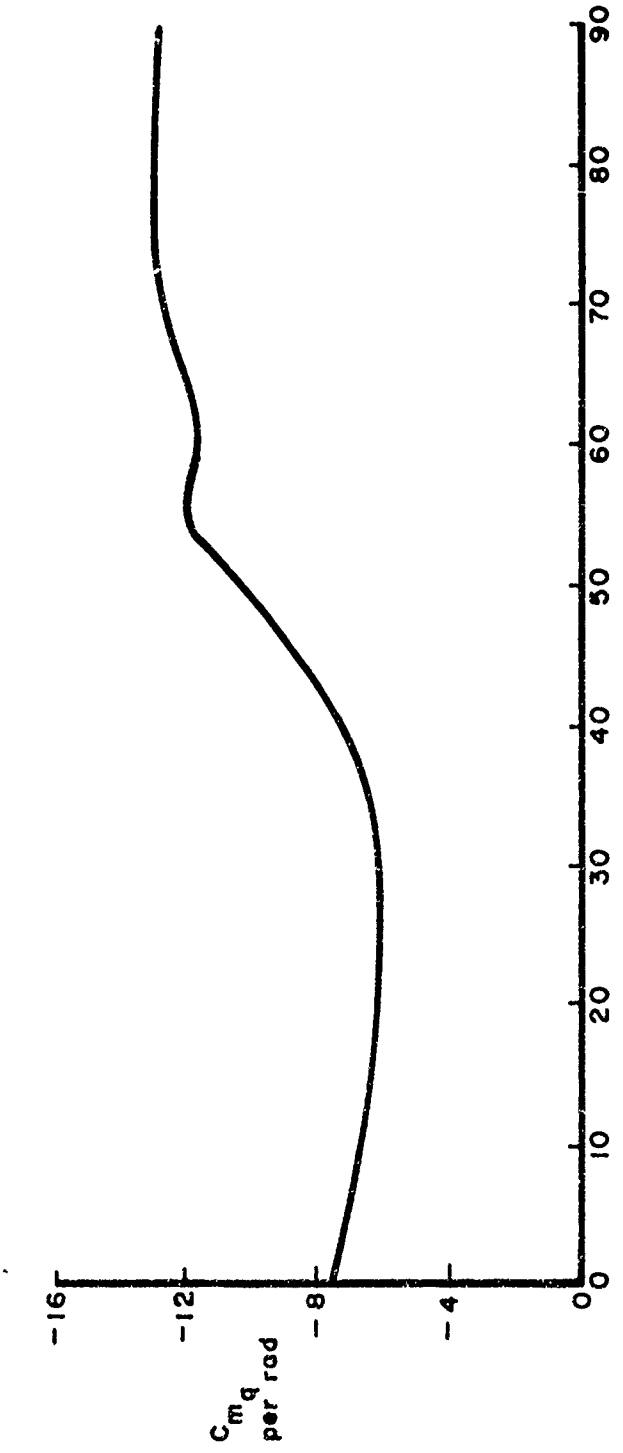

Figure 55. Variation In Pitching Moment Coefficient Due To Pitch Rate With Angle of Attack.

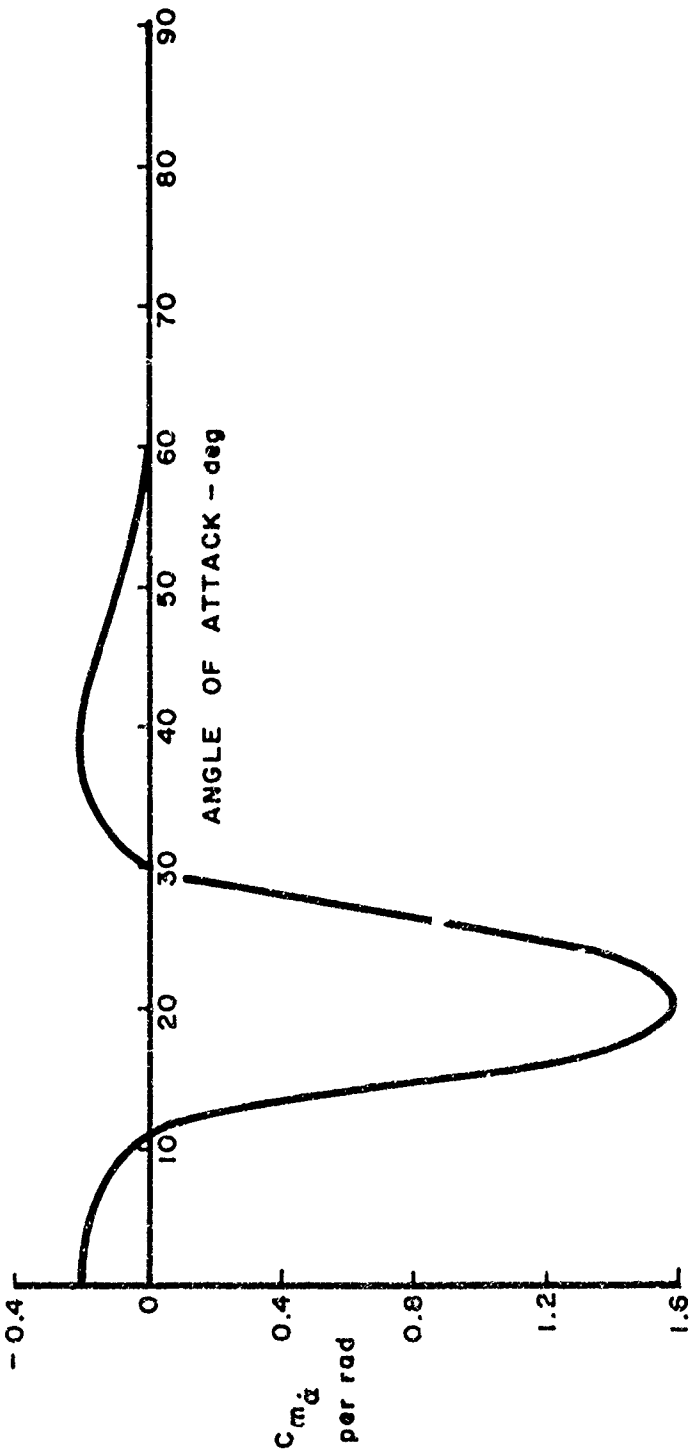

Figure 56. Variation In Pitching Moment Coefficient Due To Rate Of Change Of Angle Of Attack With Angle Of Attack

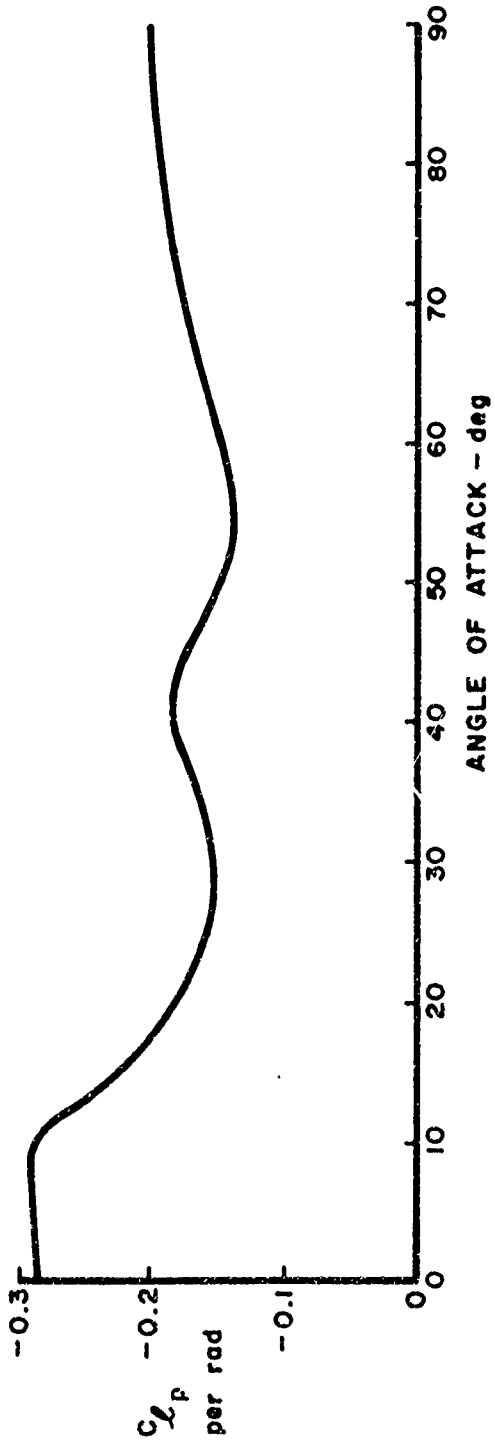

Figure 57. Variation In Rolling Moment Coefficient Due To Roll Rate With Angle Of Attack

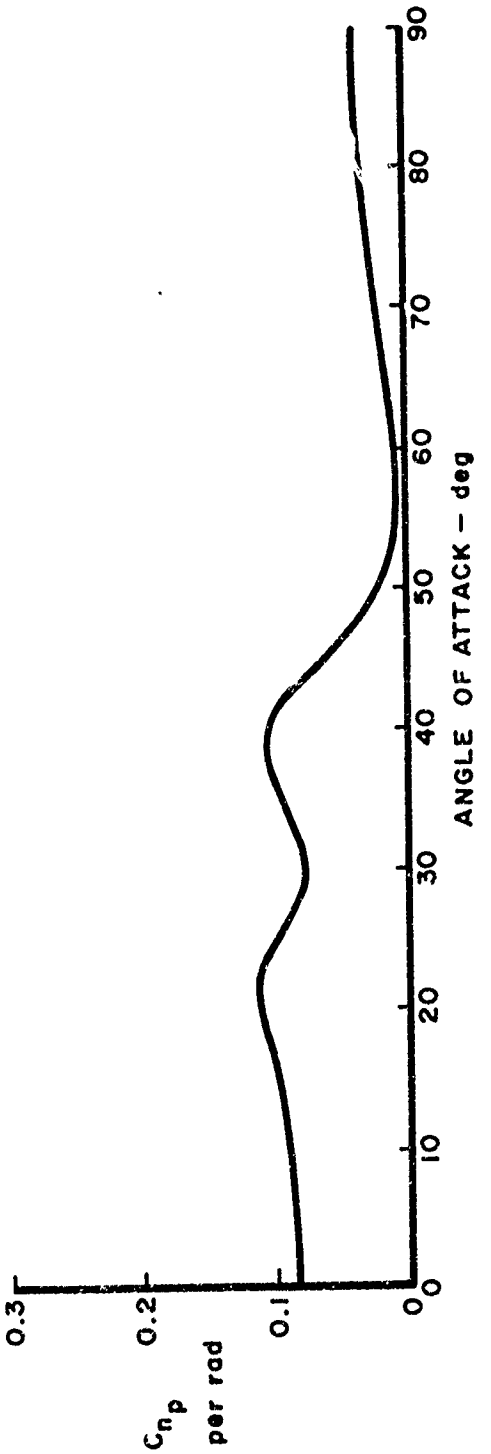

Figure 58. Variation In Yawing Moment Coefficient Due To Roll Rate With Angle Of Attack

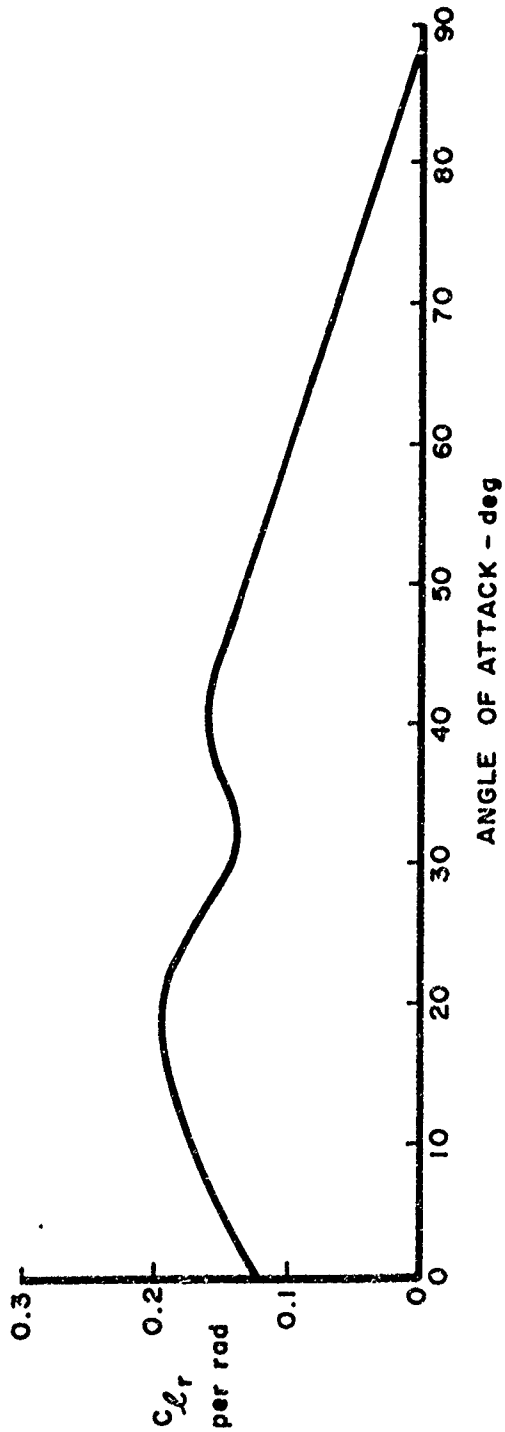

Figure 59. Variation In Rolling Moment Coefficient Due To Yaw Rate With Angle Of Attack

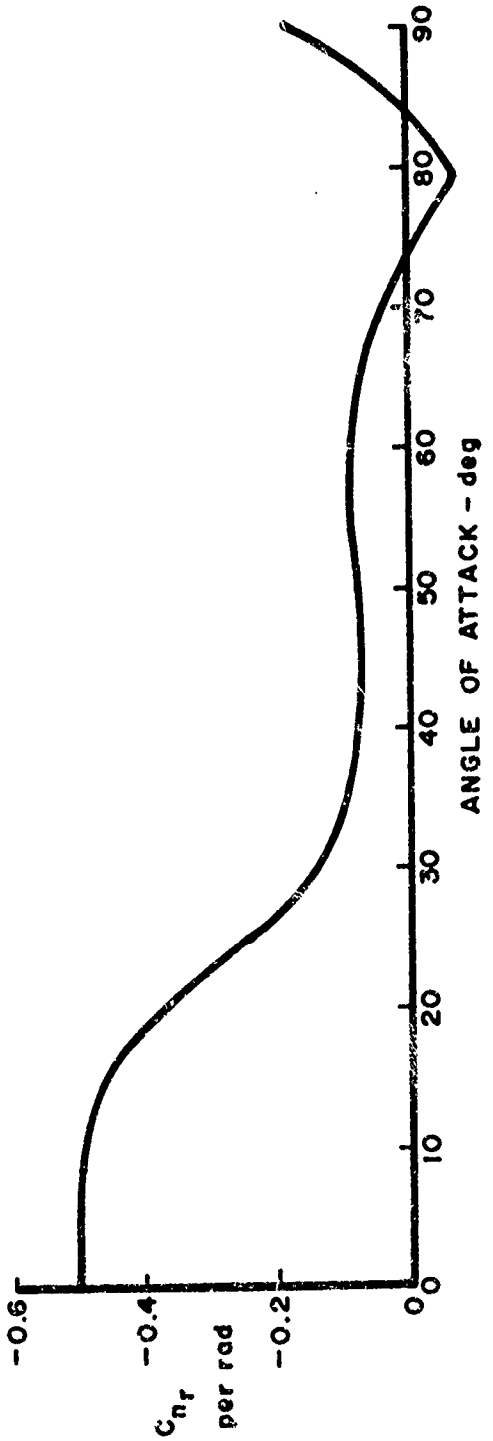

Figure 60. Variation In Yawing Moment Coefficient Due To Yaw Rate With Angle Of Attack

REFERENCES

1. Chambers, Joseph R., Analysis of Lateral-Directional Stability Characteristics of a Twin-Jet Fighter Airplane at High Angles of Attack. NASA TN D-5361, 1969.

2. Moul, Martin T., and Paulson, John W., Dynamic Lateral Behavior of High-Performance Aircraft. NACA RM L58E16, 1958.

3. Woodcock, Robert J., and Drake, Douglas E., Estimation of Flying Qualities of Piloted Airplanes. AFFDL TR-65-218, April 1966.

4. Weissman, Robert. "Influence of Inertia Characteristics on Spin Susceptibility and Spin Characteristics of Fighter-Type Airplanes." AIAA Paper No. 69-188, AIAA 7th Aerospace Sciencies Meeting, New York City, January 20-22, 1969.

BIBLIOGRAPHY

1. Burris, William R., and Hutchins, Dale E., "Effect of Wing Leading Edge Geometry on Maneuvering Boundaries and Stall Departure." AIAA Paper No. 70-904, AIAA 2nd Aircraft Design and Operations Meeting, Los Angeles, Calif., July 20-22, 1970.

2. Chambers, Joseph R., Anglin, Ernie L., and Bowman, James S., Effects of a Pointed Nose on Spin Characteristics of a Fighter Airplane Model Including Correlation with Theoretical Calculations. NASA TN D-5921, September 1970.

3. Buniel, J., Edwards, R., et al., F-5 Spin Sensitivity Study (Criteria Establishment and Comments Relative to Military Spin Specification). Northrop Corp., Norair Div., Report No. FMR-69-7, May 1969.

4. Anglin, Ernie L., Relationship Between Magnitude of Applied Spin Recovery Moment and Ensuing Number of Recovery Turns. NASA TN D-4077, August 1967.

5. Bowman, James S., "Airplane Spinning." Astronautics and Aeronautics, March 1966.

6. Neihouse, A. I., Klinar, W. J., and Scher, S. H., Status of Spin Research for Recent Airplane Designs. NASA TR R-57, 1960.

7. Wykes, J. H., Casteel, G. R., and Collins, R. A., An Analytical Study of the Dynamics of Spinning Aircraft, Part I. WADC TR 58-381, December 1958.

8. Etkin, B., Dynamics of Flight. John Wiley and Sons, Inc., New York, 1959.